CHEMICAL, PHYSICAL, AND VISCOELASTIC PROPERTIES OF HOTPRESSED HYBRID POPLAR

By

ISABELA REINIATI

A thesis submitted in partial fulfillment of
the requirements for the degree of

MASTER OF SCIENCE IN CHEMICAL ENGINEERING

WASHINGTON STATE UNIVERSITY
School of Chemical Engineering and Bioengineering

AUGUST 2009

To the Faculty of Washington State University

The members of the Committee appointed to examine the thesis of ISABELA REINIATI find it satisfactory and recommend that it be accepted.

Marie-Pierre Laborie, Ph.D., Chair

Armando McDonald, Ph.D.

Manuel Garcia-Perez, Ph.D.

Richard Zollars, Ph.D.

ACKNOWLEDGEMENT

I would like to thank numerous individuals who have devoted their time and energy to assist the completion of my degree. Special thanks to my advisor, Marie-Pierre Laborie for her guidance, constructive input, and encouragement. I would not have gone this far without her encourage for me to enter graduate school and her continuous support to complete this project. It has been a valuable learning experience and an enjoyable moment in my life. I am also grateful for the help extended by my committee members: Armando McDonald, Richard Zollars, and Manuel Garcia-Perez.

I also would like to thank WMEL personnel and chemical engineering faculty and staff for technical and administrative assistance. Special thanks to Karl Englund, Vikram Yadama, Hongzhi Liu, Robert Duncan, Scott Lewis, and Brent Olson. I thank Noridah Osman for her chemical analysis data. I appreciate my office mates and fellow graduate students for providing a stimulating and fun atmosphere, and thank Elvie Brown, Edward Jiang for their excellent mentoring. Thank you very much for going the extra mile.

Throughout my education at Washington State University, I have been blessed with several good friends, some of who became my best friends. I wish to thank Andressa Ardiani, Chi-Chi Peng, Inès de Sainte Marie, and Eric Herjanto for their understanding and friendship.

I would like to express my exceptional thanks to Paul and Lily Anderson for providing a loving environment and assistance. My immense appreciation and deepest thank goes to Mom and Dad, Betty and Didik Waluyo for their constant love, pride, and encouragement. To them I dedicate this thesis. For all these, I thank God.

CHEMICAL, PHYSICAL, AND VISCOELASTIC PROPERTIES OF

HOTPRESSED HYBRID POPLAR

Abstract

By Isabela Reiniati, M.S.
Washington State University
August 2009

Chair: Marie-Pierre Laborie

Interest in finding an alternative resource for wood-based composites has been largely influenced by the depletion of forest areas and by unstable prices for forestry products. Hybrid poplar, a fast-growing hardwood, has emerged as an important plantation tree for phytoremediation and bioenergy, and may serve as an alternative source for wood-based composites. The impacts of hotpressing on wood's viscoelastic properties, which are critical to mat consolidation, are not known. This study 1) explores the impact of wood moisture content, hotpressing temperature, and changes in wood's physical, chemical, and viscoelastic properties during hotpressing, and 2) determines the relationship between these changes. A correlation was found between stiffness, specific gravity, and cellulose crystallinity of hotpressed hybrid poplar evaluated in dry conditions. Under ethylene glycol-plasticized conditions, a relationship was found between solvent uptake, lignin thermal softening, and intermolecular coupling. This study has provided a better understanding of how moisture content and pressing temperature during

hotpressing can impact the physical, chemical, and viscoelastic properties of hybrid poplar wood. Results can be extended to breeding programs for the selection of amendable wood characteristics for composite manufacture.

TABLES OF CONTENTS

LIST OF TABLES

LIST OF FIGURES

CHAPTER 1 INTRODUCTION

1.1 Background of the Study

Hybrid poplar, a fast-growing hardwood, has emerged as an important plantation tree that offers environmental benefits with its potential use in phytoremediation (Yoon, et al., 2006) and as biomass for bioenergy (Tharakan, et al., 2003). Owing to its wide availability and low density, hybrid poplar wood has also been used for engineered wood composites such as oriented strandboard (OSB) (Kenney, et al., 1990). In addition, desirable wood quality traits can be tailored through breeding programs to meet the requirements of specific end-use products (Klasnja, et al., 2003). Therefore, hybrid poplar wood may be ideally suited and optimized for the manufacture of wood-based composites.

During hotpressing—the most critical processing step in the manufacture of wood-based composites—process temperature and pressure combine with the wood's initial properties and moisture content to create mat consolidation. In this process, changes in the chemical, anatomical, physical, and viscoelastic properties of wood influence the wood's propensity to densification and the final performance of composites (Wolcott, et al., 1990; Kamke and Wolcott, 1991). Changes in these properties are often intertwined. For example, heat treatment alters wood chemistry (Tjeerdsma, et al., 1998; Kotilatinen, et al., 1999; Yildiz, et al., 2005; Repellin & Guyonnet, 2005; Boonstra &Tjeerdsma, 2006) which in turn can influence its hygroscopicity (Kolin & Janezic, 1996; Tjeerdsma, et al., 1998; Navi & Girardet, 2000) and viscoelastic properties (Hamdan, 2000, Navi & Girardet, 2000; Jiang, et al., 2008). To date, few

studies have investigated how the chemical, physical, and viscoelastic properties of wood change during hotpressing.

The main hypothesis of this study is that during hotpressing, wood moisture content and hotpressing temperature synergistically alter the chemical, physical, and viscoelastic properties of wood. We also hypothesize that changes in chemical, physical, and viscoelastic properties of wood during hotpressing are interrelated. The two objectives of this research are to:

1) evaluate the effects of wood moisture content and hotpressing temperature and how they change wood's physical and viscoelastic properties during hotpressing; and
2) determine the relationship, if any, between changes in the chemical, physical, and viscoelastic properties of wood induced by hotpressing.

To address these goals, this thesis is organized in four chapters. Following the introduction chapter (Chapter 1), the basic structure and properties of wood are reviewed along with the known effects of heat, temperature and/or hotpressing on wood's chemical, physical, and viscoelastic properties in Chapter 2. Chapters 3 and 4 present the results of our investigation. Chapter 3 examines the effect of hotpressing conditions (wood moisture content and hotpressing temperature) on the physical and viscoelastic properties of dry wood. Properties of interest include wood's specific gravity, hygroscopic behavior, and dynamic mechanical properties in bending mode. Chapter 4 focuses on the effects of hotpressing conditions on the in situ softening of lignin through analyses of glass transition temperatures and intermolecular cooperativity associated with this transition. Chapter 5 then summarizes the major conclusions of this research.

Note that this research was performed with collaborators from the University of Idaho who specialize in the study of wood chemical properties. Therefore, while this project does not

extensively cover changes in wood's chemical properties, this thesis builds on results from these chemical studies to decipher possible relationships.

1.2 **Significance of the Study**

The study will provide comprehensive understanding of the changes in wood properties during hotpressing by linking, for the first time, aspects of wood chemistry, physics, and viscoelasticity. Results could improve the selection of processing parameters such as pressing temperature and initial moisture content to meet specific quality requirements of wood-based composites. Results can be extended to breeding programs for the selection of amenable wood characteristics for composites manufacture.

1.3 **References**

Boonstra, M.J., Rijsdijk, J.F, Sander, C., Kegel, E., Tjeerdsma, B., Militz, H., Van Acker, J., & Stevens, M. (2006). Microstructural and physical aspects of heat treated wood, Part 2: Hardwoods. Maderas. *Ciencia Y. Tecnologia, 8* (3), 209–217.

Hamdan, S., Dwianto, W., Morooka, T., & Norimoto, M. (2000). Softening characteristics of wet wood under quasi static loading. *Holzforschung, 54* (5), 557–560.

Jiang, J., Lu, J., & Yan, H. (2008). Dynamic viscoelastic properties of wood treated by three drying methods measured at high temperature range. *Wood and Fiber Science, 40* (1), 72–79.

Kamke, F.A., & Wolcott, M.P. (1991). Fundamentals of flakeboard manufacture: Wood-moisture relationships. *Wood Science and Technology, 25*, 57–71.

Kenney, W.A., Sennerbyforsse, L., & Layton, P. (1990). A review of biomass quality research relevant to the use of poplar and willow for energy-conversion. *Biomass, 21*, 163–188.

Klasnja, B., Kopitovic, S., & Orlovic, S. (2003). Variability of some wood properties of eastern cottonwood (*Populus deltoides* Bartr.) clones. *Wood Science and Technology, 37*, 331–337.

Kolin, B. & Janezic, T.S. (1996). The effect of temperature, density, and chemical composition upon the limit of hygroscopicity of wood. *Holzforschung, 50*, 263–268.

Kotilainen, R., Alen, R., & Arpiainen, V. (1999). Changes in the chemical composition of Norway spruce (*Picea abies*) at 160–260ºC under nitrogen and air atmospheres. *Paperi Ja Puu-Paper and Timber, 81* (5), 384–388.

Navi, P., & Girardet, F. (2000). Effects of thermo-hydro-mechanical treatment on the structure and properties of wood. *Holzforschung, 54,* 287–293.

Tharakan, P.J., Volk, T.A., Abrahamson, L.P., & White, E.H. (2003). Energy feedstock characteristics of willow and hybrid poplar clones at harvest age. *Biomass and Bioenergy, 25*, 571–580.

Tjeerdsma, B.F., Boonstra, M., Pizzi, A., Tekely, P., & Militz, H. (1998). Characterization of thermally modified wood: Molecular reasons for wood performance improvement. *Holz als Roh- und Werkstoff, 56*, 149–153.

Wolcott, M. P., Kamke, F. A., & Dillard, D. A. (1990). Fundamentals of flakeboard manufacture: Viscoelastic behavior of the wood components. *Wood and Fiber Science, 22* (4), 345.

Yildiz, U. C., Yildiz, S., & Gezer, E.D. (2005). Mechanical and chemical behavior of beech wood modified by heat. *Wood and Fiber Science, 37* (3), 456–461.

Yoon, J.M., Aken, B.V., & Schnoor, J.L. (2006). Leaching of contaminated leaves following uptake and phytoremediation of RDX, HMX, and TNT by poplar. *International Journal of Phytoremediation, 8*, 81–94.

CHAPTER 2 REVIEW OF LITERATURE

2.1 Introduction

This review first presents the anatomical and morphological features of hybrid poplar (HP) wood along with its chemical composition. Next, important and unique properties of the wood such as hygroscopicity, specific gravity, and porosity are described. Then, the findings of numerous researchers regarding the effects of heat and pressure on wood properties are presented, with particular attention to the effects of heat and pressure on wood structural, physical, chemical, and viscoelastic properties.

2.2 Wood Structure, Anatomy and Chemistry

This section discusses the structure of wood from both the macroscopic and microscopic standpoints, and reviews wood ultrastructure and chemical composition.

2.2.1 *Wood Macroscopic Characteristics*

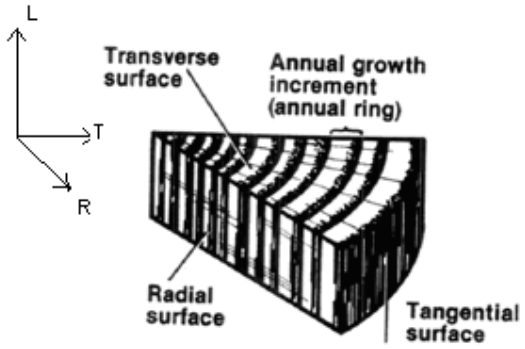

Figure 2.1 The three planes of wood cross-sections (Bowyer, et al., 2003)

Wood is not an isotropic material, but rather an orthotropic material defined by three directions or axes: longitudinal (L), radial (R) and tangential (T). As a result, wood contains three distinct surfaces: the transverse, radial, and tangential, which correspond to the direction of wood cells (Figure 2.1). The transverse surface corresponds to the direction RT, the radial surface corresponds to the direction LR, and the tangential surface corresponds to the direction LT. Wood properties thus depend on the directions and surfaces considered (Bowyer, et al., 2003). Inside a mature tree stem, two types of wood layers, the sapwood and the heartwood (Figure 2.2), can be observed on the cross-section or transverse surface.

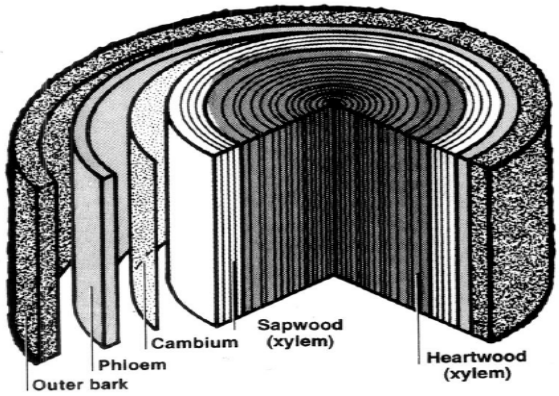

Figure 2.2 Macroscopic parts of tree stem (Bowyer, et al., 2003).

Sapwood is located next to the cambium and consists of living cells, while heartwood is located toward the center of the tree and consists of dead cells. The formation and composition of sapwood and heartwood in the tree trunk often determine the weight, permeability, or strength of the wood. The cambium, a thin layer between xylem and phloem, generates new living tissues (xylem and phloem). New cells produced by the cambium become new wood, and the outer part becomes bark (Bowyer, et al., 2003). Seasonal changes are responsible for the growth of distinct woody cells. Thin-walled wood cells are produced in the spring and constitute the less dense and

lightly colored earlywood, whereas thick-walled cells are produced during winter and constitute the denser and darker latewood. The combination of earlywood and latewood constitutes an annual growth increment or annual ring (Figure 2.1).

2.2.2 *Wood Microscopic Features*

On the microscopic level, wood structure can be seen as a massive construction of cells. Wood cells are porous and contain a cavity called the cell lumen that is surrounded by the cell wall. Cell lumens function as water transport and the diameters are on the order of microns. The wall thickness of the fiber or tracheids, the diameter of vessels, the amount of vessels and parenchyma cells together determine the density of woods (Fengel & Wegener, 1984). In hardwoods such as *Populus spec*., cells consist of fibers, vessel elements, and ray parenchyma in the following proportions: 61.8%, 26.9%, and 11.3%, respectively (Fengel & Wegener, 1984). Other hardwoods may also have longitudinal parenchyma cells which are thin walled and vertically oriented cells that function as food storage. A scanning electron micrograph of a hardwood shows the longitudinal elements, ray structure and pore distribution (Figure 2.3). As described by Fengel and Wegener (1984), the parenchyma cells of hardwoods are short and highly irregular, and cell walls are thick, with smaller lumens compared to softwoods. Vessel elements are approximately 50–100μm in diameter and surrounded by fiber cells (Tsoumis, 1991), for *Populus spec*. The vessel element is 20–150 μm in diameter and 500 mm in length (Fengel & Wegener, 1984). The tracheids/fibers have a length of 0.7–1.6 mm and diameter of 20–40μm. Vessels, fibers, and tracheids are aligned in a longitudinal direction, while ray cells (ray tracheids and ray parenchyma cells) are in horizontal alignment along the radial axis. Wood rays store carbohydrates and transport nutrients horizontally.

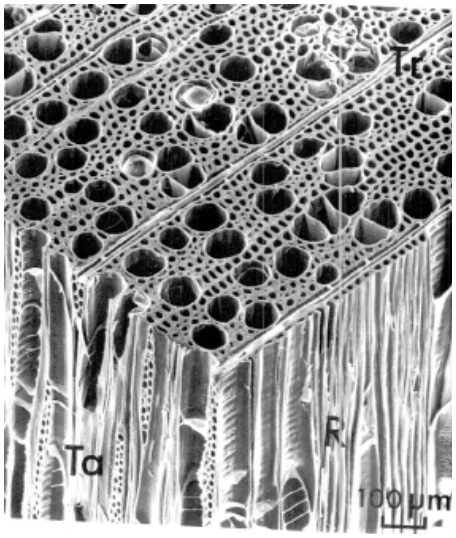

Figure 2.3 Scanning electron micrograph for yellow poplar (*Liriodendron tulipifera*) showing vessels in tranverse (Tr), tangential (Ta), and radial (R) surfaces (Siau 1995).

2.2.3 *Wood Ultrastructure*

The wood cell wall is organized with a thin primary wall and a thicker, multi-layered secondary wall around the cell lumen (Figure 2.4). Neighboring wood cells are bonded by the middle lamellae (Fengel & Wegener, 1984). In the cell wall, the smallest building blocks are the elementary fibrils, made up of approximately 40 cellulose chains and assembled into highly crystalline cellulose microfibrils. Cellulose microfibrils are 10–30 nm in diameter (Tsoumis, 1991) and can be randomly organized, as in the primary wall, or aligned to a particular angle, as in the S_1, S_2, and S_3 layers of the secondary wall. The primary cell wall is especially rich in pectin and lignin (Bowyer, et al., 2003). The middle lamellae are also rich in lignin, while the secondary cell wall layers have a higher concentration of cellulose. Within the cell wall, cellulose fibers are bonded together by a lignin matrix, thanks to the compatibilizing action of hemicelluloses. These polymers, cellulose, lignin, and hemicellulose, are the three major components of wood, and are reviewed in the next section.

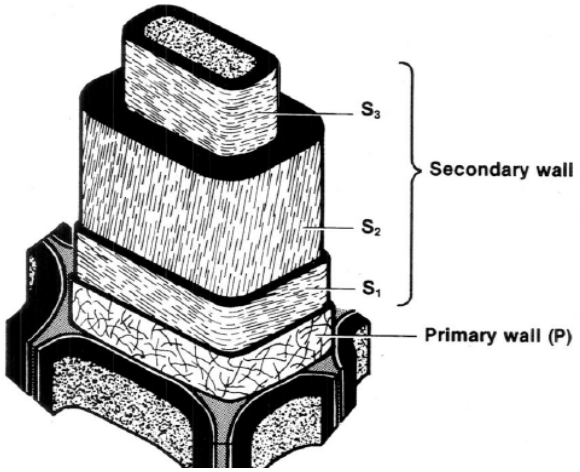

Figure 2.4 Schematic of wood cell wall structure (Bowyer, et al., 2003).

2.3 **Wood Chemistry**

Wood is comprised of three main structural polymers: cellulose, hemicelluloses, and lignin, in addition to low molecular weight compounds called extractives (Figure 2.5). Hardwoods, such as poplars, are comprised of 40–45% cellulose, 15–35% hemicelluloses, 17–25% lignin, as well as extractives and ash in small percentages (Tsoumis, 1991). In the cell wall, hemicelluloses interact with both the lignin network and cellulose chains. Hemicelluloses link to cellulose microfibrils though hydrogen bonding and with lignin through covalent bonding (Figure 2.6). Hemicelluloses act as compatibilizers between the highly ordered cellulose structure and amorphous lignin.

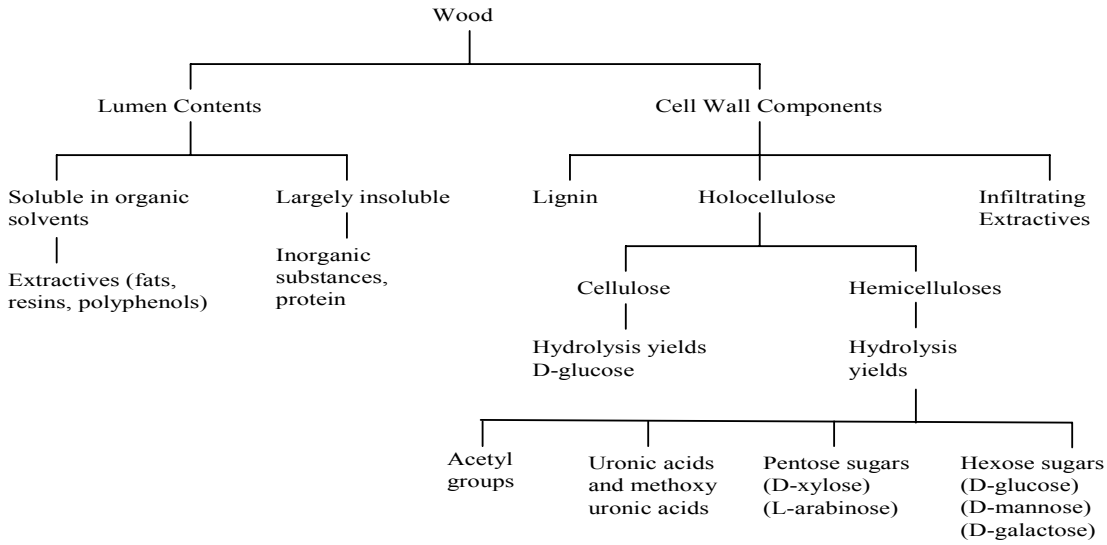

Figure 2.5 Chemical composition of wood (Hillis, 1975).

Many researchers have studied the chemical composition of poplar woods. Blakenhorn, et al. (1985a) reported the α-cellulose and hollocellulose contents of seven hybrid poplars; these contents ranged from 38.2% to 45.5% for α-cellulose and 64.3% to 80.2% for hollocellulose. In yellow poplar (*Lirodendron tulipifera*), cellulose and hemicellulose constitute approximately 47.6% and 34.1% of dry wood mass, respectively (Gardner, et al., 1993). Tuskan, et al. (1999) reported that hemicelluloses in hybrid poplar wood are comprised of 2.7% mannans, 0.5% arabinans, and 17% xylans. Xylans are therefore the predominant type of hemicelluloses in hybrid poplars.

Hemicelluloses play an important role in maintaining cohesion between the wood polymers within the cell wall, since cellulose has no affinity toward lignin and vice versa (Bowyer, et al., 2003). Due to their large number of hydroxyl groups, cellulose and hemicelluloses are highly hydrophilic and largely responsible for wood's high affinity for water

and its hygroscopicity. In contrast, lignin is a rather hydrophobic polymer with a lower affinity for water.

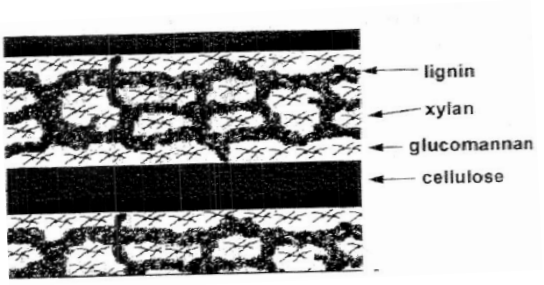

Figure 2.6 Interaction of Wood Polymers at the Molecular Level (Salmen& Olsson, 1998).

2.3.1 *Cellulose*

Cellulose is a linear chain of glucose units that are covalently linked through β-1-4-linkages, with cellobiose as the repeat unit (Figure 2.7) (Fengel and Wegener, 1984). Cellulose chains link linearly with strong intramolecular forces and dipolar interactions in the form of hydrogen bonds, and therefore form crystalline structures called cellulose microfibrils (Tsoumis, 1991).

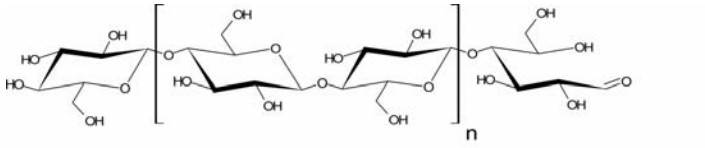

Figure 2.7 Repeating Unit (Cellobiose) of Cellulose (Fengel & Wegener, 1984).

Native cellulose, called Cellulose I, is semicrystalline in nature, and its structure can be modified when it is treated with alkali solution with or without carbon disulfide (Pettersen, 1984). This crystalline cellulose is comprised of many layers of parallel chains held by weak van der Waals's forces and intramolecular hydrogen bonds (Figure 2.8). There are also

intramolecular hydrogen bonds between the atoms of adjacent glucose molecules (Figure 2.9). Based on the orientation of the hydroxyl group, cellulose I has two distinct crystalline allomorphs, I_α and I_β. The I_β allomorph has a more stable conformation. Alkali treatment generates cellulose II, a more stable crystalline allomorph of cellulose, where chains are packed in an antiparallel fashion (Pettersen, 1984).

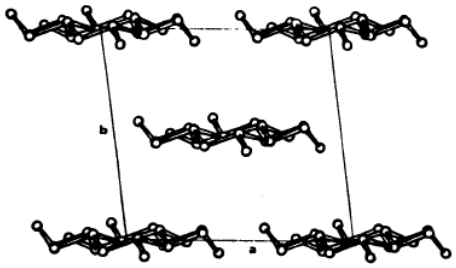

Figure 2.8 Axial projection of Cellulose I (Gardner & Blackwell, 1974).

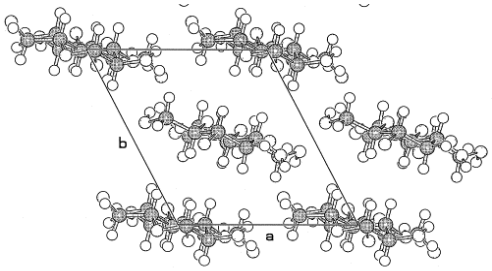

Figure 2.9 Axial projection of Cellulose II (Zugenmaier, 2001).

In hardwoods, the degree of cellulose crystallinity has been measured at around 54% (Newman & Hemmingson, 1990). The extraction of cellulose in pure form from wood is rather difficult because cellulose is insoluble in many solvents and also because of the strong interactions with other wood polymers, lignin, and hemicelluloses. As a major constituent, cellulose is a reinforcing material in the cell wall that contributes greatly to the stiffness and mechanical strength of wood (Bowyer, et al., 2003).

2.3.2 *Hemicelluloses*

Hemicelluloses are branched heteropolysaccharides based on various sugar nucleotides including glucose, mannose, galactose, xylose, arabinose, 4-O-methyl glucuronic acid, and galacturonic acid (Pettersen, 1984). Due to their heterogeneous compositions and branched structure, hemicelluloses are amorphous polymers. The xylose unit is more abundant in hardwoods (Pettersen, 1984) and in fast-growing wood species (Fengel & Wegener, 1984) such as hybrid poplars. Xylose is the building block for hemicellulose xylans. Hardwoods contain 15–30% glucoronoxylans (Figure 2.10) and 2–5% glucomannans (Figure 2.11) (Pettersen, 1984). Glucoronoxylans, the most abundant type of hemicelluloses in hardwoods, are branched and highly acetylated. Hemicelluloses are soluble in alkali and easily hydrolyzed in acids.

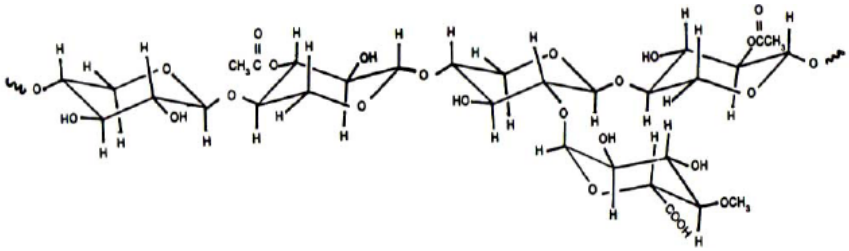

Figure 2.10 Partial chemical structure of glucoronoxylans (Pettersen, 1984).

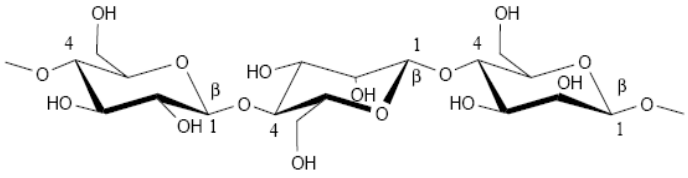

Figure 2.11 Partial chemical structure of glucomanans (Laine, 2005).

2.3.3 *Lignin*

Compared to cellulose and hemicelluloses, lignin has a more complex structure and higher molecular weight. Lignin is an amorphous polymer based on phenyl propane units.

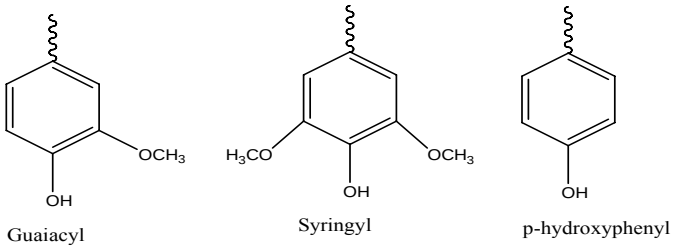

Figure 2.12 Lignin units.

The building blocks of lignin are the p-hydroxyphenyl, syringyl, and guaiacyl units (see Figure 2.12). Hardwood lignin is mostly composed of guaiacyl and syringyl units, and therefore has a high content of methoxylation (Fengel & Wegener, 1984). As a result, hardwood lignins (Figure 2.13) are believed to be less condensed than softwood lignins. It is difficult to know exactly the structure of lignin, since lignin is reactive and contains many functional groups. Some lignin units are soluble in water, while others may be soluble in acids or bases. Isolation techniques change the native structure of lignin (Fengel &Wegener, 1984). The average lignin content of hybrid poplar clones (*maximowiczii x Berolinenses, 'Angulata' x trichocarpa,* and *maximowiczii x trichocarpa*) is19% (Blakenhorn, et al., 1985b).

Lignin, principally located in the compound middle lamellae, binds with hemicelluloses covalently (Bowyer, et al., 2003), providing rigidity to the cells and improving dimensional stability, due to its relative hydrophobicity compared to that of polysaccharides. As a result, the lignified cell wall shrinks less, compared to the non-lignified one (Siau, 1995). Lignin occupies

the spaces in the cell wall which could otherwise fill with water. Removal of lignin results in discoloration and structural degradation (Bowyer, et al., 2003).

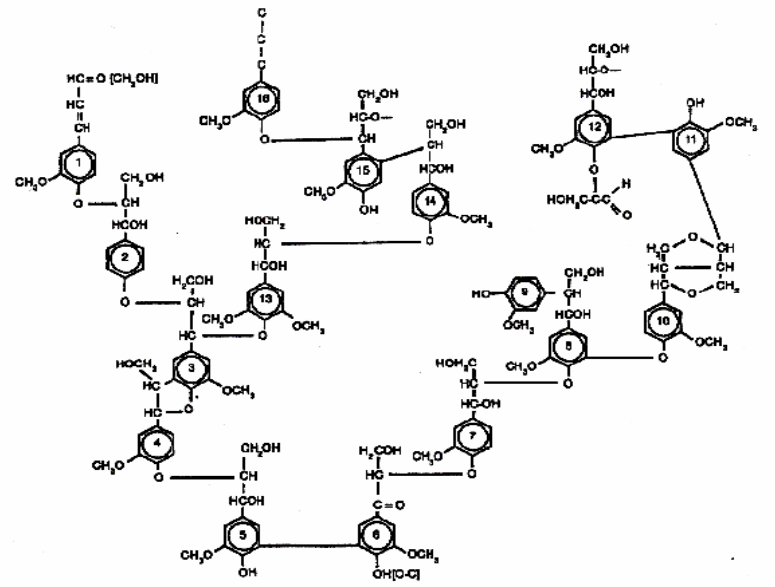

Figure 2.13 Partial chemical structure of lignin (Pettersen, 1984).

2.3.4 *Extractives*

Wood also contains a diverse collection of low-molecular-weight organic compounds called extractives. Extractives are deposited in the cell wall and can be isolated by solvent extraction (Tsoumis, 1991). These organic substances include gums, fats, resins, sugars, oils, starches, and tannins, and vary by species, from less than 1% in some poplars to approximately 10% in redwood based on oven-dry wood weight (Tsoumis, 1991). In hybrid poplar clones, Blakenhorn, et al. (1985b) reported an average 9.9% extractives content. Gardner, et al. (1993) reported 2.4% extractives in yellow poplar, while White (1987) noted 3.8% extractive content in the same species.

Extractives affect wood color, odor, decay resistance, density, flammability, and moisture absorption (Siau, 1995). Wood with less extractives can hold more water in the cell walls, and therefore extractives influence dimensional stability, shrinkage, and solvent uptake.

2.4 **Physical and Viscoelastic Properties of Wood**

2.4.1 *Wood Hygroscopicity*

Wood is highly hygroscopic and readily absorbs water. The hygroscopicity of wood is the manifestation of hydroxyl (OH) groups of cellulose and hemicelluloses (Siau, 1995). There are two kinds of water in wood: free and bound. Free water is freely flowing in the cell lumens, while bound water is trapped inside the cell walls through hydrogen bonding (Siau, 1995). Bound water is tightly held to the wood structure by surface adsorption forces (Bowyer, et al., 2003). The fiber saturation point (FSP) occurs when the cell wall is fully saturated, but there is no free water in the cell lumens, and ranges from 27% to 31% (Siau, 1995). FSP plays a significant role in the influence of water on the physical and mechanical properties of wood: at moisture contents above FSP, wood properties do not change, but below FSP, they change according to moisture content. The shrinking and solvent uptake of wood is anisotropic, since it depends on grain orientation.

2.4.2 *Wood specific gravity*

The specific gravity of wood is calculated by dividing oven-dry mass by the specimen's volume (length × width × thickness). Specific gravity is one of the important factors in wood performance evaluation (e.g., mechanical properties). In fact, wood's mechanical properties are directly related to density. Higher density results in higher mechanical properties (Tsoumis,

1991). Therefore, it is common for researchers to normalize wood properties by specific gravity and obtain a specific property that is independent of density. Thakaran, et al. (2003) investigated seven hybrid poplar clones and found that specific gravity ranged from 0.33 to 0.37, while Tsoumis (1991) found that specific gravity varies within each tree.

2.4.3 *Viscoelastic properties of wood polymers*

Because moisture and other plasticizers clearly affect the viscoelastic properties of wood, these properties have been traditionally measured under dry conditions or saturated conditions (Sadoh, 1981; Salmen, 1984; Kelley, et al., 1987; Olson & Salmen, 1997; Laborie, et al., 2004). Water is often used as the plasticizer, although other solvents, such as formamide or ethylene glycol, have been used. The technique of choice in these studies is dynamic mechanical analysis, which provides information about the elastic and viscous component of wood response via the storage modulus (E') and the loss modulus (E'') or the loss factor (tan δ=E''/E').

2.4.3.a Viscoelastic properties of dry wood

Many researchers have investigated the viscoelastic behavior of wood constituents (Hilis & Rozsa, 1978; Irvine, 1984), wood itself (Hamdan, et al., 2000; Backman & Lindberg, 2001; Lenth & Kamke, 2001) and chemically treated woods (Sadoh, 1981; Obataya, et al., 2000; Sugiyama, et al., 1998). Since isolation or extraction of wood polymers alters their structure, the in situ viscoelastic properties of wood also differ from the viscoelastic properties of isolated wood polymers.

Under dry conditions, the glass transition temperature (T_g) for cellulose, hemicelluloses, and lignin all lie in the range of 200–250ºC (Back & Salmen, 1982), which is above the

temperature range for thermal degradation. In dry wood, the ultrastructure and close interactions between wood polymers prevent researchers from making a specific assignment to a wood constituent, since only a gradual softening or decrease in modulus with increasing temperature can be observed. Indeed, in a typical dynamic mechanical analysis thermogram, clear glass transition temperature cannot be observed or assigned to a specific wood polymer.

The thermogram below (Figure 2-14) illustrates the gradual softening or decrease in storage modulus (E') and subambient relaxations in the loss factor (tan delta). As moisture content increased, the wood softened and the drop in E' became more pronounced. Obataya, et al (1998) used dynamic mechanical properties measurement under a dry nitrogen atmosphere, and noted two distinct low temperature relaxations at -100ºC and -40ºC (Figure 2.14). They identified the peak at around -100ºC for dry wood, and ascribed this to the relaxation motion of methylol groups, while the other peak at -40ºC was ascribed to relaxation motion due to adsorbed water. Obataya, et al. (1998) also found that in completely dry wood, there are many open sites and sparsely occurring intermolecular interactions. However, at higher adsorbed water content, molecules are aligned to fill the space to accommodate hydrogen bonds. In another study, Obataya, et al. (2000) investigated the mechanical relaxation process of untreated and chemically treated wood samples at low temperatures of -150 to 20ºC. They found a relaxation peak at around -53 to -33ºC for wood with adsorbed water. This peak was due to adsorbed water molecules.

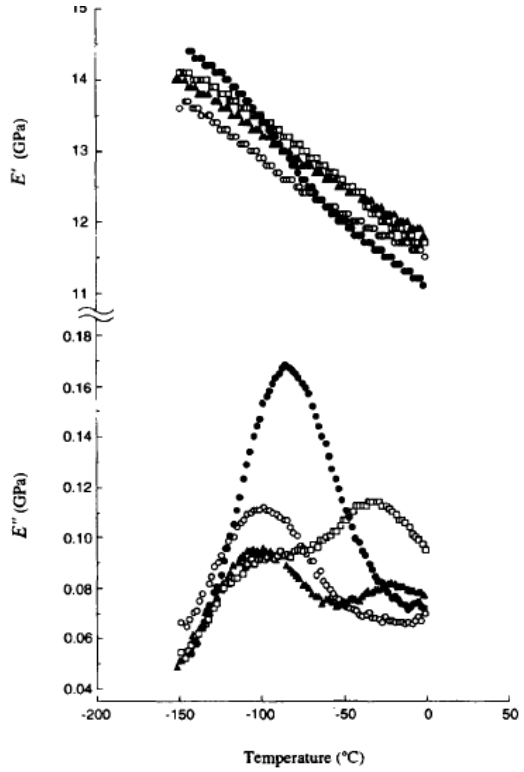

(○) absolutely dry, (▲) 0.5% moisture content (M), (□) 0.7% M, (●) 3.2% M

Figure 2.14 DMA thermogram for dry spruce wood and a trace of adsorbed water (Obataya, et al., 1998).

Sun, et al. (2007) observed that moisture in wood, even at less than 1%, affects wood chemistry, especially in low-temperature secondary relaxations. They also demonstrated that the dynamic mechanical response of wood was not altered when samples were isothermally treated for 30 minutes to 80ºC, but change did occur at 150ºC with desiccation.

2.4.3.b Viscoelastic properties of saturated wood

Moisture content and temperature play a significant role in dictating the viscoelastic behavior of wood polymers (Irvine, 1984; Obataya, et al., 1998). Moisture content can drastically

change the glass transition temperature (T_g) of lignin and hemicelluloses (Irvine, 1984; Salmen, 1984; Kelley, et al., 1987). The depression of the glass transition with moisture is due to its plasticizing effect, which allows easier chain movements. Using differential thermal analysis (DTA), Irvine (1984) reported that in water-saturated conditions, thermal softening ranged from 60–90ºC. This was ascribed to lignin glass transition (T_g), since, under wet conditions, the isolated cellulose and hemicellulose have a T_g close to 0ºC (Salmen & Back, 1977; Irvin, 1984).

Other significant studies have shown that water-saturated wood exhibits a clear softening at around 60–90°C due to lignin's glass transition, and that under these conditions, the time-temperature superposition and the Williams-Landel-Ferry (WLF) equation hold true (Salmen, 1984, Kelley, et al., 1987). Further work by Laborie, et al. (2004) showed that cooperativity analysis, which quantifies the extent of intermolecular coupling associated with alpha-relaxation, could also be applied to lignin's in situ transition. Since the T_g of lignin under plasticized conditions is detected at experimental temperatures, it has been used widely to understand the relaxation mechanism. For example, in situ T_g lignin of yellow poplar evaluated at 2Hz was reported to be 71ºC (Laborie et. al, 2004).

Sadoh (1981) reported that the torsion modulus for wood was reduced under wet condition, regardless of solvent uptake agents. The mechanical damping showed different levels of broadness, indicating different levels of solvent uptake agent distribution. The sharp mechanical damping peak corresponded to the homogeneity of wood and its solvent uptake agent, which had become composites. On the other hand, the broad mechanical damping peak demonstrated the heterogeneity of the solvent uptake agent. In Sadoh's study, wood swelled with high molecular weight, which polyethylene glycol (PEG) showed a broader mechanical damping peak compared to wood swelled with water and wood swelled with ethylene glycol (EG).

2.5 **Effects of Hotpressing on Wood Properties**

Hotpressing is a method used in the manufacturing of oriented strand board (OSB) where the wood strand is subjected to elevated temperature under compression. Wood hotpressing modifies the macroscopic structure, ultrastructure, and chemistry of wood. The physical, viscoelastic, and mechanical properties of wood are consequently altered by hotpressing. Many studies have examined the effect of hotpressing on wood's structure and properties, and these studies are summarized below.

2.5.1 *Effect of hotpressing on wood chemistry*

Many researchers have reported that heat treatment of wood, with or without compression, alters many wood properties (Hillis, 1984; Tjeerdsma, et al., 1998; Hakkou, et al., 2005; Repellin & Guyonnet, 2005, Boonstra &Tjeerdsma, 2006; Korkut & Guller, 2008; Kolin & Janezic, 1996; Tabarsa & Chui, 1997; Yildiz, et al., 2005).

It is now well established that the chemistry of wood polymers is significantly altered during hotpressing. Hsu, et al. (1988) reported that high pressure steam pretreatment caused partial hydrolysis of hemicelluloses for both softwoods and hardwoods, resulting in increased wood compressibility. After wood was steamed at 200ºC for 1 to 4 minutes, hemicelluloses hydrolyzed into low molecular weight compounds, while lignin and cellulose did not seem to decompose (Hsu, et al., 1988). Under such conditions, hemicelluloses and lignin were significantly removed from the wood (Ito, et al., 1998).

Dwianto, et al. (1999) also observed hemicellulose degradation, in addition to lignin cleavage. Prolonged application of heat induced lignin cross-linking, combined with condensation reactions between free phenolic units and hemicelluloses degradation products

(such as furfural compounds and acetic acid) created a more rigid structure around cellulose microfibrils (Tjeerdsma, et al., 1998). Condensation reactions and thus reduction in free hydroxyl groups restricted the extent of hydrogen bonding between water and cellulose microfibrils or cellulose chains, and hindered the penetration of water molecules in the cell wall (Tjeerdsma, et al., 1998).

Heat treatment was also found to enhance wood polymers' mobility and alter their morphology. For example, Gardner, et al. (1993) observed an increase in cellulose crystallinity with hotpressing temperature when using ^{13}C CP/MAS NMR. Additional work suggests that the observed increase in relative crystallinity results from a substantial increase in cellulose crystalline fraction and not from a loss of amorphous components (Ito, et al., 1998).

2.5.2 *Effect of hotpressing on wood's physical and viscoelastic properties*

The high temperature and pressure applied to wood during hot pressing changes its physical properties, such as density and hygroscopicity. For example, Tjeerdsma, et al. (1998) and Navi & Girardet (2000) found that heat treatment and hotpressing of wood reduces its hygroscopicity. This is linked to the chemical changes induced by hotpressing, particularly the deacetylation of hemicelluloses and the reduction of hydroxyl groups (Hilis, 1984). As a result, heat treatment also decreases the FSP (Repellin & Guyonnet, 2005).

Interestingly, when wood is hotpressed under steam (thermo-hydro mechanical treatment, THM) it adsorbed less water compared to wood compressed without steam (thermo-mechanical, TM). Navi & Girardet (2000) concluded that both THM and TM reduced the hygroscopicity of wood, and that THM produced wood with less hygroscopicity. Thus, steam during hotpressing enhanced dimensional stability.

Kutnar, et al. (2008) found that the densification process altered surface characteristics of treated wood. When compression was applied to viscoelastic thermal compressed wood (VTC) in a softened state, changes in surface chemistry, wettability, and surface free energy occurred. In that study, the VTC process caused hydrophobicity to increase and total surface energy to drop significantly for samples heated above 200ºC, while chemical changes were insignificant. The trend increased with the degree of densification. The breaking of intermolecular and intramolecular chemical bonds intensifies as temperature increases, starting at temperatures above 100°C, and compressive strength decreases due to the depolymerization of hemicelluloses (Yildiz, et al., 2005). At 200°C and 6 hours of heating, the effect was 7 times more than heating at 180°C for the same amount of time. As discussed above, the combination of heat and pressure treatment on wood, with or without steam, introduced cell wall fractures and decreased lumens. Dense wood has less total porosity and hygroscopicity since access of water to the hydroxyl groups in cellulose microfibrils is limited (Kolin & Janezic, 1996). In addition, the increase in microfibrils' regularity promoted more crystalline formations within the cell wall.

When the wood was compressed in the presence of moisture, cell walls already softened by the combination of water and high temperature experienced greater deformation. This caused the lumens to close completely and irreversibly. Navi and Girardet (2000) found that TM-treated wood exhibited fewer cell wall fractures compared to the THM-treated wood (see Figure 2.15). Densification of wood intensifies at higher pressing temperature and compression level (Tabarsa & Chui, 1997) because the degree of fracture is higher at higher pressing temperature and compression levels.

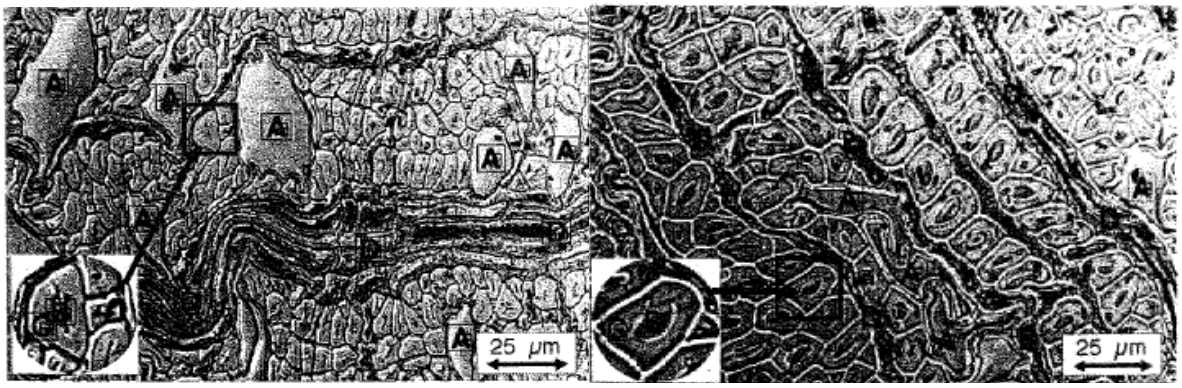

Figure 2.15 Micrograph of Beech Densified Wood by THM (left) and TM (right), where A=vessels, B=lumen, C=cell wall, and D=rays (Navi &Girardet, 2000).

2.6 **References**

Back, E.L., & Salmen, N.L. (1982). Glass transitions of wood components hold implications for molding and pulping processes. *Tappi Journal, 65*(7), 107–110.

Backman, A.C, & Linberg, K.A. (2001). Differences in wood material responses for radial and tangential direction as measured by dynamic mechanical thermal analysis. *Journal of Material Science, 36,* 3777–3783.

Blakenhorn, P.R., Bowersox, T.W., Kuklewski, K.M., Stimely, G.L., & Murphey, W.K. (1985a). Comparison of selected fuel and chemical content values for seven *Populus* hybrid clones. *Wood and Fiber Science, 17*(2), 148–158.

Boonstra, M.J., Rijsdijk, J.F, Sander, C., Kegel, E., Tjeerdsma, B., Militz, H., Van Acker, J., & Stevens, M. (2006). Microstructural and physical aspects of heat treated wood. Part 2. Hardwoods. Maderas. *Ciencia Y. Tecnologia, 8* (3), 209–217.

Bowyer, J.L., Shmulsky, R., & Haygreen, J.G. (2003). Forest products and wood science: An introduction (4th ed.). Ames: Blackwell Publishing.

Dwianto, W., Morooka, T., Norimoto, M., & Kitajima, T. (1999). Stress relaxation of sugi (*Cryptomeria japonica* D. Don) wood in radial compression under high temperature steam. *Holzforschung, 53*, 541–546.

Dwianto, W., Tanaka, F., Inoue, M., & Norimoto, M. (1996). Crystallinity changes of wood by heat or steam treatment. *Wood Research, 83*, 47–48.

Dwianto, W., Morooka, T., & Norimoto, M. (1998). The compressive stress relaxation of albizia (*Paaraserienthes falcate* Becker) wood during heat treatment. *Mokuzai Gakkaishi, 44* (6), 403–409.

Fengel, D., & Wegener, G. (1984). Wood: Chemistry, ultrastructure, and reactions. New York: Walter de Gruyter.

Ferry J.D. (1980). Viscoelastic properties of polymers (2nd ed.). New York: John Wiley and Sons.

Gardner, D.J., Gunnells, D.W., Wolcott, M.P., & Amos, L. (1993). Changes in wood polymers during the pressing of wood-composites. In J. F. Kennedy, G. O. Phillips and P. A. Williams (eds.), *Cellulosics, Chemical, Biochemical and Material Aspects* (pp. 513–518). New York: Ellis Horwood.

Gardner, K.H., & Blackwell, J. (1974). The hydrogen bonding in native cellulose. *Biochimica Biophysica Acta, 343*, 232–237.

Hamdan, S., Dwianto, W., Morooka, T., & Norimoto, M. (2000). Softening characteristics of wet wood under quasi static loading. *Holzforschung, 54*(5), 557–560.

Hilis, W.E. (1984). High temperature and chemical effects on wood stability. *Wood Science and Technology, 18*, 281–293.

Hilis, W.E., & Rozsa, A.N. (1978). The softening temperatures of wood. *Holzforschung, 32*, H.2, 68–73.

Hillis, W.E. (1975). Ethylene and extraneous material formation in woody tissues. *Phytochem. 13*(25), 2559–2562.

Hsu, W.E., Schwald, W., Schwald, J., & Shields, J.A. (1988). Chemical and physical changes required for producing dimensionally stable wood-based composites. Part I: Steam pretreatment. *Wood Science and Technology, 22*, 281–289.

Inoue, M., Morooka, T., Norimoto, M., Rowell, R.M., & Egawa, G. (1992). Permanent fixation of compressive deformation of wood (II) mechanisms of permanent fixation. *FRI Bull N. Z., 176*, 181–189.

Inoue, M., Norimoto, M., Tanahashi, M., & Rowell, R.M. (1993). Steam or heat fixation of compressed wood. *Wood and Fiber Science, 25*, 224–235.

Irvine, G.M. (1984). The glass transition of lignin and hemicellulose and their measurement by differential thermal analysis. *Tappi Journal, 67* (5), 118.

Ito, Y., Tanahashi, M., Shigematsu, M., & Shinoda, Y. (1998). Compressive molding of wood by high pressure steam treatment: Part 2: Mechanism of permanent fixation. *Holzforschung, 52*, 217–221.

Jiang, J., Lu, J., Yan, H. (2008). Dynamic viscoelastic properties of wood treated by three drying methods measured at high temperature range. *Wood and Fiber Science, 40* (1), 72–79.

Kelley, S.S., Rials, T.G., & Glasser, W.G. (1987). Relaxation behaviour of the amorphous components of wood. *Journal of Materials Science, 22*, 617–624.

Kolin, B., & Janezic, T.S. (1996). The effect of temperature, density, and chemical composition upon the limit of hygroscopicity of wood. *Holzforschung, 50*, 263–268.

Korkut, S., Akgul, M., & Dundar, T. (2008). The effects of heat treatment on some technological properties of Scots pine (*Pinus sylvestris* L.) wood. *Bioresource Technology, 99*, 1861–1868.

Kotilainen, R., Alen, R., & Arpiainen, V. (1999). Changes in the chemical composition of Norway spruce (*Picea abies*) at 160–260ºC under nitrogen and air atmospheres. *Paperi Ja Puu-Paper and Timber, 81*(5), 384–388.

Laborie, M.P.G., Salmen, L., & Frazier, C.E. (2004). Cooperativity analysis of the in situ lignin glass transition. *Holzforschung, 58,* 129–133.

Laine, C. (2005). Structures of hemicelluloses and pectins in wood and pulp. (Doctoral Dissertation, Helsinki University of Technology, Espoo, Finland).

Menard, K.P. (1999). Dynamic mechanical analysis: A practical introduction. Boca Raton, FL: CRC Press LLC.

Navi, P., & Girardet, F. (2000). Effects of thermo-hydro-mechanical treatment on the structure and properties of wood. *Holzforschung, 54*, 287–293.

Newman, R.H., & Hemmingson, J.A. (1990). Determination of the degree of cellulose crystallinity in wood by carbon-13 nuclear magnetic resonance spectroscopy. *Holzforschung, 44* (5), 351–355.

Obataya, E., Norimoto, M., & Tomita, B. (2000). Mechanical relaxation processes of wood in the low temperature range. *Journal of Applied Polymer Science, 81*, 3338–3347.

Obataya, E., Norimoto, M., & Gril, J. (1998). The effects of adsorbed water on dynamic mechanical properties of wood. *Polymer, 39*(14), 3059–3064.

Olsson, A.M., & Salmen, L. (1997). Humidity and temperature affecting hemicellulose softening in wood. Proc. Int. Conf. of COST Action E8, June 16–17, Copenhagen, 269.

Olsson, A.M., & Salmen, L. (1992). Chapter 9: Viscoelasticity of in situ lignin as affected by structure: Softwood vs. hardwood. *Journal of the American Chemical Society (489)*, 133–143.

Petterson, R.C. (1984). The chemical composition of wood. *in* Rowell, R. M. (ed.), The chemistry of solid wood. Advances in chemistry series 207. Washington, D.C.: American Chemical Society.

Repellin, V., & Guyonnet, R. (2005). Evaluation of a heat-treated wood solvent uptake by differential scanning calorimetry in relation to chemical composition. *Holzforschung, 59,* 28–34.

Sadoh, T. (1981). Viscoelastic properties of wood in solvent uptake systems. *Wood Science and Technology. 15*(1), 57–66.

Salmen, L. (1984). Viscoelastic properties of in situ lignin under water saturated conditions. *Journal of Material Science, 19* (9), 3090.

Salmen, L. (1986). Directional viscoelastic properties of wood, progress and trends in rheology II. Proceedings of the Second Conference of European Rheologists, Prague June 17–20, 234–235.

Salmen, N.L., & Back, E.L. (1977). The influence of water on the glass transition temperature of cellulose, *Tappi, 60* (12), 137.

Salmen, L., & Olsson, A.M. (1998). Interaction between hemicelluloses, lignin and cellulose: structure–property relationships. *Journal of Pulp and Paper Science, 24*, 99–103.

Siau, J.F. (1995). Elementary wood structure. In Wood: Influence of moisture on physical properties. Virginia Polytechnic Institute and State University Publishing, VA.

Stamm (1964). Wood and cellulose science. New York: Ronald Press.

Sun, N., Das, S., & Frazier, C.E. (2007). Dynamic mechanical analysis of dry wood: Linear viscoelastic response region and effects of minor moisture changes. *Holforschung, 66*, 28–33.

Tabarsa, T., & Chui, Y. (1997). Effect of hot-pressing on properties of white spruce. *Forest Products Journal, 47*(5), 71–76.

Tharakan, P.J., Volk, T.A., Abrahamson, L.P., & White, E.H. (2003). Energy feedstock characteristics of willow and hybrid poplar clones at harvest age. *Biomass and Bioenergy, 25*, 571–580.

Tjeerdsma, B.F., Boonstra, M., Pizzi, A., Tekely, P., & Militz, H. (1998). Characterization of thermally modified wood: molecular reasons for wood performance improvement. *Holz als Roh- und Werkstoff, 56*, 149–153.

Tsoumis, G. (1991). Science and technology of wood: Structure, properties, utilization. New York: Van Nostrand Reinhold.

Tuskan, G.A., West, D.C., Davis, M., & Bradshaw, H.D. (1999). Proceedings of the 2nd International Poplar Symposium, INRA, Orleans, France, Sept. 13–17, 93.

White, R.H. (1987). Effect of lignin content on extractives on the higher heating value of wood. *Wood and Fiber Science, 19* (4), 446–452.

Wolcott, M.P., Kamke, F.A., & Dillard, D.A. (1990). Fundamentals of flakeboard manufacture: Viscoelastic behavior of wood components. *Wood and Fiber Science, 22* (4), 345–361.

Yildiz, U. C., Yildiz S., & Gezer, E.D. (2005). Mechanical and chemical behavior of beech wood modified by heat. *Wood and Fiber Science, 37*(3), 456–461.

Zugenmaier, P. (2001). Conformation and packing of various crystalline cellulose fibers. *Progress in Polymer Science, 26 (*9),1341–1417.

CHAPTER 3 PHYSICAL AND VISCOELASTIC PROPERTIES OF HOTPRESSED HYBRID POPLAR IN THE DRY STATE

3.1 Introduction

Heat treatment has long been used by the wood industry to improve wood properties such as dimensional stability, density, and fungal resistance. It is well established that subjecting wood to high temperatures alters its chemistry, as first evidenced by its weight loss (Kotilainen, et al., 1999; Reinprecht, et al., 1999; Hakkou, et al., 2005a; Yildiz, et al., 2005; Repellin & Guyonnet, 2005; Boonstra & Tjeerdsma, 2006). Mass losses in poplar and beech heated for 8 hours increase at treatment temperatures above 200ºC (Hakkou, et al., 2005a). Kotilainen, et al. (1999) investigated the changes in the chemical composition of Norway spruce and reported that mass loss was highly dependent on treatment temperature, with significant degradation above 220ºC. Kotilainen, et al. (1999) found that hemicellulose, the least stable wood polymer compared to lignin and cellulose, degraded first and contributed to most of the mass loss. Hemicelluloses decompose at heating temperatures above 200ºC (Tjeerdsma, et al., 1998; Kotilainen, et al., 2001), and the galactoglucomannans and arabinoglucoronoxylans are the most heat-sensitive heteropolysaccharides (Kotilainen, et al., 1999). Navi & Heger (2004) found that in steamed, hot-pressed wood treated at 180ºC and 200ºC, hemicelluloses such as arabinose, galactose, mannose, and xylose began to decompose. Acetic acid, furfural, and formaldehyde form upon decomposition of such hemicelluloses (Tjeerdsma, et al., 1998).

Thermal treatment affects lignin and cellulose as well. Reduction of lignin molecular weight was induced by lignin depolymerization that occurs at elevated temperature. Tjeerdsma,,

et al. (1998) hypothesized that heat enhanced the demethoxylation of guaiacyl and syringyl units in lignin, thereby increasing the amount of reactive hydroxyl lignin sites available for reaction. They also found that the cross-linking of free phenolic units to furfural compounds and acetic acid created a more rigid structure around cellulose microfibrils and hindered water molecules' penetration of the cell wall. This mechanism maybe responsible for the improvement in dimensional stability of heat-treated wood. Ito, et al. (1998) postulated that semicrystalline cellulose was disturbed and damaged during compressive deformation, and thus released the inner stress within cellulose microfibrils. Under moist conditions, the water becomes steam, which facilitates the rearrangement of the cellulose chains, and forms additional crystalline regions (Ito, et al., 1998; Bhuyian, et al. 2000). An intense interaction between glucomannan and cellulose was reported (Salmen & Olsson, 1988) and the decomposition of glucomannan led to an increase of a more orderly carbohydrate backbone. In addition, conformational changes in polysaccharides due to the desorption of water (Hakkou, et al., 2005b) and the possibility of crystallization of quasicrystalline amorphous regions were postulated to increase the cellulose crystallinity (Akgul, et al., 2007). As a result, heat-treated wood exhibits improved dimensional stability and decreased hygroscopicity. For example, Tjeerdsma, et al. (1998) found that extreme thermal treatments enhanced wood's dimensional stability by decreasing the equilibrium moisture content (EMC). In wood conditioned at 96% relative humidity (RH), moisture content decreased from 30% to roughly 10%, while the wood exhibited only a minor decrease in strength. However, depending on conditions, heat treatment of wood can increase or decrease mechanical properties. In general, heat treatment increases stiffness but reduces strength. Korkut, et al. (2008) demonstrated that compression strength, bending strength, modulus of elasticity,

and other mechanical properties were reduced by heat treatment. However, at a processing temperature of 120ºC and 2 hours, these properties were not significantly affected.

During hotpressing, similar chemical changes might be expected and complicated by the combined action of pressure and densification. Indeed, compression can either fracture cell walls or allow viscoelastic and plastic deformation, depending on the wood polymers' viscoelastic behavior under the compression conditions (Navi & Girardet, 2000; Penneru, et al., 2006). In particular, at high hotpressing temperatures and wood moisture contents, densification of wood can intensify due to the higher deformability of wood polymers and higher level of cell wall fracture (Tabarsa & Chui, 1997).

Clearly, moisture content and compression levels, as well as the chemical changes induced by heat, all affect how wood responds to hotpressing. However, little is known about the combined effects of pressure and temperature on wood's chemical and viscoelastic properties. Only one study (Gardner, et al., 1993) reports on the chemical changes caused by hotpressing in conditions relevant to the manufacture of wood-based composites. They reported that hotpressing induced the formation of free phenolic units on lignin by virtue of demethoxylation of syringil and guaiacyl moieties. Gardner, et al. (1993) also found that different pressing conditions did not alter the elemental composition at the wood surface. The increased mobility of amorphous components of wood and the expansion of void volume above lignin T_g (expected at around 65°C) allowed the reorientation of the hydrophobic functionalities of amorphous polymers toward the surface. Enhanced crystallization of cellulose at temperatures near lignin T_g was also proposed.

The potential of hybrid poplar as an alternative resource for wood-based composites requires a deeper understanding of how hotpressing changes bulk wood properties. In particular,

the impact of hotpressing on wood's viscoelastic properties, which are critical to mat consolidation, is not known. Our research hypothesizes that wood moisture content and hotpressing temperature interact to dictate changes in the physical, chemical, and viscoelastic properties of wood during hotpressing. We also hypothesize the presence of a correlation between the chemical changes and viscoelastic changes induced by hotpressing.

3.2 **Objectives**

The overall goal of this work is to investigate the effect of hotpressing conditions on the chemical, physical, and viscoelastic properties of hybrid poplar wood. The specific objectives of this study are 1) to understand the impact and possible interaction of wood initial moisture content and hotpressing temperature on wood specific gravity and bending dynamic mechanical properties, and 2) to evaluate possible relationships between the changes in physical, viscoelastic, and chemical properties induced by hotpressing.

3.3 **Materials and Methods**

3.3.1 *Sample preparation and hotpressing treatments*

Wet hybrid poplar OP-367 supplied by Potlatch Corporation was sliced into flatsawn veneers (Figure 3.1). The bottom part was selected and divided into three positions within the bottom log (top, middle, bottom). For a control in each hotpressing group, 4 sets of 8 replicates, each totaling 32 replicates, were prepared using a numbering system and position code to represent the whole tree. Hotpressing conditions were selected based on tests of the impact of temperature, moisture content, and their possible interactions (Table 3.1). Two moisture contents (0% and 9%) and three hotpressing temperatures (150°C, 200°C, 250°C) were selected, resulting

in 6 hotpressing conditions or treatments. Initially, all wood samples were dried using high-vacuum drying at room temperature. For the 0% wood moisture content hotpressing group, high-vacuum-dried wood samples were kept in a vacuum dessicator filled with the drying agent $CaSO_4$ until hotpressing. The 9% moisture content was induced by conditioning high-vacuum-dried wood samples at 65% relative humidity at 21ºC. Veneers, 10 x 10 cm with thickness of 2.3 mm in nominal dimensions, were hotpressed in a 46 x 46 cm Wabash hot press of 3.4 MPa for 5 minutes under various conditions of wood moisture content and hotpressing temperature. Upon hotpressing, sample thickness was reduced to approximately 1.0 mm.

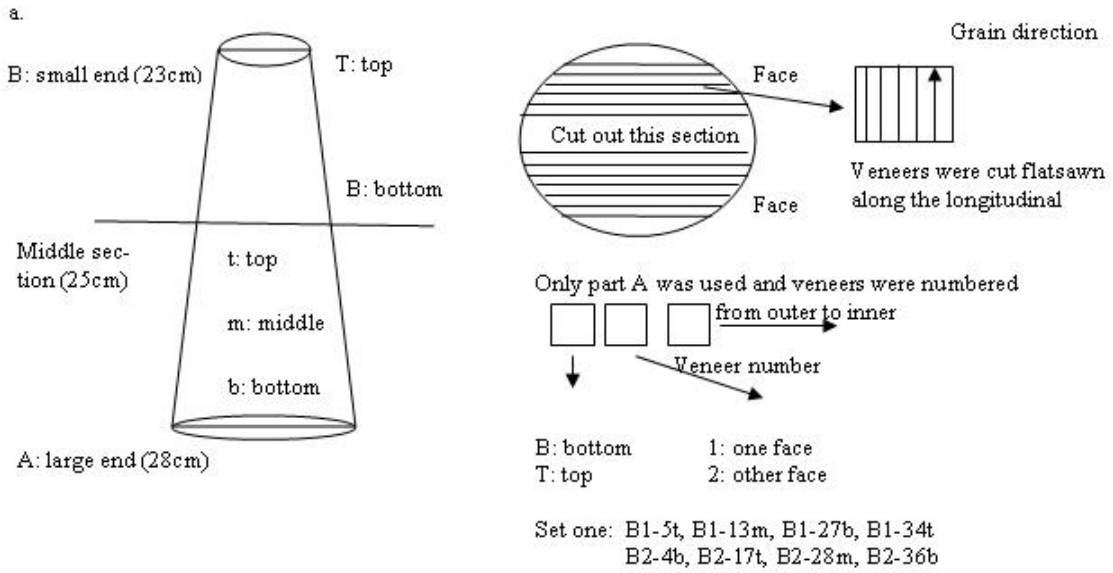

Figure 3.1 Cutting scheme of a log, and veneer labeling of samples.

Table 3.1 Hotpressing conditions

	Wood Moisture Content (%)	Pressing Temperature (°C)
Control	-	-
(9%, 150°C)	9	150
(9%, 200°C)	9	200
(9%, 250°C)	9	250
(0%, 150°C)	0	150
(0%, 200°C)	0	200
(0%, 250°C)	0	250

3.3.2 *Specific gravity measurement*

The specific gravity (SG) of hybrid poplar wood samples was calculated for the non-hotpressed (control) and the hotpressed samples by dividing the weight of a specimen by its volume, based on its oven dry dimensions (Equation 3-1).

$$SG_{0,OD} = \frac{mass_{ovendry}}{volume_{ovendry}} \qquad \text{Equation 3-1}$$

The mass was recorded on the Metler Toledo electronic weighing scale with 0.0001 g accuracy. Dimensions were 50 mm along the grain and 12 mm wide (measured by digital calipers), with a thickness of 2.3 mm with variability of 0.1 mm (measured by a dial gauge with 0.01 mm precision). Specific gravity for all oven dry samples ($SG_{0,OD}$) was calculated following ASTM D 2395-07. The $SG_{0,OD}$ was important for thorough examination of the characterized viscoelastic properties. The degree of densification (%) was calculated by taking the ratio of the difference in $SG_{0,OD}$ for control (before) and hotpressed (after) hybrid poplar (Kutnar, et al., 2009) according to Equation 3-2:

$$Densification(\%) = \frac{SG_{0,OD,after} - SG_{0,OD,before}}{SG_{0,OD,before}} * 100\% \qquad \text{Equation 3-2}$$

3.3.3 *Characterization of wood viscoelastic properties by dynamic mechanical analysis (DMA).*

Rectangular flatsawn samples of 50 mm along the grain by 12 mm by 2.3 mm (control samples) or 1 mm (hotpressed samples) were tested along the grain in 3-point bending mode on a Tritec 2000 DMA instrument. Before testing, the samples were freeze dried to less than 0.7% moisture content under vacuum and were kept in a vacuum desiccator with P_2O_5 until DMA testing. DMA tests were then performed in the linear viscoelastic range, as determined by strain scans performed at the most extreme test temperature possible for dry wood without causing significant thermal degradation (120°C). Following rapid cooling (with liquid nitrogen) at approximately 5°C/min to 25±2°C, a temperature scan was performed from 30°C–120°C at 1 Hz and a heating rate of 2°C/min. After the temperature scan, the furnace was cooled again (5°C/min) and subjected to a frequency sweep from 0.005 Hz to 50 Hz at 10°C intervals from 30°C to 120°C. This step-isothermal frequency sweep utilized a heating rate of 1.5°C/min. This data was then utilized for time-temperature superposition. For each sample group (the control and 6 hotpressing conditions), at least triplicate DMA tests were conducted. The storage and loss moduli (E' and E") data from the step frequency sweeps were then used to develop master curves using the time-temperature superposition principle (TTS) (Ferry, 1980). The reference temperature was arbitrarily selected at 80°C for all groups, and isotherms were horizontally shifted to that reference isotherm in order to create smooth master curves. When needed, vertical shifting was applied after horizontal shifting.

3.3.4 *Sorption tests*

The water adsorption isotherms were constructed by equilibrating samples in a controlled humidity chamber at 20ºC. Initially, 12 replicates for control and hotpressed groups, with dimensions of 50 mm along the grain, a width of 12 mm and a thickness of 2.3 mm for the control, and roughly 1 mm for the hotpressed samples, were cut using a table saw from 10 cm x 10 cm veneers (Figure 3.1). These 50 x 12 mm samples were freeze-dried at 0.02 mbar at -50°C using a Labconco FreeZone 4.5-Liter Benchtop Freeze Dry System for 24 hours under a vacuum (~ 0.7% moisture content). The mass was measured on a Metler Toledo electronic scale with 0.0001 g accuracy. Dimensions were 50 mm along the grain, a width of 12 mm (measured by digital caliper) and a thickness of 2.3 mm (measured by a dial gauge with 0.01 mm precision). Next, these freeze-dried (FD) samples were subjected to humidity conditioning series in a humidity chamber (G-64 Elite Russell's Technical Products) at 20±1°C, starting at 30±1% relative humidity (RH), until the mass was constant and % RH was increased to 45, 60, 80, and 90±1% relative humidity in the same manner. The mass was recorded daily, and the equilibrium condition was achieved after approximately 5 to 10 days of conditioning. The wood equilibrium moisture content (EMC) was calculated based on freeze-dried mass, as described in Equation 3-3,

$$EMC(\%) = \frac{m_{wet} - m_{dry}}{m_{dry}} \qquad \text{Equation 3-3}$$

where EMC(%) was the equilibrium moisture content, m_{dry} was the mass after freeze-vacuum drying, and m_{wet} was the mass after equilibrium was achieved at the set condition. Adsorption isotherms were then constructed by plotting the EMC corresponding to each relative humidity at 20°C.

3.3.5 *Statistical Analyses*

As there is a well-established correlation between wood's dynamic mechanical properties and density, all measured properties were first tested for dependency on specific gravity. In statistical viscoelastic properties evaluation, specific gravity corresponds to the oven-dried specific gravity ($SG_{0,OD}$). When such a dependency was observed, an analysis of covariance (ANCOVA), using specific gravity as a covariate, was performed at an α level of 0.05 to determine significant differences between properties measured in hotpressed and control samples (using SAS 9.1 statistical software). With ANCOVA, the effect of hotpressing treatment on moduli could be determined regardless of its impact on specific gravity. Normalization of these properties was conducted by dividing the properties by specific gravity. Significant differences in these "specific properties" were then detected by conducting an analysis of variance (ANOVA) at an α level of 0.05. ANOVA analysis was also conducted in the case of properties showing no dependence on specific gravity. When a significant difference was detected, we also conducted Tukey-Kramer post-hoc analyses to establish grouping among treated and control samples. We conducted these analyses on numerous measured properties, including specific gravity, and storage and loss moduli at 30 and 120°C, along with the percentage of drop in moduli between these temperatures, as well as the peak observed on the loss modulus and the range of log frequency in the master curves.

3.4 **Results and Discussion**

3.4.1 *Specific gravity*

The specific gravity discussed in this section corresponds to $SG_{0,OD}$. As expected, hotpressing increased wood specific gravity significantly (p value = 0.0001) (Figure 3.2). Using

Tukey-Kramer's three classifications of specific gravity, we found that the specific gravity of all hotpressed samples differed significantly from control samples (at least 4 replicates).

The control wood samples had an average specific gravity of 0.35±0.03, while hotpressed samples displayed a higher specific gravity, varying from 0.90±0.06 to 0.64±0.16. Different hotpressing conditions led to different increases in specific gravity. The lowest specific gravity increase was observed for samples hotpressed at conditions of 0% at 150ºC (Group B) (Table 3.2 and Figure 3.2).

Table 3.2 Average specific gravity for control and hotpressed (treated) hybrid poplar samples. Letters are the grouping from ANOVA at an α=0.05 and Tukey-Kramer analyses.

	Oven Dry Specific Gravity, $SG_{0,OD}$	% Densification = $(SG_{after}-SG_{before})/SG_{before}*100$
Control	0.35 ± 0.03 C	-
9%,150°C	0.90 ± 0.06 A	154
9%,200°C	0.90 ± 0.06 A	153
9%,250°C	0.80 ± 0.10 A,B	132
0%,150°C	0.64 ± 0.16 B	81
0%,200°C	0.85 ± 0.12 A	141
0%,250°C	0.80 ± 0.05 A,B	124

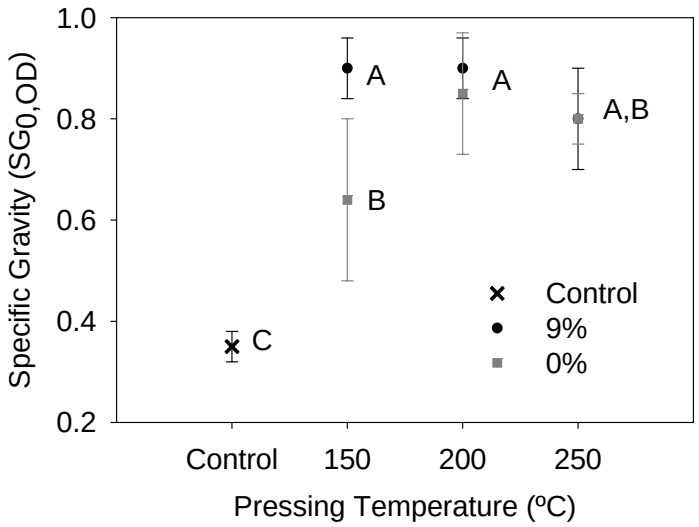

Figure 3.2 Average specific gravity for not-hotpressed (control) and hotpressed hybrid poplar wood samples and its Tukey-Kramer grouping.

Hotpressing increased the SG of hybrid poplar wood by at least 2 fold. The increase in specific gravity was expected because of the decrease of pore sites due to cell wall collapse and compaction during compression. In the absence of moisture, the cell wall became rigid and was easily distorted and crushed during hotpressing. Hsu, et al. (1988) reported that high-pressure steam pre-treatment causes partial hydrolysis of hemicelluloses for both softwoods and hardwoods, resulting in increased wood compressibility. At 9% wood MC, the variability of the SG measurement was higher. However, the lowest hotpressing temperature of 150°C created higher densification compared to the equivalent at 0% MC. This was expected because water becomes steam during hotpressing, and steam plasticizes the cell wall and facilitates better densification (Wolcott, et al., 1990).

3.4.2 *Viscoelastic property*

We also investigated the effect of hotpressing on the viscoelastic properties of hybrid poplar wood. Temperature scans were performed from room temperature to 120°C, and E' and E" were also recorded. For both control and hotpressed samples, E' decreased with increasing temperature, as expected (Figure 3.3 and Figure 3.4). However, this was not the case with the E". A peak in E" was observed around 50°C. At temperatures above 80–100°C, the loss modulus started to increase, likely due to higher loss of thermal energy. The increase of loss modulus indicated increase of heat dissipation from the molecular movements to the surroundings.

According to Sugiyama, Obataya & Norimoto (1998), a tan δ peak (tan δ =E"/E') was observed at around 75°C on oven-dried wood, but this was not explained. Jafarpour, et al. (2008) reported a relaxation peak at around 39°C on a dried poplar and cellulose powder sample, using dielectric analysis, and ascribed this to entrapped water. In their study, the peak was not observed on the second temperature scan at up to 120°C, and this was attributed to the desorption of water molecules. Sun, et al. (2007) postulated that the peak on tan δ of absolutely dry wood between 75°C and 150°C was extremely sensitive to moisture changes, even between 0% to 0.7%, perhaps due to the glass transition of hemicelluloses. In addition, a loss peak observed around 40°C to 56°C for wood with an approximately 7% moisture content was not detected at 4% moisture content (Backman & Lindberg, 2001). Instead, a new peak was shown at around 80°C (Backman & Lindberg, 2001) and confirmed by what Kelley, et al. (1987) reported as the glass transition peak of hemicelluloses. Thus, the peak observed at approximately 50°C may be the manifestation of glass transition of hemicelluloses or of molecular motions from adsorbed water molecules.

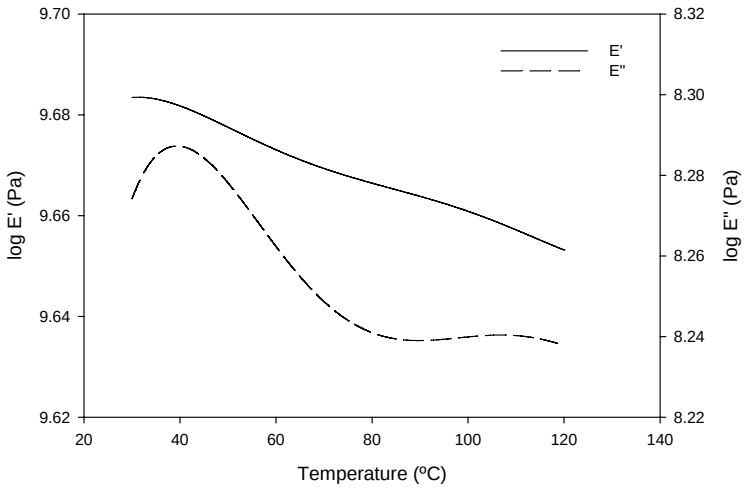

Figure 3.3 Typical DMA temperature scan of hybrid poplar wood at 1Hz utilizing 2°C/min heating rate for control samples tested in 3-point bending mode along the grain.

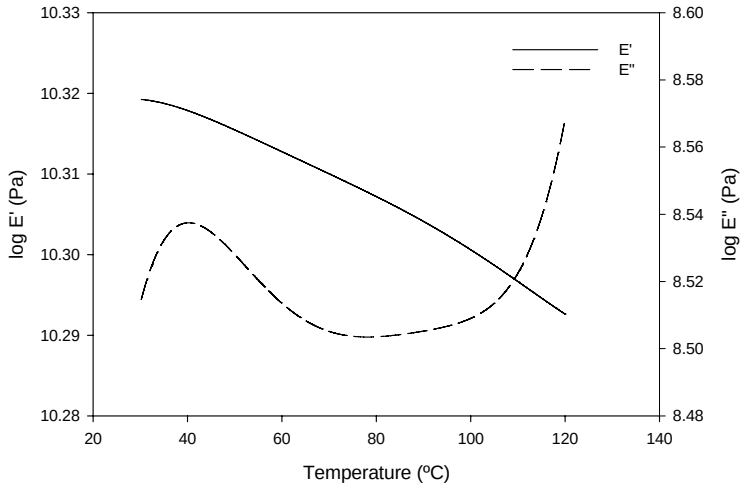

Figure 3.4 Typical DMA temperature scan at 1Hz utilizing 2°C/min heating rate for hotpressed hybrid poplar samples (9%, 250ºC) tested in 3-point bending mode along the grain.

To quantitatively compare the effect of treatments on wood viscoelastic properties, we compared the values of the storage modulus at 30°C ($E'_{(30°C)}$) and 120°C ($E'_{(120°C)}$), along with the relative drop over that temperature range (Equation 3-4).

$$E'_{decrease}(\%) = \frac{E'_{(30°C)} - E'_{(120°C)}}{E'_{(30°C)}} * 100 \qquad \text{Equation 3-4}$$

Figure 3.5 shows that hotpressing affected the absolute value of the moduli.

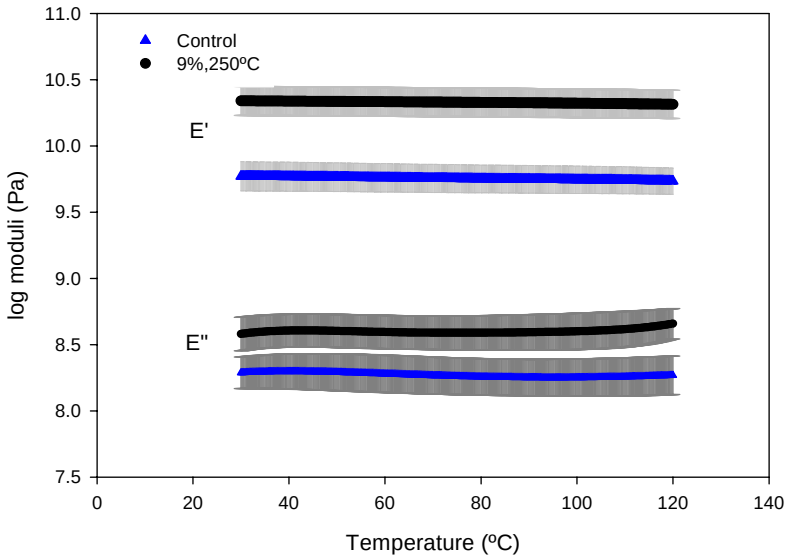

Figure 3.5 Average storage and loss moduli curves during a temperature scan for control and hotpressed samples (9% MC, 250°C) at 1Hz with a 2°C/min heating rate. Samples were tested in 3-point bending mode along the grain with at least 3 replicates (with standard deviation).

As expected, the storage modulus for all hotpressed samples was higher than that of the control, indicating a stiffening of wood samples during hotpressing. This may be due to the increase in SG or densification induced by hotpressing. Indeed, it is well established that wood strength and stiffness are linearly related to density (Bowyer, et al., 2003). To confirm whether specific gravity directly affected viscoelastic properties, we explored dependencies between the two. Specific gravity corresponds to $SG_{0,OD}$.

Figure 3.6 shows that E' at both 30°C and 120°C for all samples linearly increases with $SG_{0,OD}$ (R^2=0.84). Therefore, the 200–500% increase in the storage modulus upon hotpressing could largely be attributed to an increase in density. This corresponded well with a maximum

densification of roughly three times upon hotpressing. One might ask whether the increase in storage modulus was strictly due to densification or also to hotpressing conditions independent of the density increase. To answer this question, an ANCOVA (analyis of covariance) was performed with specific gravity as the covariate. The hotpressing treatment had a significant effect on $E'_{(30°C)}$ (p value=0.0038) and $E'_{(120°C)}$ (p value=0.0054), in addition to the effect of specific gravity (p value =0.0015**)** (Table 3.3).

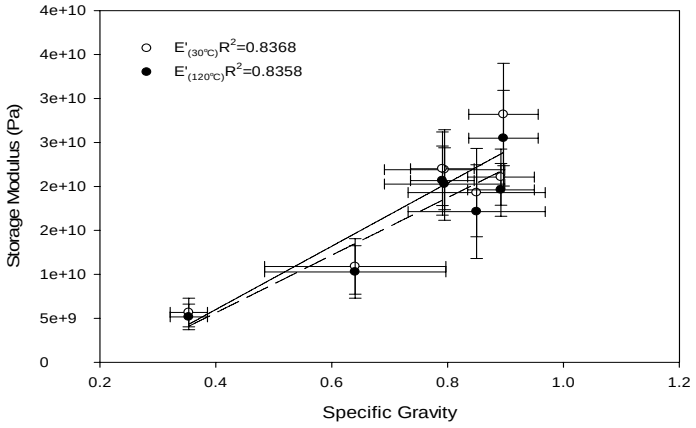

Figure 3.6 Relationship between the storage modulus and oven-dry specific gravity.

In contrast, $E'_{decrease\ (\%)}$ did not depend on specific gravity (R^2=0.0125) (Figure 3.7), nor on the hotpressing treatment. No significant difference between control and hotpressed samples was found with ANOVA analysis (p value=0.1417) (Table 3.3).

Table 3.3 The oven dry specific gravity and storage modulus data and evaluation of statistical analysis at an α=0.05 (with at least 3 replicates). Letters are grouping from ANOVA with an α=0.05 and Tukey-Kramer analyses.

	Oven dry Specific Gravity, $SG_{0,OD}$	Storage Modulus, E'(GPa)		Specific Storage Modulus, ($E'/SG_{0,OD}$) (GPa)		$E'_{decrease,} = \frac{(E'_{30°C} - E'_{120°C})}{E'_{30°C}}$
Treatment	Specific Gravity, SG	30℃	120°C	30°C	120°C	(°C)
Control	0.35 ± 0.03 C	5.7 ± 1.6	5.2 ± 1.5	16.4 ± 6.1 B	14.9 ± 5.4 C	9 ± 3
9%, 150°C	0.90 ± 0.06 A	28.2 ± 5.8	25.5 ± 5.4	31.7 ± 7.1 A	28.6 ± 7.1 A	10 ± 2
9%, 200°C	0.90 ± 0.06 A	21.1 ± 3.2	19.6 ± 3.1	23.6 ± 2.9 A,B	22.0 ± 2.8 A,B,C	7 ± 2
9%, 250°C	0.80 ± 0.10 A,B	21.9 ± 4.5	20.3 ± 4.1	27.6 ± 5.1 A	25.5 ± 3.9 A,B	7 ± 2
0%, 150°C	0.64 ± 0.16 B	10.9 ± 3.2	10.3 ± 3.0	16.9 ± 2.3 B	16.0 ± 2.4 C	6 ± 2
0%, 200°C	0.85 ± 0.12 A	19.3 ± 5.0	17.1 ± 5.3	22.5 ± 3.5 A,B	19.8 ± 4.0 B,C	12 ± 8
0%, 250°C	0.80 ± 0.05 A,B	22.0 ± 4.2	20.7 ± 3.9	27.8 ± 4.9 A	26.1 ± 4.5 A,B	6 ± 1
ANOVA p value	0.0001	-	-	0.0001	0.0001	0.1417
ANCOVA	p value (treatment)	0.0038	0.0054	-	-	-
	p value (SG)	0.0015	0.0007	-	-	-

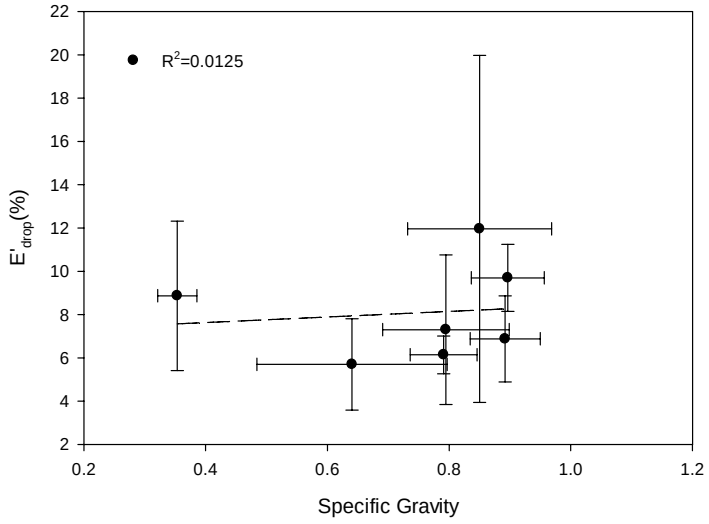

Figure 3.7 Relationship between specific gravity and the drop of storage modulus [(E'$_{30°C}$-E'$_{120°C}$)/ E'$_{30°C}$*100].

To further delineate the effects of hotpressing conditions on storage modulus, the storage modulus for each group was normalized by its specific gravity, leading to specific modulus properties. The specific storage modulus for some hotpressed samples differed significantly from that of control samples (ANOVA p value=0.0001) (Table 3.3). Specifically, the Tukey-Kramer grouping indicated that regardless of moisture content, samples hotpressed at 250°C had higher specific storage moduli than control samples. Surprisingly, this was also the case for the 9% MC sample hotpressed at 150°C. All other hotpressing conditions (at 150°C and 200°C) resulted in no change in specific storage moduli. With the extreme hotpressing temperature at 250°C, a change in the morphology of wood polymers may be expected. For example, an increase in stiffness could be attributed to the changes of amorphous and crystalline cellulose chemistry.

This finding coincides with results from a study investigating the effects of compressive strain and press temperature. Tabarsa & Chui (1997) found that differences in mechanical

properties in hotpressed white spruce were small at pressing temperatures of 150 and 200°C with a wood moisture content of 15%.

To further investigate the reason for moduli increases, project collaborators at the University of Idaho, Osman, et al. (2009), evaluated cellulose crystallinity using Fourier Transform Infra-Red (FTIR) spectroscopy. Figure 3.8 shows their results. They evaluated cellulose crystallinity from two different calculations using a method described by Akerholm, et al. (2004). The IR ratio H_{1429}/H_{897} is the ratio between different peak heights of the CH_2 bending vibration in crystallized cellulose I and amorphous cellulose (Hakkou, et al., 2005) to the vibration for the β-glucosidic chain (Nelson & O'Connor, 1964). This peak ratio correlates well with increase of crystallinity, and the relationship is relatively linear (Akerholm, et al., 2004). Another peak ratio of H_{1372}/H_{2900} was also used for the cellulose crystallinity determination. Akerholm, et al. (2004) found that the peak height ratio H_{1372}/H_{2900} had a linear relationship up to only 50% *Cladophora* cellulose which is rich in cellulose I_α. This indicates the limitation of the peak height ratio H_{1372}/H_{2900} when used to explain the higher index of crystallinity which was problematic when considering the crystallinity of wood that, in general, is rich in crystalline cellulose.

Therefore, in our study, the peak height ratio H_{1429}/H_{897} is used to further examine the relationship of cellulose crystallinity and stiffness. The height ratio of H_{1429}/H_{897} followed the general trend of a proportional increase of the peak height ratio with the increase in cellulose crystallinity. Illustrated in Figure 3.8, the peak height ratios of H_{1429}/H_{897} of the hotpressed group at 0% and 9% at 200ºC, as well as at 0% and 150ºC, were the same as those of the control group, indicating no change in crystallinity. Surprisingly, hotpressing at a 9% wood moisture content showed the lowest crystallinity of all groups at 150ºC, and the highest at 250ºC. The trend that

was observed for peak height ratio consists of a slight increase of crystallinity at hotpressing temperatures 200ºC and 150ºC, and a rapid increase afterwards. The peak increase occurred at 9% and 250ºC, indicating that hotpressing at this condition promotes cellulose crystallization more than the equivalent pressing temperature at 0%.

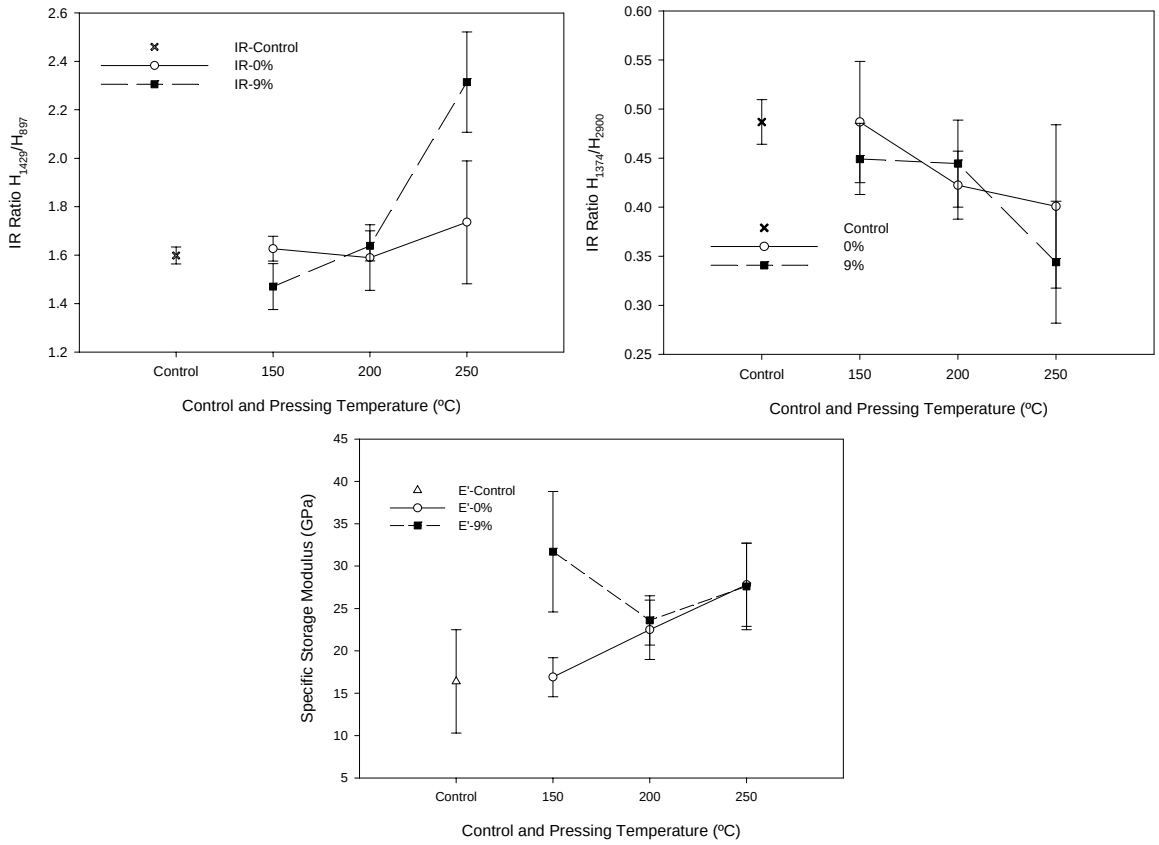

Figure 3.8 IR peak height ratio H_{1429}/H_{897} and H_{1374}/H_{2900} (Osman, et al., 2009) and specific storage modulus at 30ºC for control and hotpressed hybrid poplar samples.

Figure 3.8 also illustrates the stiffness for each hotpressing treatment and control. The lowest crystallinity was observed for control hybrid poplar, and crystallinity tended to increase as pressing temperature increased, with the exception of the hotpressed group at 9% MC and 150ºC. Interestingly, this hotpressed group (9%, 150ºC) showed the highest stiffness of all groups. Note

that the storage modulus measured for this group had a very large standard deviation. Overall, the crystallinity determination using FT-IR peak height ratios of H_{1429}/H_{897} showed that the increase in the storage modulus at higher pressing temperatures (250ºC) was due to the increase in cellulose crystallinity.

Similar analysis performed on the storage modulus was conducted on loss modulus data (Table 3.4) and monitored the loss peak. Again, for the control and treated wood samples together, the loss modulus was shown to be linearly dependent on specific gravity ($R^2_{E'(30°C)}$=0.77 and $R^2_{E'(120°C)}$=0.91) (Figure 3.9). ANCOVA analysis showed that there was no significant difference in loss moduli ($E''_{(30°C)}$ p value=0.54 and $E''_{(120°C)}$ p value=0.78) due to treatment compared to the control, evaluated at α=0.05. ANOVA analysis on specific loss moduli (sE") confirmed that the loss modulus was not significantly affected by treatment ($sE''_{(30°C)}$ p value=0.52 and $sE''_{(120°C)}$ p value=0.72). Finally, loss peak temperature did not differ significantly among all the groups (p value=0.99), indicating that hotpressing did not alter the relaxation related to the water adsorption sites of wood polymers.

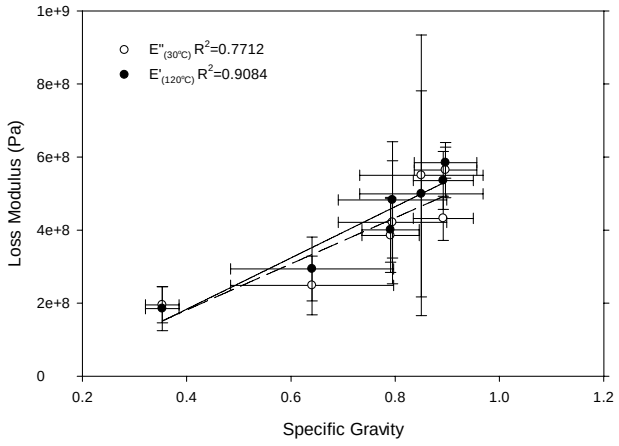

Figure 3.9. Relationship between loss modulus and specific gravity.

Table 3.4 Oven-dry specific gravity, loss modulus data, and evaluation of statistical analysis at an α=0.05 (at least 3 replicates). Letters are used for ANOVA groupings (α=0.05) and Tukey-Kramer analyses.

Treatment	Oven Dry Specific Gravity, $SG_{0,OD}$		Loss Modulus, E"(GPa)		Specific Loss Modulus, E"(GPa)		E" peak (°C)
			30°C	120°C	30°C	120°C	°C
Control	0.35 ± 0.03	C	0.6 ± 0.2	0.5 ± 0.2	0.6 ± 0.2	0.5 ± 0.2	48 ± 10
9%, 150°C	0.90 ± 0.06	A	0.6 ± 0.1	0.7 ± 0.1	0.6 ± 0.1	0.7 ± 0.1	47 ± 4
9%, 200°C	0.90 ± 0.06	A	0.5 ± 0.1	0.6 ± 0.1	0.5 ± 0.1	0.6 ± 0.1	50 ± 6
9%, 250°C	0.80 ± 0.10	A,B	0.5 ± 0.3	0.6 ± 0.2	0.5 ± 0.3	0.6 ± 0.2	50 ± 10
0%, 150°C	0.64 ± 0.16	B	0.4 ± 0.1	0.5 ± 0.1	0.4 ± 0.1	0.5 ± 0.1	48 ± 3
0%, 200°C	0.85 ± 0.12	A	0.6 ± 0.3	0.6 ± 0.2	0.6 ± 0.3	0.6 ± 0.2	50 ± 13
0%, 250°C	0.80 ± 0.05	A,B	0.5 ± 0.1	0.5 ± 0.1	0.5 ± 0.1	0.5 ± 0.1	-
ANOVA p value	0.0001		-	-	0.5220	0.7196	0.99
ANCOVA	p value (treatment)		0.5440	0.7794	-	-	-
	p value (SG)		0.0125	0.0058	-	-	

3.4.3 *DMA/master curve analysis*

Master curves were built for the control samples and for the following hotpressed samples: 0%-150°C; 0%-250°C; 9%-150°C; and 9%-250°C. The typical raw data from frequency scans for control and hotpressed hybrid poplar wood are shown in Figure 3.10. The isotherms of storage and loss moduli were plotted only up to 10 Hz because, at testing, frequencies of higher than 10 Hz (close to the system resonance frequency) appeared to be erroneous (Figure 3.11)

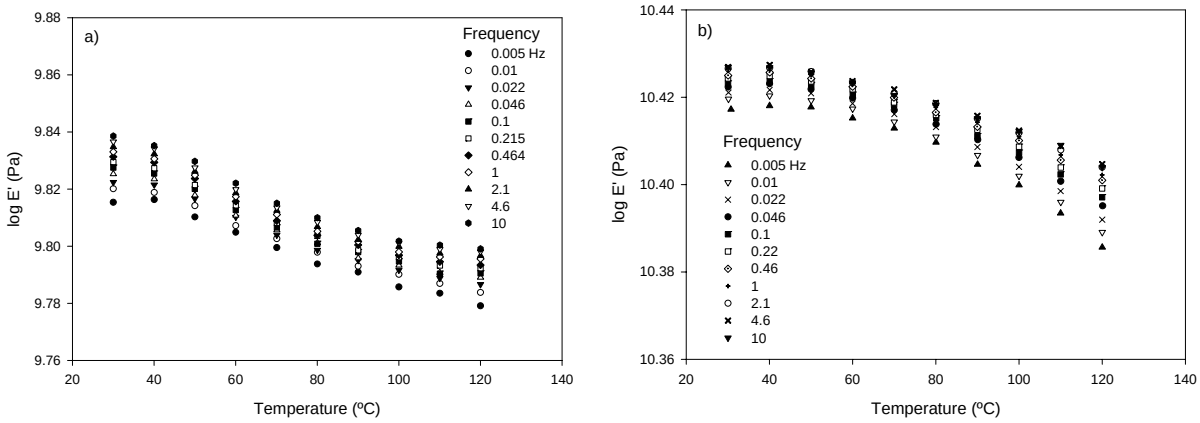

Figure 3.10 Raw data from frequency scans (0.005–10Hz) from 30ºC to 120ºC for control (a) and hotpressed samples (9%, 250ºC) (b).

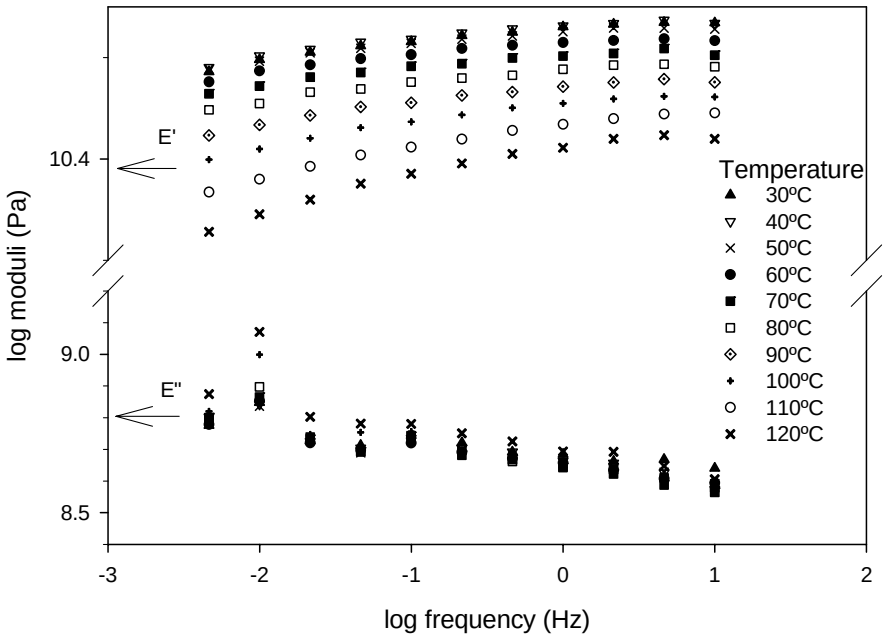

Figure 3.11 Raw E' and E" isotherms for (9%, 250ºC) hotpressed hybrid poplar wood.

The storage and loss moduli were used to construct master curves using the time-temperature superposition principle. Namely, isotherms were horizontally shifted towards the selected reference temperature until they were superposed, in order to generate a smooth master

curve. We selected 80ºC as the reference temperature for all master curves because it fell in the middle of the evaluated temperature range. The horizontal shift factor (a_τ) is a ratio of a relaxation time at the reference temperature $\tau_{(Tr)}$ and the relaxation time at a specific temperature $\tau_{(T)}$ and was described as $a_\tau = \tau_{(T)} / \tau_{(Tr)}$. Master curves for storage modulus using horizontal shifting were quite smooth and continuous for dry wood (Figure 3.12), and showed the expected trend: as frequency increased, samples appeared to be stiffer (showing an increase in storage modulus) while the viscous component (loss modulus) decreased. However, horizontal shifting alone did not allow for a smooth loss modulus superposition (Figure 3.13).

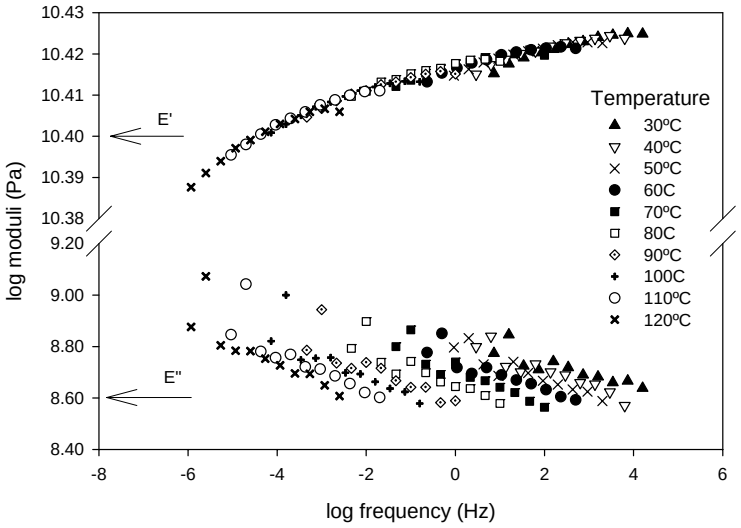

Figure 3.12 Typical E' and E" master curve of (9%, 250ºC) obtained from horizontal shifting alone to the reference temperature isotherm at 80ºC.

The fact that viscoelastic functions did not superpose well with the horizontal shift factor alone suggests that the dry wood system is probably too heterogeneous in this case. The method of reduced variables introduced by Ferry (1980) did not apply. In complex systems, vertical shifting is often required to account for fluctuations in materials density and thermal expansion

as temperature changes (Ferry, 1980). The temperature dependence of the vertical shift factor (b_τ) can be described based on the dilute solution principle and/or theory of rubber elasticity as described in

$$b_\tau = \frac{\rho_r(T_r)}{\rho T} \qquad \text{Equation 3-5}$$

where T is the absolute temperature, the subscript "r" indicates reference conditions, and ρ is the density at the corresponding temperature. For elastomers, many researchers initially ignored the need for the vertical shift factor (Ferry, 1980); one reason being the small magnitude of vertical shift needed relative to the horizontal shift (O'Connell & McKenna, 1997).

In the case of freeze-dried wood, fluctuations in density and moisture content as temperature varies might complicate viscoelastic behavior and create a need for vertical shifting. Therefore, vertical shifting was attempted here to correct for the potential effect of density and moisture content variations during the DMA experiment. When vertical shifting in conjunction with horizontal shifting was used, smooth E' and E" master curves were obtained (Figure 3.13) with the corresponding shift factor (inset of Figure 3.13).

All control and hotpressed wood samples required the application of both horizontal and vertical shift factors to develop smooth master curves for both storage modulus and loss modulus in the dry state. While the need for a vertical shift to conduct TTS on wood has not been reported before, it is not surprising, considering the complexity of wood. In fact, vertical shift has been observed in several complex materials, such as highly filled nanocomposites (Duperray & Leblanc, 1982) and fiber-filled composites (Mohanty & Nayak, 2007).

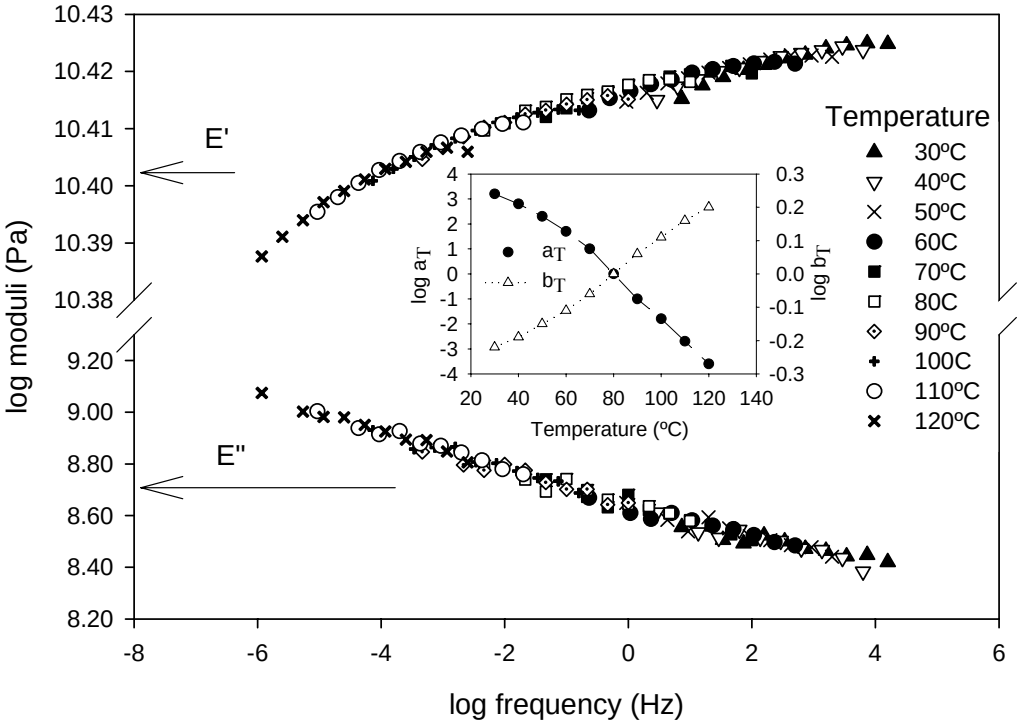

Figure 3.13 Typical E' and E" master curve of (9% MC, 250ºC) obtained with horizontal shifting to the reference temperature isotherm at 80ºC with an addition of vertical shift for the E". Inset shows the shift factors.

Note, however that in the case of wood, the horizontal shift factor was the same for loss and storage moduli, while the vertical shift factor differed for the two viscoelastic properties. In fact, the vertical shift factor was mainly necessary for the loss modulus. Even though the magnitude of the vertical shift was much smaller than that of the horizontal shift, the application of vertical shift was necessary to achieve satisfactory overlap. No explanation for this behavior can be given with certainty. However, one might speculate that fluctuations in density and moisture content along with test temperature could affect the relative magnitude of moduli beyond what is expected, from the time-temperature equivalence of relaxation. Regardless of the material changes that induce this need for a vertical shift, this phenomenon appears to affect loss moduli more significantly than storage moduli, which required little or no vertical shifting.

Figure 3.14 shows the reproducibility of master curves. Master curves for control hybrid poplar samples and samples hotpressed at 9% MC, 250°C are depicted with the corresponding shift factor (Figure 3-14 and Figure 3-15). These graphs illustrate the typical representation of master curve comparison for the control group and the hotpressed group. Each treatment condition was evaluated using at least three replicates to construct the master curves. The reproducibility of the dry wood master curve is considered satisfactory, since wood is a complex system. The shift factor for hotpressed samples did not differ much compared to the control.

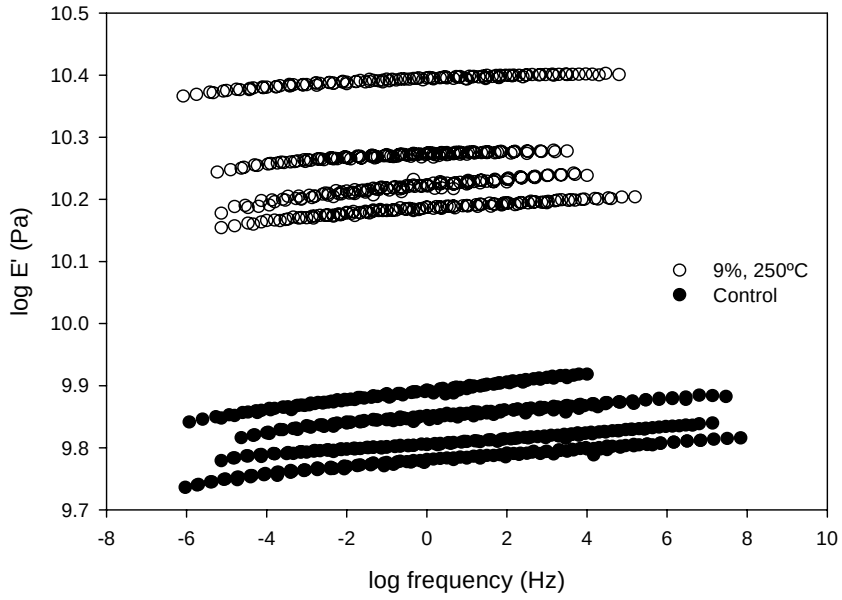

Figure 3.14 Master curve of control hybrid poplar and one of the hotpressed samples (4 replicates) referenced to 80ºC isotherm.

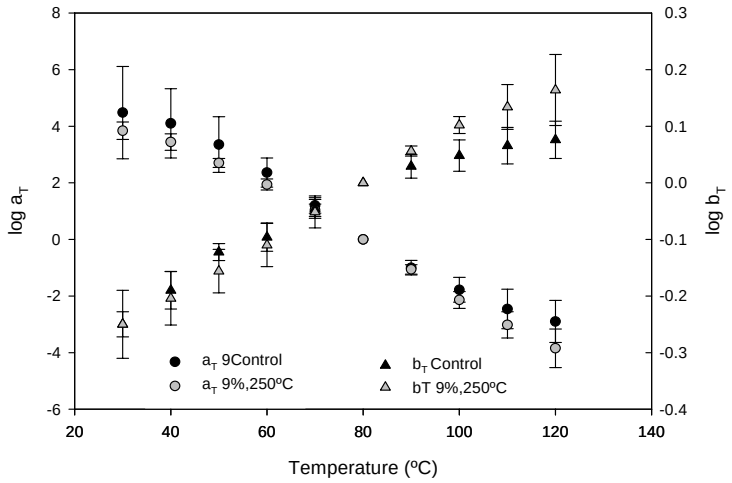

Figure 3.15 Average shift factor for control and 0% MC, 250°C for master curves shifted to reference temperature at 80ºC.

Table 3.5 shows the difference in log frequency range for E' master curves. The breadth of log frequency presents information about molecular mobilization distribution and the relaxation behavior of wood polymers. To quantify the extent of log frequency, the value of minimum frequency (at 120°C, 0.005 Hz) was subtracted from the maximum frequency (at 30°C, 11 Hz). A longer breadth of master curves is explained by the heterogeneity of molecules within the polymer matrix and the longer time required for them to start relaxing. In this study, the breadth of master curves of hotpressed samples did not differ significantly with the control (p value=0.094). Nonetheless, this difference might be significant if ANOVA was performed at a 90% confidence level. Under dry conditions, the time-temperature dependent relaxations of wood are not altered by hotpressing.

Table 3.5 The breadth of master curves.

Treatment	Δlog frequency
Control	12 ± 2
9%, 150°C	11 ± 0
9%, 200°C	-
9%, 250°C	11 ± 1
0%, 150°C	10 ± 2
0%, 200°C	-
0%, 250°C	10 ± 1
ANOVA p value	0.094

The small variation among samples from the same treatment group condition may have been due to their more uniform organization upon densification. Possibly, the temperature-dependent properties of hotpressed wood could not be captured under dry conditions. Indeed, in natural conditions, wood is heterogenous. In control samples, the available void volume and the structure of cell walls were more diverse. The collapsing of cell walls during pressing reduced the free volume and limited the space available in cell walls.

The experimental temperatures were selected to imitate industrial strand board manufacturing practice. For the viscoelastic analysis, the log frequency at two extreme temperatures (150ºC and 250ºC) were evaluated to magnify effects of hotpressing. Wood chemical composition was not altered below 150ºC (Sun, et al., 2007). Rapid hemicellulose decomposition and creation of free lignin phenolic units occurred above 200ºC (Tjeerdsma, et al., 1998; Kotilainen, et al., 1999). The reduction of carbohydrates and the molecular cleavage of lignin facilitated the increased mobility of chain motion. With the alteration of space confinement, we expected that relaxation behavior would change. However, hotpressing conditions significantly affected viscoelastic functions such as storage modulus. Hotpressing

conditions did not affect loss modulus or the time-temperature dependence indicated by the range of log frequency.

3.4.4 *Wood Hygroscopicity*

Figure 3.16 presents the results of sorption tests for control and hotpressed samples at 20ºC at various relative humidities. Hotpressing clearly decreases wood hygroscopicity, as evidenced by lower wood equilibrium moisture content (EMC) for hotpressed samples compared to control samples. A general trend can be observed where more severe hotpressing conditions (higher temperature) lead to a lower EMC. In other words, wood samples hotpressed at 250°C equilibrate at a lower EMC than those hotpressed at 200°C, which in turn equilibrate at a lower EMC than those pressed at 150ºC. The effect is quite significant; for example, samples hotpressed at 250ºC equilibrate to approximately 10% EMC at 90% RH, compared to 18% EMC for control samples in the same environment. At pressing temperatures of 150 and 200°C, samples hotpressed at 9% MC adsorbed less moisture compared to those hotpressed at 0% MC. Samples hotpressed at 250°C showed the opposite trend, with 9% MC, indicating more adsorption capability. Kolin & Janezic (1996) reported that the FSP of poplar at 20ºC is approximately 30%. This experimental value was close to the fiber saturation point of beech (a hardwood) at 20%, measured at 18ºC (Navi & Girardet, 2000). Others found a decrease in FSP due to heat treatment (Navi & Girardet, 2000; Repellin & Guyonnet, 2005).

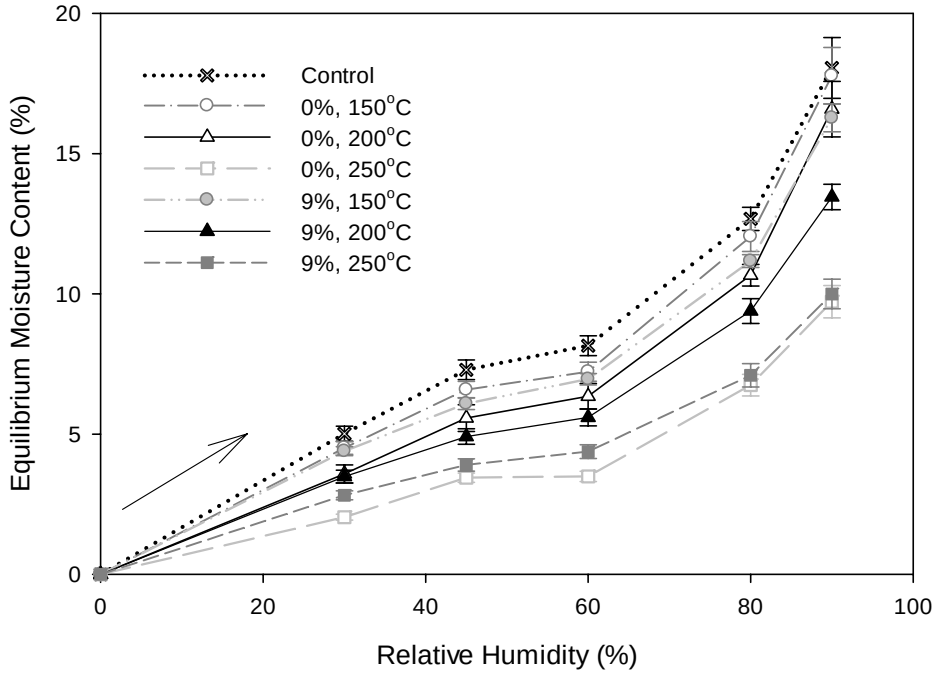

Figure 3.16 Adsorption isotherms of control and hotpressed hybrid poplar wood at 20°C at (%MC, TºC) (12 replicates each).

In this project, pressing temperature clearly influenced the moisture adsorption ability of wood by lowering hygroscopicity with an increase in pressing temperature, agreeing with results from other researchers (Kolin & Janezic, 1996; Tabarsa & Chui, 1997). Moisture definitely affected hygroscopicity; samples hotpressed at 9% MC showed lower moisture adsorption than those hotpressed at 0% MC. In general, wood samples exhibit less hygroscopicity when pressed at higher temperatures and higher moisture contents, indicated by a lower EMC. This result corresponds to findings by Navi and Girardet (2000), where steamed, hotpressed wood showed less FSP and less hygroscopicity than hotpressed wood that was not steamed. The limit of hygroscopicity of heat-treated wood was highly influenced by its cellulose content; thus, hydrogen bonding within amorphous cellulose determined the sorption capacity of wood (Kolin & Janezic, 1996).

Even though the moisture adsorption was noted to be lower at higher pressing temperature, for hotpressing at 0% MC, the trend was reversed at the highest pressing temperature, illustrated by higher adsorbed moisture content for wood samples pressed at 9% MC. Moisture affected chemistry changes during hotpressing, especially at 250 ºC. The least hygroscopic samples were those hotpressed at 0% MC and 250°C.

This reduction of wood hygroscpicity could be due to the reduction of high water-affinity molecules, such as hydroxyl groups in hemicelluloses and cellulose, and therefore wood's ability to adsorb moisture was subsequently limited. Almeida, et al. (2009) reported that hotpressing at temperatures above 190ºC removed some hemicelluloses from the wood matrix and therefore reduced the amount of hydroxyl groups available for the water molecule to bind. At temperatures above 220ºC, this effect on hygroscopicity was even more prominent (Almeida, et al., 2009). Chemical analysis by project collaborators at University of Idaho, Osman, et al. (2009) supported the evidence of increase of crystallinity upon hotpressing up to 250°C. This crystallinity increase could be due to reduced amorphous content in wood, and to cellulose chain-like realignment. As temperature increases above 100°C, intermolecular and intramolecular chemical bond breakage intensifies and compressive strength decreases, mainly due to the depolymerization of hemicelluloses (Yildiz, et al., 2005). However, at a higher pressing temperature of 260°C, cellulose chains become depolymerized and damage the crystalline structure (Hakkou, et al., 2005b). In fact, a complete amorphous state occurs at about 270°C (Fengel & Wegener, 1984).

In addition to the changes occurring to wood carbohydrates, changes to lignin may play a role in alteration of wood hygroscopicity as well. Tjeerdsma, et al. (1998) hypothesized that heat enhances the demethoxylation of guaiacyl and syringyl units in lignin, which increases the amount of reactive phenolic lignin sites available for reaction. Once the lignin demethoxylation

and cross-linking of free phenolic units that occurred at approximately 220°C formed furfural compounds and acetic acid, a more rigid structure was created around cellulose microfibrils and hindered water molecules' penetration to the cell wall (Tjeerdsma, et al., 1998).

3.5 **Conclusions**

This work assessed how the heat and pressure of hotpressing and their interaction modify wood properties. The combination of heat and pressure altered specifically the viscoelastic properties of absolutely dry hybrid poplar wood. The hotpressing conditions were found to significantly increase the specific gravity and stiffness of the wood. In this study, hotpressing was observed to have a significant effect on the increase of the hotpressed wood stiffness, irrespective of its density effect. Conversely, the hotpressing did not significantly affect the loss modulus and the drop in storage modulus values evaluated by thermal scan from 30°C to 120°C, or the loss peak observed in the range of 50°C.

The increase in wood stiffness resulted mainly from an increase in crystallinity. This could be related to the reduction of amorphous hemicelluloses and less-ordered celluloses. This could also drive the formation of a more ordered cellulose structure, thereby increasing crystallinity. Movement of cellulose chains was limited, and wood samples maintained their stiffness at 250°C. This explains the increase in stiffness and the low hygroscopicity of hotpressed samples. Further chemical analysis, such as an analysis of lignin and carbohydrates in hotpressed samples, could provide a deeper understanding of hotpressing's effect on the physical, chemical, and the viscoelastic properties of wood.

This study found that hotpressed hybrid poplar samples were less hygroscopic, especially when pressed at higher temperatures with some adsorbed moisture, in particular, hotpressing at

0% MC and 250°C showed the least hygroscopic behavior. This suggests that moisture and pressing temperature, as well as how they interact together, contribute to physical and viscoelastic property changes during hotpressing. The study evaluated the viscoelastic properties of wood hotpressed at extreme temperatures of 150°C and 250°C under dry conditions, and utilized dynamic mechanical analysis and master curve construction. Master curves were smooth, and superposed well with the addition of a vertical shift for the loss modulus. Results showed that the breadth of log frequency of hotpressed samples was the same as that of the control. This indicates that the temperature- and time-dependent properties of wood polymers were not significantly altered by hotpressing, a surprising result that countered our original hypothesis. However, the fact that there was no difference in master curve shape and frequency range could be due to the fact that the isotherms were very flat, with a gradual storage modulus decrease, and were highly dependent on the application of vertical shift. The vertical shift in this study was mainly applied to the loss modulus.

3.6 **References**

Almeida, G., Brito, J.O., & Perre, P. (2009). Changes in wood-water relationship due to heat treatment assessed on micro-samples of three *Eucalyptus* species. *Holzforshung, 66*, 80–88.

Akerholm, M., Hinterstoisser, B., & Salmen, L. (2004). Characterization of the crystalline structure of cellulose using static and dynamic FT-IR spectroscopy. *Carbohydrate Research. 339*, 569–578.

Backman, A.C. & Linberg, K.A. (2001). Differences in wood material responses for radial and tangential direction as measured by dynamic mechanical thermal analysis. *Journal of Materials Science, 36,* 3777–3783.

Bhuyian, Md. T.R., Hirai, N., & Sobue, N. (2000). Changes of crystallinity in wood cellulose by heat treatment under dried and moist conditions. *Journal of Wood Science*, *46*, 431–436.

Boonstra, M.J., Rijsdijk, J.F, Sander, C., Kegel, E, Tjeerdsma, B., Militz, H., Van Acker, J., & Stevens, M. (2006). Microstructural and physical aspects of heat treated wood. Part 2. Hardwoods. Maderas. *Ciencia Y. Tecnologia, 8* (3), 209–217.

Bowyer, J.L., Shmulsky, R., & Haygreen, J.G. (2003). Forest products and wood science: An introduction. (4th ed.). Ames, Iowa: Blackwell Publishing.

Duperray, B. and Leblanc, J.L. (1982). The time-temperature superposition principle as applied to filled elastomers. *Kautschuk +Gummi Kunststoffe, 35*, 298–307.

Fengel, D. & Wegener, G. (1984). Wood: Chemistry, ultrastructure, and reactions. New York: Walter de Gruyter.

Ferry, J.D. (1980). Viscoelastic properties of polymers, (2nd ed.). New York: John Wiley and Sons.

Gardner, D.J., Gunnells, D.W., Wolcott, M.P., & L. Amos (1993). Changes in wood polymers during the pressing of wood-composites. In J. F. Kennedy, G. O. Phillips and P. A. Williams, (Eds.) *Cellulosics, Chemical, Biochemical and Material Aspects (pp. 513–518).* New York: Ellis Horwood.

Hakkou, M., Petrissans, M., El Bakali, I., Gerardin, P., & Zoulalian, A. (2005a). Wettability changes and mass loss during heat treatment of wood. *Holzforschung, 59*, 35–37.

Hakkou, M., Petrissans, M., & Zoulalian, A., & Gerardin, P. (2005b). Investigation of wood wettability changes during heat treatment on the basis of chemical analysis. *Polymer Degradation and Stability, 89*, 1–5.

Hsu, W.E., Schwald, W., Schwald, J., & Shields, J.A. (1988). Chemical and physical changes required for producing dimensionally stable wood-based composites. Part I: Steam pretreatment. *Wood Science and Technology, 22*, 281–289.

Ito, Y., Tanahashi, M., Shigematsu, M., & Shinoda, Y. (1998). Compressive molding of wood by high pressure steam treatment: Part 2: Mechanism of permanent fixation. *Holzforschung, 52*, 217–221.

Jafarpous, G., Dantras, E., Boudet, A., & Lacabanne, C. (2008). Molecular mobility of poplar cell wall polymers studied by dielectric techniques. *Journal of Non-Crystalline Solids,* 354, 3207–3214.

Kelley, S.S., Rials, T.G., & Glasser, W.G. (1987). Relaxation behaviour of the amorphous components of wood. *Journal of Materials Science, 22*, 617–624.

Kolin, B. & Janezic, T.S. (1996). The effect of temperature, density, and chemical composition upon the limit of hygroscopicity of wood. *Holzforschung, 50*, 263–268.

Korkut, S., Akgul, M., & Dundar, T. (2008). The effects of heat treatment on some technological properties of Scots pine (*Pinus sylvetris* L.) wood. *Bioresource Technology, 99*, 1861–1868.

Kotilainen, R., Alen, R., & Arpiainen, V. (1999). Changes in the chemical composition of Norway spruce (*Picea abies*) at 160–260ºC under nitrogen and air atmospheres. *Paperi Ja Puu-Paper and Timber, 81*(5), 384–388.

Kotilainen, R., Alen, R., Toivanen, T. (2001). Chemical changes in black alder (*Alnus glutinosa*) and European aspen (*Populus tremula*) during heating at 150–220º in a nitrogen atmosphere. *Cellulose Chemical Technology, 35*(3-4), 275–284.

Kutnar, A., Kamke, F.A., and Sernek, M. (2009). Density profile and morphology of viscoelastic thermal compressed wood. *Wood Science Technology, 43*, 57–68.

Mohanty, S., and Nayak, S.K. (2007). Dynamic and steady state viscoelastic behavior and morphology of MAPP treated PP/sisal composites. *Materials Science and Engineering, 443*, 202–208.

Navi, P. & Girardet, F. (2000). Effects of thermo-hydro-mechanical treatment on the structure and properties of wood. *Holzforschung, 54*, 287–293.

Navi, P. & H**e**ger, F. (2004). Combined densification and thermo-hydro-mechanical processing of wood. *MRS Bulletin, 29* (5), 332–336.

Nelson, M.L. & O'Connor, R.T. (1964). *Journal of Applied Polymer Science.*, 1325–1341.

Obataya, E., Norimoto, M., & Gril, J. (1998). The effects of adsorbed water on dynamic mechanical properties of wood. *Polymer, 39* (14), 3059–3064.

Osman, N., McDonald, A.G. & Laborie, M-P. (2009). Thermal Compression of Hybrid Poplar Wood: Vibrational spectroscopy analysis on the effects and behaviors of hot-pressed heat treatment (abstract). In: FPS 63rd International Convention, June 21-23; Boise, Idaho. Madion (WI): Forest Products Society.

Ott, L.R. (1999). An introduction to statistical methods and data analysis, (4th ed.). Belmont, California: Wadsworth Publishing Company.

Penneru, A.P., Jayaraman, K., & Bhattacharyya, D. (2006). Viscoelastic behavior of solid wood under compressive loading. *Holzforschung, 60* (3), 294–298.

Reinprecht, L., Kacik, F., & Solar, R. (1999). Relationship between the molecular structure and bending properties of the chemically and thermally degraded maplewood. *Cellulose Chemistry and Technology, 33*, 67–79.

Repellin, V. & Guyonnet, R. (2005). Evaluation of a heat-treated wood solvent uptake by differential scanning calorimetry in relation to chemical composition. *Holzforschung, 59,* 28–34.

Sun, N., Das, S., & Frazier, C.E. (2007). Dynamic mechanical analysis of dry wood: Linear viscoelastic response region and effects of minor moisture changes. *Holforschung, 66*, 28–33.

Tabarsa, T. & Chui, Y. (1997). Effect of hot-pressing on properties of white spruce. *Forest Products Journal, 47*(5), 71–76.

Tjeerdsma, B.F., Boonstra, M., Pizzi, A., Tekely, P., & Militz, H. (1998). Characterization of thermally modified wood: Molecular reasons for wood performance improvement. *Holz als Roh- und Werkstoff, 56*, 149–153.

Wolcott, M.P., Kamke, F.A., & Dillard, D.A. (1990). Fundamentals of flakeboard manufacture: Viscoelastic behavior of wood components. *Wood and Fiber Science, 22* (4), 345–361.

Yildiz, U.C., Yildiz, S., & Gezer, E.D. (2005). Mechanical and chemical behavior of beech wood modified by heat. *Wood and Fiber Science, 37*(3), 456–461.

CHAPTER 4 THE IMPACT OF HOTPRESSING ON LIGNIN IN SITU SOFTENING

4.1 Introduction

Hotpressing is an important step in wood-based composites manufacturing, and is achieved by submitting wood to a compressive force at an elevated temperature. During hotpressing, processing temperature and wood moisture content (MC) play a substantial role in the modification of wood polymers' chemical, physical, and viscoelastic properties, which were discussed in Chapter 3. These changes, in turn, affect the densification and performance of mat consolidation (Wolcott, et al., 1990). Pressing temperature and moisture content impact the dry wood system, but in the glassy state, polymer chains are immobilized and configurational changes are limited; only gradual viscoelastic changes have been observed (Ferry, 1980). Conversely, the viscoelastic functions of polymers are highly dependent on temperature near the transition region between the glassy and rubbery states, while maintaining time dependence. Viscoelastic behavior is noted to be distinct around polymers' thermal softening. It is important to understand the phenomenon since typical temperatures for wood-based composites manufacturing processes are often in the range of the wood polymers' thermal softening, i.e., lignin glass transition. Because the physical, chemical, and viscoelastic changes caused by hotpressing affect the quality of the end product, the manufacturing industry will benefit from having more control over these changes. We hypothesize that the lignin glass transition is impacted by hotpressing, and that the pressing temperature and wood moisture content interact in this process.

4.1.1 *Thermal softening of wood polymers*

Degradation of wood polymers is an inevitable result of the thermal softening or glass transition (T_g) in dry state. Under dry conditions, the T_g of extracted lignin and hemicelluloses are around 134–235ºC and 167–217ºC, respectively (Goring, 1963), while the T_g for the wood polymers cellulose, hemicellulose, and lignin range from 200–250ºC (Back & Salmen, 1982). Extracted wood components exhibit different T_g, compared to those evaluated in situ, because the in situ glass transition is strongly influenced by interaction with other wood constituents. The thermal softening and viscoelastic behavior of lignin and hemicelluloses are quite moisture-sensitive, and the thermal softening of amorphous polymers has been found to decrease as water sorption and diluent uptake increases (Goring, 1963; Irvine, 1984; Kelley, et al., 1987). Under water-saturated conditions, isolated cellulose and hemicelluloses exhibit thermal softening at close to 0ºC (Irvine, 1984). The depression of the glass transition with moisture is due to its plasticizing effect, which allows easier chain movements (Kelley, et al., 1987). Indeed, the glass transition of those isolated amorphous polymers differs greatly compared to that of the in situ material due to the absence of neighboring interactions.

Moisture is necessary to detect the glass transition of amorphous polymers and a careful moisture control is needed. To ease the complication, many studies of viscoelastic properties were conducted for wood swollen with water and solvent such as glycols (Sadoh & Ohgoshi, 1974; Sadoh, 1981). In the earlier study, the in situ glass transition of lignin was detected at around 80ºC using a forced oscillation in torsion apparatus for both water-saturated wood and ethylene glycol-swollen wood. Using a differential thermal analyzer (DTA), Irvine (1984) showed clearly the effects of moisture in wood polymers and reported the water-saturated lignin glass transition in the 60–90ºC range.

4.1.2 *Viscoelastic properties evaluation via time-temperature superposition*

Salmen (1984) first demonstrated the ability of dynamic mechanical measurement to detect in situ lignin glass transition, and applied the principle of time-temperature equivalence to the lignin glass transition. This was successfully expressed with the Williams-Landel-Ferry (WLF) equation. Salmen's work represented a breakthrough in the application of the time-temperature superposition (TTS) principle for master curve construction on wood, by relating the temperature dependence of lignin relaxation to wood's mechanical properties. The WLF equation is described in Equation 4-1 (Ferry, 1980):

$$\log a_\tau = \log \frac{\tau(T)}{\tau(T_r)} = \frac{-C_1(T - T_r)}{C_2 + (T - T_r)} \qquad \text{Equation 4-1}$$

where a_τ is a ratio of relaxation time at the reference temperature $\tau_{(Tr)}$ and the relaxation time at a specific temperature $\tau_{(T)}$, C_1 and C_2 are WLF constants. The WLF constants were once considered universal with values of C_1=16.7 and C_2=51.6K for many amorphous polymers when referenced to the glass transition. However, it has been noted that different values apply for different polymers (Ngai & Roland, 1993). The empirical modeling proposed by Williams, Landel, and Ferry, who constructed the TTS principle and the WLF equation, successfully describes the viscoelastic properties of complex composites such as wood (Salmen, 1984; Kelley, 1987). The applicability of the WLF equation to the viscoelastic behavior of polymers at T_g suggests that a common phenomenon occurs around the glass transition that is related to the viscoelastic properties of glass.

4.1.3 *Cooperativity analysis to describe molecular motion*

At a glass transition region, segmental relaxation of amorphous polymers causes temperature dependence to deviate from Arrhenius behavior (Ferry, 1980). Plazek and Ngai proposed a coupling model that aids in interpreting the correlation of time and temperature dependence for the segmental relaxation of polymers at the glass transition temperature. The following equation (Equation 4-2) describes the effect of intermolecular coupling in molecular motion:

$$\tau^*(T) = [((1-n))\omega_c{}^n \tau_0(T)]^{1/(1-n)} \qquad \text{Equation 4-2}$$

where τ^* represents relaxation time at temperature T, τ_0 * represents primitive relaxation time, n is the coupling constant range from 0 to 1.0, and ω_c is the cross-over frequency for the independent relaxation or couple relaxation. The coupling constant represents the strength of non-bonded molecules influencing the segmental motion of neighboring molecules (Ngai & Roland, 1993). This interaction is called cooperativity. The segmental motion is amplified near the glass transition, and therefore the correlation of the n and T_g can be used to explain molecular behavior. If the value of n is zero, the equation is simply an exponential relaxation function with a characteristic relaxation time of τ_0. This is a simple Maxwell model, and means that no cooperativity occurs. A higher value for the coupling constant, n indicates a higher intermolecular interaction between the segment motions of neighboring molecules. The more intermolecular coupling interaction that occurs, the bigger the distribution of the relaxation mechanism, since segmental motion is influenced by surrounding molecules. The coupling model described by Plazek & Ngai (1991) is shown in Equation 4-3.

$$(1-n)\log a_T = (1-n)\log\frac{\tau^*(T)}{\tau^*(T_r)} = \frac{-C_1\left(\frac{T-T_g}{T_g}\right)}{C_2+\left(\frac{T-T_g}{T_g}\right)} \qquad \text{Equation 4-3}$$

The constants C_1=5.49 and C_2=0.141 for this model apply to many polymers and are bound to be universal (Plazek & Ngai; 1991). This could be because of equal temperature dependence for primitive relaxation. The coupling constant, n, can be calculated by plotting the shift factor obtained from time-temperature superposition on the fractional deviation of temperature $(T-T_g)/T_g$. The coupling constant bears structural characteristics of the polymer backbone, such as steric hindrance, polarity, and chain backbone symmetry (Ngai & Roland, 1993). Salmen and Olsson (1998) proposed that the thermal softening of one wood polymer was influenced by other wood polymers and therefore, the postulated interaction was significant in affecting wood polymers' relaxation behavior. Laborie, et al. (2004) demonstrated the applicability of cooperativity analysis for lignin glass transition in wood. This suggests that cooperativity analysis by Plazek and Ngai (1991) can also be applied to in situ lignin glass transition of hotpressed wood and be utilized to detect changes in thermal softening behavior caused by hotpressing.

Attempts to correlate physical and chemical changes during hotpressing have been numerous. However, exactly how these chemical changes relate to viscoelastic changes, and how they are, in turn, affected by wood moisture content and pressing temperature, has not been addressed. Thermal softening is an important parameter in wood-based composites manufacturing. We hypothesize that there is a correlation between wood moisture content and pressing temperature, causing changes in the in situ thermal softening of lignin and the intermolecular cooperativity associated with this transition.

4.2 **Objectives**

The objective of this work is to investigate the impact of hotpressing conditions (wood moisture content and pressing temperature) on the chemical, physical, and viscoelastic properties of hybrid poplar wood. This chapter aims to 1) explore the impact of hotpressing on the thermal softening of lignin, and 2) investigate the intermolecular interaction among polymers affected by hotpressing conditions.

4.3 **Materials and Methods**

4.3.1 *Sample preparation and hotpressing treatments*

Wet hybrid poplar OP-367 supplied by Potlatch Corporation was sliced into flatsawn veneers (Figure 3.1). The labeling, veneers selection, conditioning, and hotpressing were conducted in a similar manner as previously explained in Chapter 3. Hotpressing conditions were selected based on tests of the impacts of temperature and moisture content and their possible interactions (Figure 3.1). Two moisture contents (0% and 9%) and three hotpressing temperatures (150°C, 200°C and 250°C) were selected, resulting in 6 hotpressing conditions or treatments (Table 3-1). Veneers of 10 x 10 cm with a thickness of 2.3 mm in nominal dimensions were hotpressed for 5 minutes in a 46 x 46 cm Wabash hot press of 3.4 MPa under various conditions of wood moisture content and hotpressing temperature. Upon hotpressing, sample thickness was reduced to approximately 1 mm.

4.3.2 *Solvent Uptake*

Control samples were rectangular and flatsawn, 50 mm long along the grain by 12 mm wide by 2.3 mm thickness. Hotpressed samples were 1 mm thick**.** Before testing, freeze-dried

samples (<1% moisture content) were kept under vacuum in a desiccator with P_2O_5 until solvent uptake analysis. Since solvent uptake has been shown to influence the relaxation of polymer chains, complete saturation was desired. Ethylene glycol (EG) was chosen as the diluent because its high boiling point (approximately 150ºC) provided a large experimental temperature window. Solvent uptake relates to the sorption of bound water, and EG, a polar solvent, behaves like water in plasticizing the cell wall. Saturation was achieved by immersing freeze-dried wood samples (<1% moisture content) in an ethylene glycol bath under atmospheric pressure at 120±5ºC. After samples were conditioned for 2 hours (or 3 hours for samples hotpressed at 0% MC and 150ºC) in the EG bath, they reached full saturation. Samples were then ready for viscoelastic measurement. Mass of the freeze-vacuumed dried samples was recorded before submersion (w_{dry}), after submersion and before the strain scan, and after viscoelastic measurements. The percent of solvent uptake (mass gained) was calculated as follows (Equation 4-4):

$$solvent\ uptake\ (\%) = \frac{(mass_{wet} - mass_{dry})}{mass_{dry}} * 100\% \qquad \text{Equation 4-4}$$

The term "wet" implied saturation after each viscoelastic measurement (e.g., before and after the strain scan, after the temperature scan, and after the frequency scan). The percent of solvent uptake was recorded from at least 3 replicates for each treatment group.

4.3.3 *Dynamic mechanical analysis (DMA)*

The well-saturated control and hotpressed samples were tested in single cantilever bending mode along the grain with a Tritec 2000 DMA instrument. Samples were immersed in ethylene glycol in a 100 mL aluminum cup located in the DMA furnace throughout the

viscoelastic measurements. DMA tests were then performed in the linear viscoelastic range, as determined by strain scans performed at the most extreme test temperature possible without significant thermal degradation (120°C). The furnace was cooled at approximately 5°C/min to 25 ± 2°C using liquid nitrogen prior to the temperature scan, which was performed from 30°C–120°C at 1 Hz and a heating rate of 2°C/minute. The furnace was then cooled again (5°C/min) and subjected to a frequency sweep from 0.005 Hz to 50 Hz at 10°C intervals from 30°C to 120°C. This step isothermal frequency sweep utilized a heating rate of 1.5°C/min. The storage and loss moduli (E' and E") data from the step frequency sweeps were then used to develop master curves using the TTS (Ferry, 1980). For each sample group (the control and the 6 hotpressing conditions), at least triplicate DMA tests were conducted.

4.3.4 *Data analysis*

To analyze DMA results from the step isothermal frequency, a method proposed by Olsson and Salmen (1992) was used, by fitting the log storage modulus (log E')–temperature curves at each experimental frequency range to fifth-order polynomials (Figure 4.1).

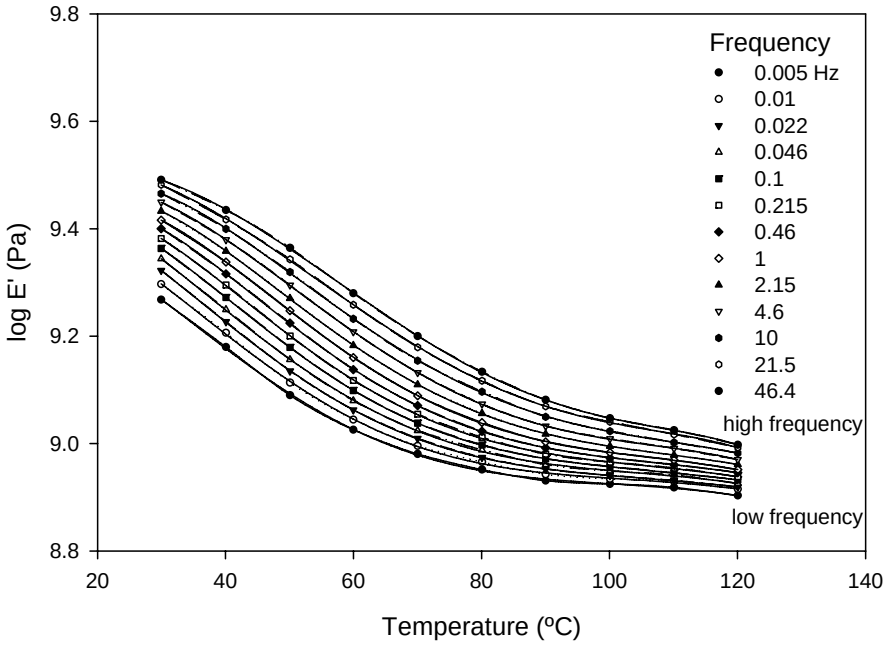

Figure 4.1 Polynomial fit of the logarithm of storage modulus as a function of temperature at a range of frequencies.

The best fit was then used to generate isotherms every ±3 or 4ºC (Figure 4.2). The temperature at which the maximum tan δ was found was the glass transition temperature (T_g), and was used as the reference temperature (T_r).

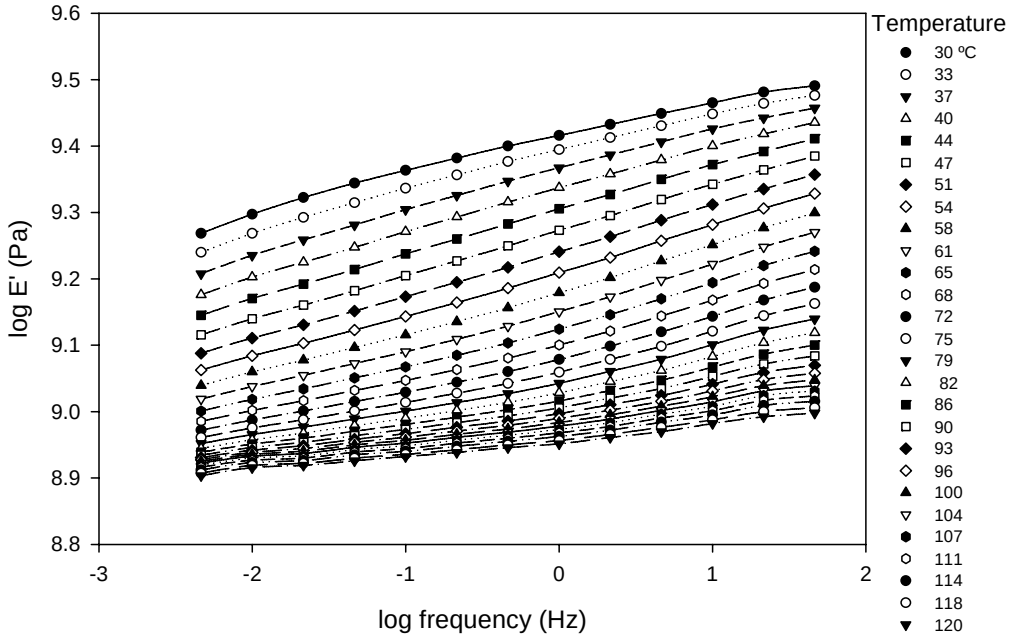

Figure 4.2 Isotherms from 30º–120ºC generated from the 5th order polynomial fit with increments of 3–4ºC.

Horizontal shifting factor, a_T, was then employed to superpose the adjacent isotherms to generate a master curve. The shift factor was obtained and the WLF constants (C_1 and C_2) were determined by linearizing WLF equation into the form of Equation 4-9 as shown in Figure 4.3.

$$\frac{T-T_{ref}}{\log a_\tau} = \frac{-(T-T_{ref})}{C_1} - \frac{C_2}{C_1} \qquad \text{Equation 4-5}$$

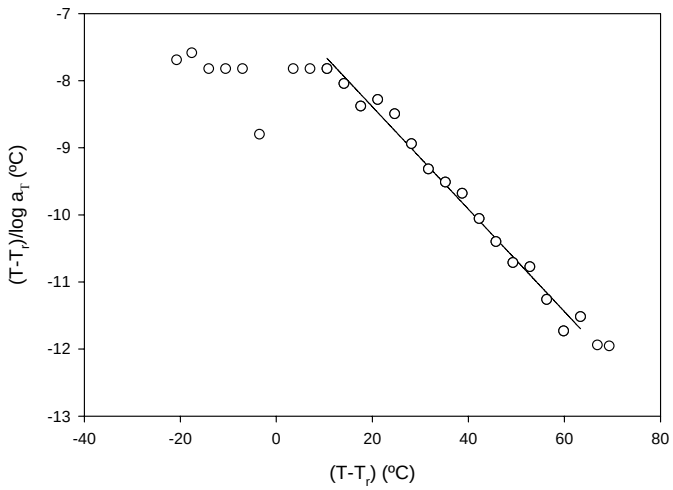

Figure 4.3 Determination of WLF constants (C_1 and C_2) using the linearized form of the WLF equation.

The basic principles of the relationships of time, temperature, and viscoelastic properties of polymers requires further understanding of molecular motion. At low temperatures, molecules are in a glassy state and tightly compacted, and as temperature increases, the material warms up and expands, creating more volume for chain motions and bond movements (Menard, 1999). The phenomenon of glass formation is explained by free volume theory in (Equation 4-6) (Ferry, 1980).

$$f(T) = f_g + \Delta\alpha_f (T - T_g) \qquad \text{Equation 4-6}$$

where T_g is the glass transition, f_g is the fractional free volume at the T_g not occupied by matter (V_f) to the total volume (V), and $\Delta\alpha_f$ is the difference in the thermal expansion coefficient ($\Delta\alpha_f$ = (1/v)(dv/dT)) between the liquid and glassy state. Viscosity and molecular rearrangement are solely dependent on free volume. Doolittle's equation relating temperature dependency to viscosity is similar to that of the free volume described in Equation 4-7 (Doolittle**,** 1951):

$$\ln \eta_0 = \ln A + B(v - v_f)v_f \qquad \text{Equation 4-7}$$

where A and B are empirical constants and η_o is viscosity. Knowing that

$f = \frac{V_f}{V}, a_T = \frac{\eta_T}{\eta_{T\,g}} = \frac{\tau_T}{\tau_{T_g}}$ then the shift factor a_T can be described by Equation 4-8:

$$\log a_T = \frac{B}{2.303}\left(\frac{1}{f} - \frac{1}{f_0}\right) \qquad \text{Equation 4-8}$$

Next, after substituting Equation 4-6 into Equation 4-7, the following equation is obtained

$$\log a_T = \frac{-B}{2.303 f_g} \frac{T - T_g}{(f_g / \alpha_f + T - T_g)} \qquad \text{Equation 4-9}$$

This is the same as the Williams-Landel-Ferry (WLF) (Equation 4-1) for shift factor temperature dependence (in a temperature window of Tg+100ºC) (Ferry, 1980).

Using Equation 4-9 and Equation 4-1, WLF constants can be equated to the thermal properties of polymers at a glass transition. These properties include the relaxation activation energy, the fractional free volume (f_g), and the difference thermal expansion of the free volume ($\Delta\alpha_f$) accordingly (Ferry, 1980). (Equation 4-10 and Equation 4-11):

$$C_1 = B / 2.303 f_g \qquad \text{Equation 4-10}$$

$$C_2 = f_g / \alpha_f \qquad \text{Equation 4-11}$$

where B is set equal to unity. For water-saturated wood, f_s varies among species from 0.021 for European spruce to 0.0144 for Norway spruce (Olsson & Salmen, 1992), while $\Delta\alpha_f$ ($x10^{-4}deg^{-1}$) has been reported to be 1.86 for the former and 0.82 for the latter. The activation energy at the softening region, $E_{a(WLF)}$, was calculated at the reference temperature ($T_r = T_g$), found using (Equation 4-12).

$$\Delta Ea_{(WLF)} = 2.303R(\delta(\log a_\tau) / \delta(1/T)) \qquad \text{Equation 4-12}$$

where T is the glass transition temperature and R is the gas constant. For in situ lignin glass transition of water-saturated wood, activation energy was estimated at around 450 kJ/mol (Salmen, 1984). In addition, the shift factor was normalized to the fractional deviation from the $T_{g,}$ resulting in the plot of log a_T vs. $(T-T_g)/T_{g\,,}$ and yielding cooperativity plots. Further, individual cooperativity plots for each specimen were constructed, as well as an average cooperativity plot using the method explained by Jensen (1999).

4.3.5 *Statistical analysis*

First, properties measured were tested for their correlation to solvent uptake . When a correlation was observed, covariance (ANCOVA) was analyzed at α level of 0.05 to evaluate the effect of treatments on properties measured for hotpressed and control samples. Properties measured included storage modulus (E'), loss modulus (E"), E' decrease ($[E'_{(30°C)}- E'_{(120°C)}]/ E'_{(30°C)}$*100%), lignin glass transition (T_g), activation energy (E_a), and solvent uptake, where the last was hypothesized to be a covariable. Using ANCOVA, the effect of hotpressing treatment on properties could be determined regardless of the impact on wood solvent uptake. To normalize properties, the properties were divided by the percentage of solvent uptake before the strain scan. An analysis of variance (ANOVA) was conducted at α level of 0.05 for normalization products, and for the properties that showed no correlation with solvent uptake. When a significant difference was detected, Tukey-Kramer post-hoc analyses were also conducted to establish groupings among all groups (treated and control). These analyses were conducted on various measured properties including solvent uptake, E' and E" at 30°C and 120°C along with the % E' drop between these temperatures, as well as the tan δ, E_a, f_g, α_g, Δlog frequency, and coupling constant (n). The statistical evaluation was performed using SAS 9.1 statistical software.

4.4 **Results and Discussion**

4.4.1 *Solvent Uptake*

Changes in dimensions, especially in thickness, were observed along with differences in wood mass increase. Nonetheless, the quantification of solvent uptake was not as accurate as mass measurement, so for this study, the solvent uptake of hybrid poplar hotpressed at different conditions was used to quantify the effect of hotpressing on solvent absorption. The liquid bath for all samples turned yellowish brown after saturation, which has been found to be due to solvolysis (Bouchard, et al., 1993). Samples hotpressed at higher temperatures created a darker solution color. However, there was no further study on solvent color after saturation. For ease of terminology, samples hotpressed at 9% wood moisture content (MC) and at pressing temperatures (T) of 150ºC , will be noted as (9%, 150), and this (MC%,TºC) notation will be used throughout the paper.

Table 4.1 shows the average solvent uptake data for control and hotpressed hybrid poplar wood before and after viscoelastic measurement, based on the freeze-dried mass. All samples, regardless of hotpressing conditions, tripled their dry mass upon saturation. Wood samples were completely saturated after 2 hours (3 hours for 9%, 150ºC) submersion in EG. Solvent uptake before strain scan (the beginning of viscoelastic measurement) and after lengthy frequency scan measurement at ~20hours (the last viscoelastic measurement) differed by approximately 30% at maximum (control samples) and 4% at minimum (9%, 250ºC) (Table 4.1). Despite this increase, solvent uptake of hotpressed samples relative to the control was negligible, indicated by the same Tukey-Kramer grouping for the 0% and 9%, for solvent uptake before the strain scan (solvent uptake$_{bef}$), and after the frequency scan (solvent uptake$_{af}$). Since the strain scan was the first DMA measurement, it made sense to use solvent uptake before the strain scan as the basis for the

properties normalization used in this study. Figure 4.4 shows the trend of solvent uptake for control and hotpressed samples before viscoelastic measurements and its Tukey-Kramer's grouping.

It was observed that hotpressing conditions significantly affected solvent absorption (ANOVA p value = 0.005) (Table 4.1). All hotpressed samples had the same solvent uptake as the control group, but among hotpressed samples there was solvent uptake variation depending on the hotpressing condition. Samples hotpressed at pressing temperature of 250ºC at 0% MC and 9% MC exhibited the lowest solvent uptake, at 172 ± 9% for (9%, 250ºC) and 229 ± 51% for (0%, 250ºC). In fact, the hotpressed samples at 9% MC and 250ºC displayed the least solvent uptake, which differed significantly from other samples hotpressed at 150 and 200ºC. Hotpressing at 250ºC produced wood with a lower absorption of polar solvent EG.

Table 4.1 Average solvent uptake for control and hotpressed hybrid poplar wood in EG before and after viscoelastic measurement.

	Solvent uptake (%)	
Treatment	Before strain scan	After frequency scan
Control	245 ± 27 A,B	278 ± 21 A,B
9%, 150ºC	306 ± 36 A	329 ± 36 A
9%, 200ºC	281 ± 44 A	293 ± 46 A
9%, 250ºC	172 ± 9 B	177 ± 9 B
0%, 150ºC	283 ± 29 A	304 ± 36 A
0%, 200ºC	274 ± 64 A	291 ± 66 A
0%, 250ºC	229 ± 51 A,B	229 ± 5 A,B
ANOVA p value	0.0051	0.0027

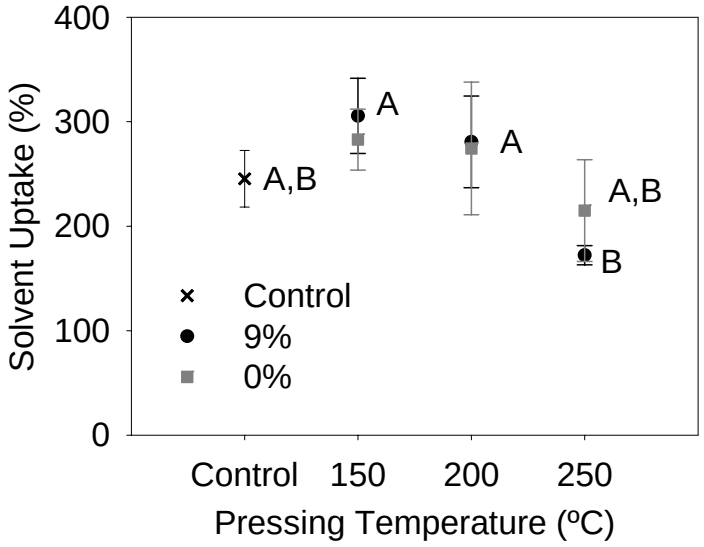

Figure 4.4 Average solvent uptake for control and hotpressed hybrid poplar wood in EG for hotpressing at both 9% and 0% wood moisture content before the viscoelastic measurement (at least 3 replicates).

This indicated that hotpressing at 250ºC drastically changed the chemistry or physical attributes of wood polymers and promoted less affinity toward polar solvent. EG (molecular mass of 62 gram/mol) is a polar solvent that behaves like water, acting as a plasticizer in solvent uptake wood but has two hydroxyl groups. Lower EG uptake may be explained by reduction of hydroxyl groups available as well as lower accessibility of polar groups to bind with hydroxyl groups in the wood polymers. In fact, hemicelluloses degrade at temperatures above 200ºC (Hsu, 1988; Reinprecht, 1999) and the loss of amorphous components consequently led to the reduction of hydroxyl groups available to bond with EG. The wood vessels became deformed by compression, and available pore sites for the penetration of solvent were reduced dramatically. This created a tighter space and a lower amount of lumens available for EG to position itself in the cell wall and bind with wood polymers through hydrogen bonding.

4.4.2 *Dynamic mechanical analysis (DMA) and Cooperative Analysis*

4.4.2.a Glass transition temperature

Submersion dynamic mechanical analysis was performed to detect the in situ lignin glass transition on EG plasticized hybrid poplar control wood and hotpressed wood. The applicability of DMA to detect in situ lignin glass transition in wood has been previously demonstrated (Laborie, et al., 2004). This experimental T_g, interchangeably called the apparent T_g in this paper, was determined at the temperature where the tan δ peak reached the maximum. Figure 4.5 illustrates typical DMA temperature scan results conducted in this study.

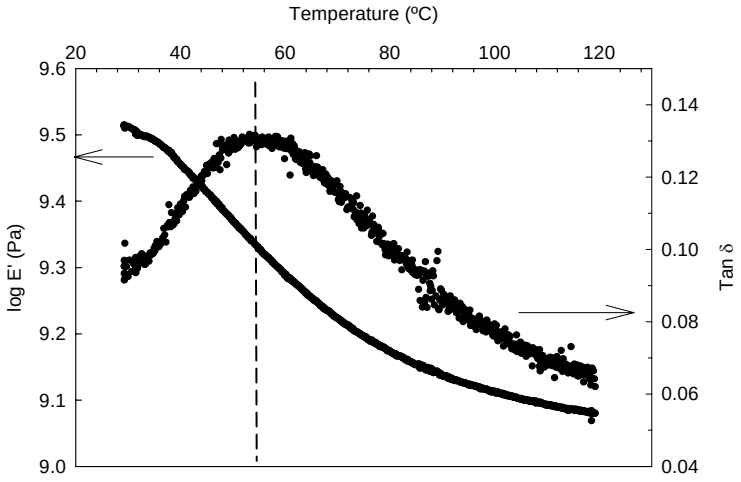

Figure 4.5 DMA temperature scan performed from 30–120°C at a heating rate of 2°C/min at 1Hz for EG plasticized hybrid poplar wood.

The storage modulus (E') dropped significantly as temperature increased. A tan δ peak was observed between 40 and 70ºC. The apparent T_g , $T_{g(App)}$, for control hybrid poplar wood saturated in EG evaluated at 1 Hz occurred at around 65 ± 8ºC. This is close to the findings of Laborie, et al. (2004), at 71ºC for yellow poplar evaluated at 2 Hz. Ethylene glycol has been found to behave in a similar manner with either water or PEG as a solvent uptake agent at

approximately of 80ºC (Sadoh & Ohgoshi, 1974; Sadoh, 1981).

Table 4.2 shows the wood solvent uptake and the glass transition of lignin for control and hotpressed hybrid poplar EG-saturated wood. Samples hotpressed at both 0% and 9% at 150ºC and 200ºC exhibited lower $T_{g(App)}$, ranging from 47 to 54ºC, while those hotpressed at 250ºC were similar to those of control at around 67 ± 2ºC. This corresponded well with solvent uptake (%) recorded before the strain scan, as shown in Figure 4.6a), where an inverse relationship between wood solvent uptake and $T_{g(App)}$ was noted (R^2=0.7073). When such a linear dependence was noted, it is reasonable to question whether a higher $T_{g(App)}$ for hotpressing samples at 250°C was strictly due to less solvent uptake or to hotpressing conditions independent of the solvent uptake. To answer this question, analysis of covariance (ANCOVA) was performed for hybrid poplar wood, using solvent $uptake_{bef}$ as a covariate.

Table 4.2 Average wood solvent uptake accompanied with the apparent and normalized glass transition temperature. (Letters are for Tukey-Kramer grouping).

Treatment	Solvent $uptake_{bef}$ (%)	$T_{g\,(App)}$ (ºC)	Normalized $T_{g\,(App)}$ (ºC) $T_{g\,(App)}$ /Solvent $uptake_{bef}$
Control	245 ± 27 A,B	65 ± 8	0.27 ± 0.06 A,B
9%, 150ºC	306 ± 36 A	50 ± 6	0.16 ± 0.03 C
9%, 200ºC	281 ± 44 A	47 ± 3	0.17 ± 0.02 C
9%, 250ºC	172 ± 9 B	67 ± 2	0.35 ± 0.05 A
0%, 150ºC	283 ± 29 A	53 ± 10	0.18 ± 0.04 C
0%, 200ºC	274 ± 64 A	54 ± 2	0.21 ± 0.04 B,C
0%, 250ºC	229 ± 51 A,B	67 ± 2	0.29 ± 0.07 A
ANOVA p value	0.0051		0.0001
ANCOVA treatment p value	-	0.0001	-
ANCOVA solvent uptake p value	-	0.9513	-

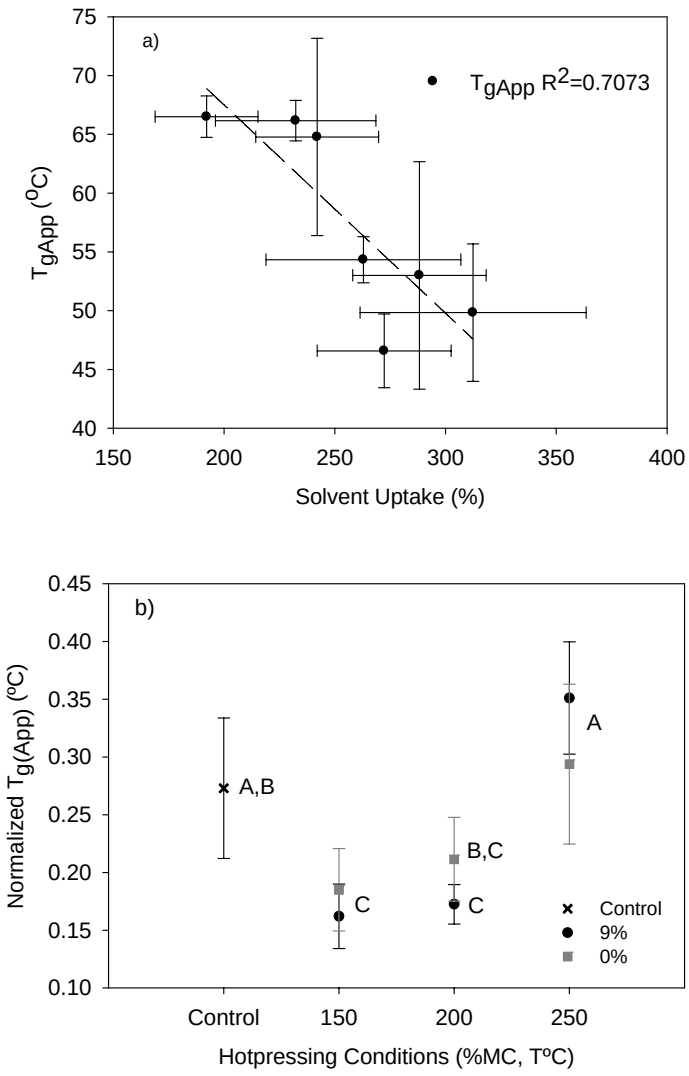

Figure 4.6 a) Relationship of wood solvent uptake to its apparent lignin glass transition; b) Normalized apparent lignin glass transition for control and hotpressed hybrid poplar wood.

To further analyze the influence of treatment irrespective of solvent uptake, $T_{g(App)}$ was normalized by dividing it by solvent uptake, leading to normalized apparent lignin glass transition, $nT_{g(App)}$ (Figure 3.6 a). Then $nT_{g(App)}$ for hotpressed samples differed significantly from control samples (ANOVA p value=0.0001) (Table 4.2). Hotpressing reduced $nT_{g(App)}$ by 60% from 0.27 ± 0.06 ºC to approximately 0.17 for conditions of 200ºC and (0%, 150ºC) (Table 4.2).

This was expected, because thermal treatment affects lignin chemistry such as its structure by cleavage of the β-O-4 linkages (Wikberg & Maunu, 2004) and demethoxylation of guaiacyl and syringyl units in lignin creating more condense lignin structure (Tjeerdsma, et al., 1998). Dwianto, et al. (1999) postulated that lignin cleavage occurred when wood was steamed below 200ºC. This depolymerization and cleavage of lignin creates lower molecular lignin-phenolic groups and thus explains the observed lower value of $nT_{g(App).}$ However, the decreased of $nT_{g(App)}$ hotpressed at 150 and 200ºC relative to the control and the higher temperature of hotpressing groups can be explained by work of Wikberg and Maunu (2004) reporting that the cleavage of the β-O-4 linkages in hardwood evaluated by NMR was more extensive compared to the depolymerisation of softwood lignin. This means that lower molecular weight of lignin in hardwood was created by broken of aryl ether linkages. Interestingly, samples pressed at the highest temperature displayed no change in $nT_{g(App)}$ relative to the control group.

In prolonged thermal treatment, continuous demethoxylation of guaiacyl and syringyl can thereby increase the amount of reactive hydroxyl lignin sites and thus it is possible in creating more condense lignin structure (Tjeerdsma, et al., 1998). The formation of complex networks resulting from the cross-linking of free phenolic units to furfural compounds and acetic acid may be responsible for an increased of $T_g,n_{(App)}$ from hotpressing at 250°C relative to other hotpressing conditions (Tjeerdsma, et al., 1998; Olsson & Salmen, 1992). The condensed structure of lignin displayed similar thermal softening to that of the control group.

Rapid hemicellulose decomposition and creation of free lignin phenolic units occurred above 200ºC (Tjeerdsma, et al., 1998; Kotilainen, et al., 1999). With prolonged thermal treatment, this decomposition and depolymerization may occur at lower temperatures—as low as 160ºC (Wikberg and Maunu, 2004). The reduction of carbohydrates and the molecular cleavage

of lignin facilitated the increased mobility of chain motion. With the alteration of space confinement, it was expected that relaxation behavior would change. In fact, continuous thermal application (above 220ºC) was likely to enhance lignin cross-linking and condensation (Gardner, et al., 1993; Tjeerdsma, et al., 1998).

4.4.2.b Dynamic moduli

Dynamic mechanical properties such as storage modulus, drop of storage modulus, and loss modulus were determined. The value of the rubbery modulus (E') of EG-saturated wood was similar to that reported by Laborie, et al. (2004), with a log E' of 9.5 Pa (E'=3.2 GPa). This appeared to be independent of lignin cross-link density (Olsson & Salmen, 1992).

Firstly, storage modulus was found to be linearly dependent to solvent uptake, as shown in Figure 4.7 (R^2 $E'_{(30°C)}$=0.60 and R^2 $E'_{(120°C)}$=0.66). An ANCOVA analysis found that both treatment (ANCOVA $E'_{(30°C)}$ pvalue=0.39 and $E'_{(120°C)}$=0.31) and solvent uptake (ANCOVA $E'_{(30°C)}$ p value=0.14 and $E'_{(120°C)}$=0.11) did not affect E' at all at an α level of 0.05 (Table 4.3). This is rather surprising, considering that the relationship between solvent uptake and E' was linear. However, the normalized storage modulus ($n'E_{(30°C)}$ p value=0.004 and $nE'_{(120°C)}$ p value=0.0012) showed a significant difference within treatments; however, there was no change relative to the control group. The $nE'_{(30ºC)}$ increased with pressing temperature, as noted on the 9% wood moisture content hotpressing samples.

To quantitatively compare the effect of treatments on wood's viscoelastic properties, the values of the storage modulus at 30°C and at 120°C were recorded, along with the relative drop in that temperature range (Equation 4-13).

$$E'_{decrease}(\%) = \frac{E'_{(30°C)} - E'_{(120°C)}}{E'_{(30°C)}} * 100 \qquad \text{Equation 4-13}$$

This E' decrease was significantly affected by treatment for hotpressed samples of 9%, 150°C and 9%, 200°C that exhibited a lower stiffness drop compared to the control group (ANOVA p value=0.0004) (Table 4.3) and independent of solvent uptake (Figure 4.8). The E' drop was approximately 55% to 65%. This data was comparable to the modulus drop calculated for water-saturated wood (found by strictly dividing the E'_{rubber}/E'_{glass}), as reported by Olsson and Salmen (1992).

Table 4.3 Average wood solvent uptake and storage modulus data, including its normalized data and evaluation of statistical analysis at α=0.05 (with at least 3 replicates) and ANOVA Tukey-Kramer groupings letters.

		Storage Modulus (GPa)		Normalized Storage Modulus = $E'_{(T°C)}$/Solvent $uptake_{bef}$		E'decrease Equation 4-13
Treatment	Solvent (%)	$E'_{(30°C)}$	$E'_{(120°C)}$	$nE'_{(30°C)}$	$nE'_{(120°C)}$	(%)
Control	245 ± 27	2.6 ± 0.8	0.9 ± 0.3	10.8 ± 3.9 A,B,C	3.8 ± 0.9 A,B,C	65 ± 4 A
9%, 150ºC	306 ± 36	2.0 ± 0.6	0.8 ± 0.2	6.7 ± 02.3 B,C	2.7 ± 0.9 C	60 ± 5 A,B
9%, 200ºC	281 ± 44	2.0 ± 0.6	0.9 ± 0.3	7.5 ± 2.3 B,C	3.4 ± 1.1 B,C	56 ± 2 B
9%, 250ºC	172 ± 9 B	3.0 ± 0.5	1.3 ± 0.2	16.1 ± 4.8 A	7.0 ± 1.7 A	56 ± 3 B
0%, 150ºC	283 ± 29	2.0 ± 0.4	0.7 ± 0.1	7.1 ± 1.8 B,C	2.6 ± 0.7 C	63 ± 5 A
0%, 200ºC	274 ± 64	3.0 ± 1.7	1.1 ± 0.8	12.0 ± 7.7 A,B,C	4.7 ± 3.4 A,B,C	62 ± 4 A,B
0%, 250ºC	229 ± 51	3.3 ± 1.0	1.3 ± 0.4	15.4 ± 8.9 A,B	6.1 ± 3.4 A,B	60 ± 1 A,B
ANOVA p	0.0051	-	-	0.0040	0.0012	0.0004
ANCOVA	treatment p value	0.3859	0.3085	-	-	-
ANCOVA	solvent uptake p value	0.1420	0.1087	-	-	-

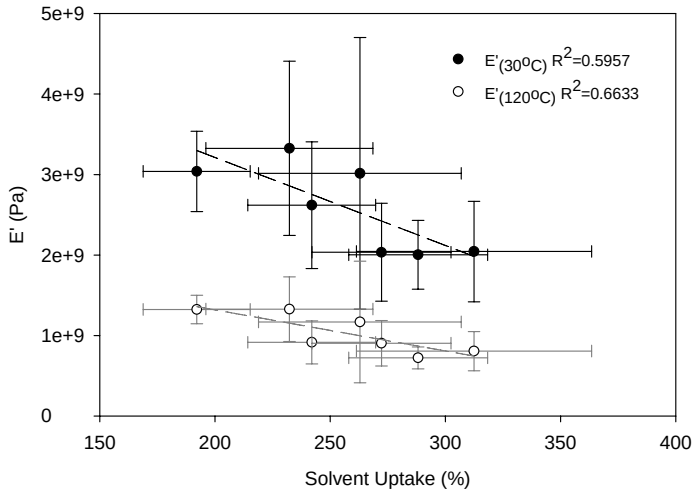

Figure 4.7 Relationship of wood solvent uptake to the storage modulus for both ($E'_{(30°C)}$ and $E'_{(120°C)}$).

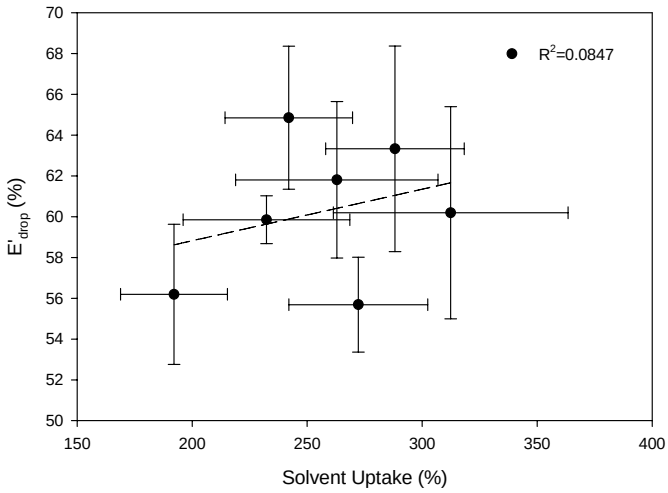

Figure 4.8 Relationship between solvent uptake and E'decrease [$(E'_{(30°C)}-E'_{(120°C)})/E'_{(30°C)}$].

To further delineate the effects of hotpressing conditions on loss modulus, the loss modulus for each group was normalized by its solvent $uptake_{bef}$, leading to normalized modulus properties, $nE''_{(T°C)}$ (Figure 4.9). ANOVA evaluation confirmed that the nE" for some hotpressed samples differed significantly from that of control samples (p value=0.0001) (

Table 4.4). Specifically, the Tukey-Kramer grouping indicated that regardless of moisture content, samples hotpressed at 250°C had an nE" of at least three times higher than control samples. As expected, the effects of hotpressing on the viscous component could be determined for plasticized wood but not dry wood (Chapter 3). In a dry state, wood polymers are in a glassy, plasticized condition and polymer chains are more mobile. Thus, viscoelastic measurement under plasticized conditions facilitates the detection of the increase of dissipated heat due to chain motion.

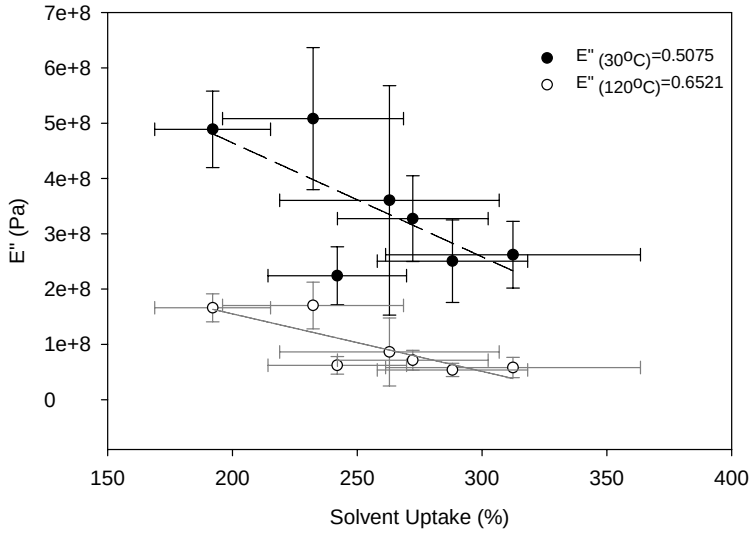

Figure 4.9 Relationship of wood solvent uptake to the loss modulus ($E"_{(30°C)}$ and $E"_{(120°C)}$).

This result implies that energy dissipated by hybrid poplar wood samples hotpressed at 250ºC were much higher compared to that of other treatment groups'. The amount of dissipated heat corresponded to an increase in chain mobility, which could be due to the increased number of shorter branch chains or lower molecular weight chains as a result of polymer degradation or bonds cleavage. The decomposition of polysaccharides during heat treatment (mainly

hemicelluloses and amorphous cellulose) possibly affected the increase of energy dissipated by the segmental chains since many bonds between hemicelluloses and lignin as well as between hemicelluloses and cellulose were broken, making chain movements were more feasible. It appears that hotpressing enchances the formation of smaller polymer molecules from hemicellulose and amorphous cellulose decomposition, and from lignin cleavages. This, in turn, induces rapid molecular movements during DMA experiments, and dissipates large amounts of heat at higher experimental temperatures.

Table 4.4 Average wood solvent uptake and loss modulus data, including normalized data and evaluation of statistical analysis at an α=0.05 (with at least 3 replicates) followed by ANOVA Tukey-Kramer groupings letters.

		Loss Modulus (10^8Pa)		Normalized Loss Modulus (MPa)= $E''_{(T°C)}$/Solvent $uptake_{bef}$	
Treatment	Solvent (%)	$E''_{(30°C)}$	$E''_{(120°C)}$	$nE''_{(30°C)}$	$nE''_{(120°C)}$
Control	245 ± 27 A,B	2.2 ± 0.5 C	0.60 ± 0.2 B	0.9 ± 0.2 C	0.3 ± 0.1 B
9%, 150ºC	306 ± 36 A	2.6 ± 0.6 B,C	0.58 ± 0.2 B	0.9 ± 0.3 C	0.2 ± 0.1 B
9%, 200ºC	281 ± 44 A	3.3 ± 0.8 A,B	0.86 ± 0.2 B	1.2 ± 0.3 C	0.3 ± 0.1 B
9%, 250ºC	172 ± 9 B	4.9 ± 0.7 A,B	1.66 ± 0.3 B	2.6 ± 0.6 A	0.9 ± 0.2 A
0%, 150ºC	283 ± 29 A	2.5 ± 0.8 C	0.54 ± 0.1 C	0.9 ± 0.3 C	0.2 ± 0.1 B
0%, 200ºC	274 ± 64 A	3.6 ± 2.1 A,B,C	0.86 ± 0.6 B	1.4 ± 0.9 B,C	0.3 ± 0.3 B
0%, 250ºC	229 ± 51 A,B	5.1 ± 1.3 A	1.7 ± 0.4 A	2.3 ± 81.2 A,B	0.8 ± 0.4 A
ANOVA p value	0.0051	-	-	0.0001	0.0001
ANCOVA treatment p value	-	0.0005	0.0001	-	-
ANCOVA solvent uptake p	-	0.0426	0.0353	-	-

It is notable that the thermal energy dissipated due to motion was expected to be small, since cross-linking limited molecular movements and segmental chain motions, indicated by higher apparent glass transition temperature. This indicates that lignin was not responsible for the increased loss of thermal energy due to molecular motion; in fact, cellulose chains of lower molecular weight were responsible. The storage and loss moduli were highly correlated to solvent uptake however, hotpressing was found to be significantly important in determining the stiffness and viscous component of hybrid poplar wood.

4.4.2.c Evaluation of time–dependent behavior and cooperativity analysis

Time-temperature superposition to describe the complete viscoelastic properties of hybrid poplar samples, resulted in smooth master curves for the logarithm of the storage modulus (log E') as a function of log frequency. Initially, the apparent lignin glass transition was used as the reference temperature for the construction of a master curve. The shift factor for each specimen was determined from master curves obtained by shifting the E' isotherm to the adjacent reference temperature. A typical master curve of hybrid poplar plasticized in EG both for E' and E" is presented in Figure 4.10.

It has been reported that the WLF equation describes the temperature-dependence of an amorphous polymer only at temperatures above glass transition. Below T_g, material properties such as density are not in equilibrium, and WLF behavior applies only to properties with equilibrium density. Many researchers have shown the applicability of WLF for describing the temperature-dependence of plasticized wood system (Salmen, 1984; Kelley, et al, 1987; Olsson & Salmen, 1992; Laborie, et al., 2004).

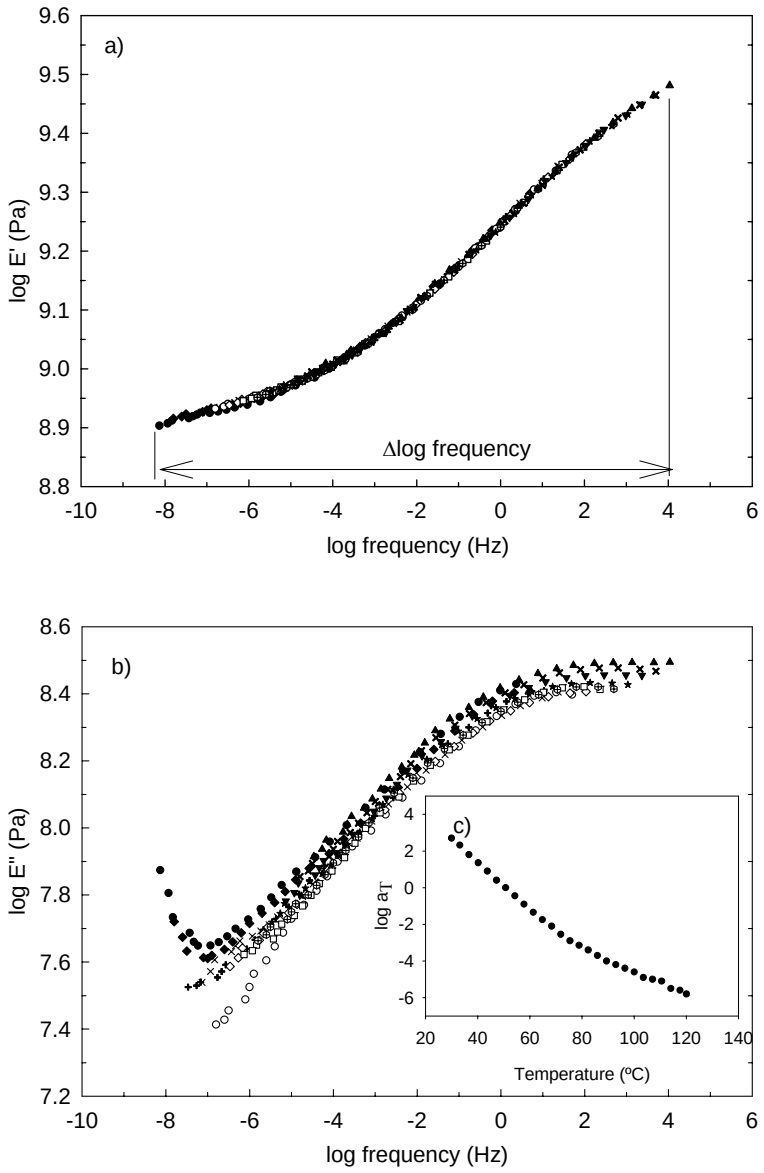

Figure 4.10 Illustration of smooth master curves for a) storage modulus and b) loss modulus using the same c) shift factor for EG plasticized hybrid poplar control wood referenced to T_g.

$T_{g(App)}$ was used as the reference temperature to obtain the shift factor from a master curve. Figure 4.11 shows the shift factor plotted against the temperature difference for the master curve of EG plasticized hybrid poplar wood. The equilibrium T_g which occurred at $T-T_g=0$ was observed to be actually 4ºC lower than the $T_{g(App)}$ (Figure 4.11). This equilibrium T_g was

interpreted as the temperature where the apparent T_g equals fitted values based on the WLF equation, thus the equilibrium T_g is referred to as $T_{g(WLF)}$. Therefore, in order to accurately describe viscoelastic behavior modeled by WLF equation, reconstruction of a master curve was performed by utilizing the newly determined glass transition $T_{g\,(WLF)}$. This shifting factor was later used in the cooperativity analysis.

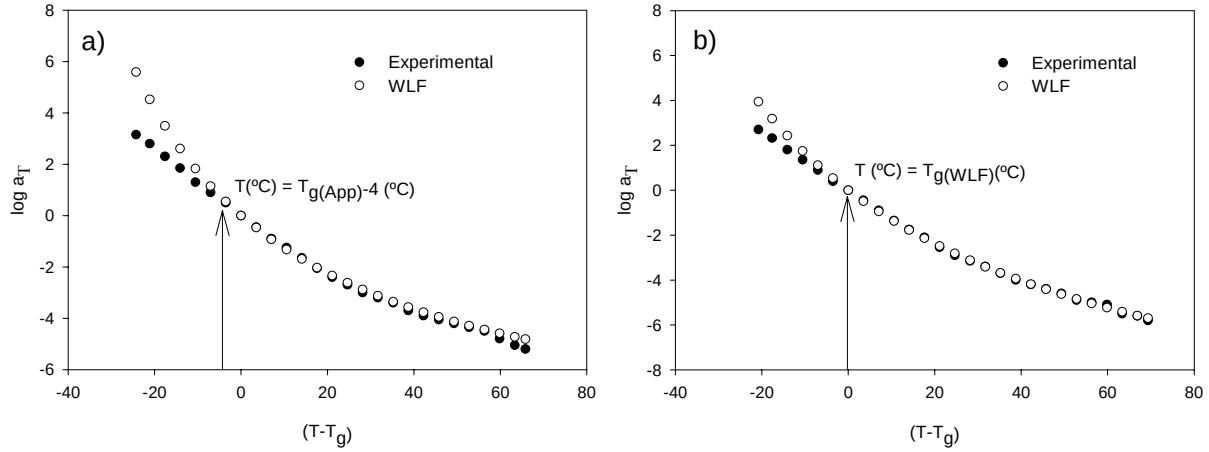

Figure 4.11 Determination of $T_{g(WLF)}$ from the observed apparent glass transition; shift factor obtained for EG plasticized hybrid poplar wood from 30ºC to 120ºC.

Figure 4.12 displays the master curve obtained after reconstruction using $T_{g(WLF)}$ as the reference temperature, and shows its reproducibility. Smooth master curves for the elastic component (log E' vs. log frequency) were attained on nearly all tested samples; however, the corresponding viscous component (log E" vs. log frequency) exhibited dispersion at the lower frequency and high temperature.

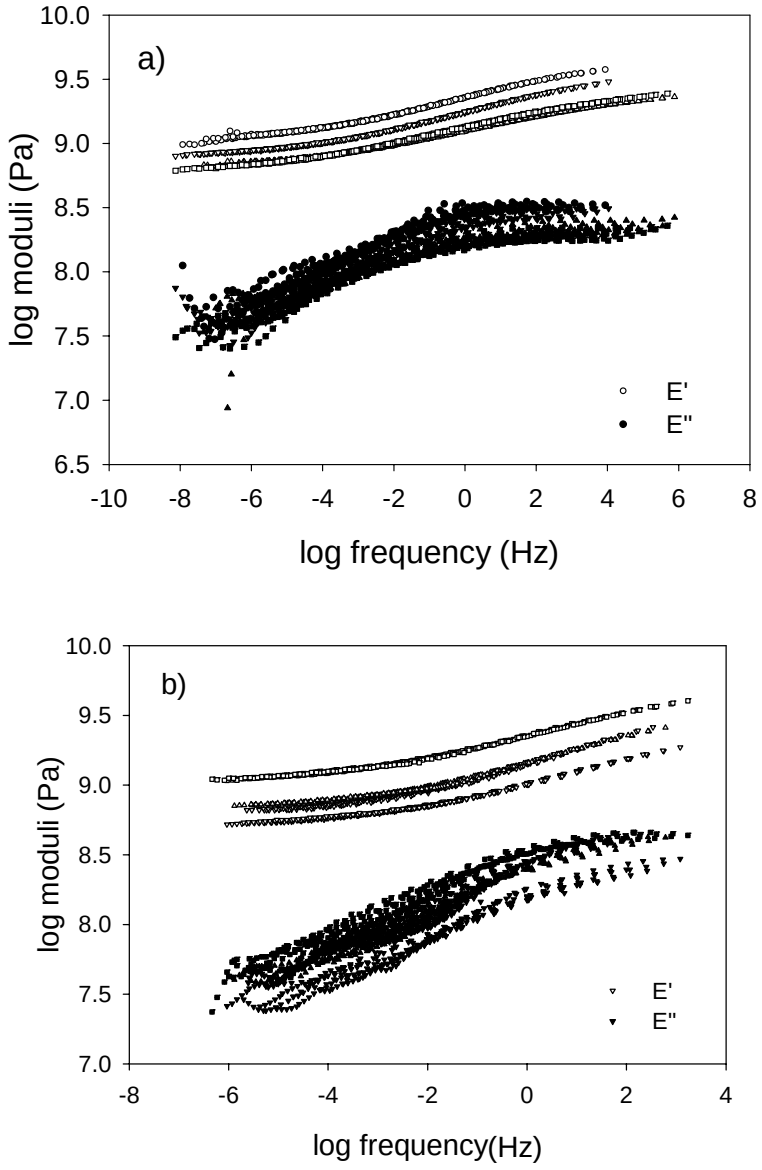

Figure 4.12 Reproducibility of master curves for a) control and b) hotpressed samples of (9%, 200ºC) (4 replicates).

As noted previously, the resonant frequency might be nearly equal to the testing frequency. Though the two highest isotherms (117ºC and 120ºC) were already eliminated, poor superposition occurred on the loss modulus superposition, and was more pronounced in hotpressed samples. It is possible that either resonant frequency affected the viscous component

more, or that another factor induced dispersion or influenced molecular mobility. Because the apparent lignin glass transition is sensitive to solvent uptake, the equilibrium lignin glass transition is also suspected to be highly dependent on solvent uptake.

Figure 4-13a) shows that $T_{g(WLF)}$ is highly dependent on solvent uptake (R^2=0.89). ANCOVA analysis using solvent uptake as a covariate further confirmed that the treatment had significantly impacted the $T_{g(WLF)}$ (p value =0.0011) (Table 4.5), while solvent uptake was not significant. This contradicted the observed linear dependence of the $T_{g(WLF)}$ on solvent uptake. Furthermore, the $T_{g(WLF)}$ was normalized by solvent uptake, and hotpressed samples differed significantly from control samples (ANOVA p value=0.0001) (Table 4.5). The normalized $T_{g(WLF)}$ of hotpressed samples was lower compared to the control group, with the exception of samples hotpressed at 9% and 0% at 250°C, which showed a higher $T_{g(WLF)}$ than control samples Figure 4.13 b). This result agreed with the $T_{g(App)}$ found earlier.

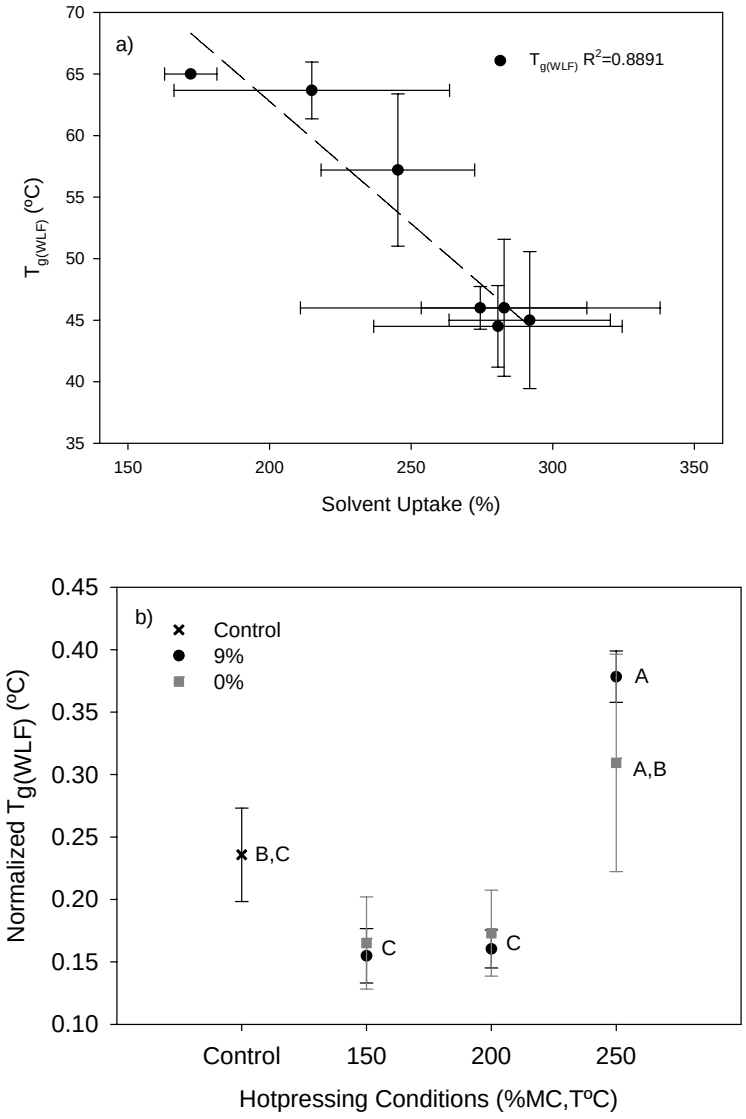

Figure 4.13 a) Relationship between $T_{g(WLF)}$ and solvent uptake, b) the grouping of normalized $T_{g(WLF)}$ for control and hotpressed hybrid poplar wood (at least 3 replicates).

A lower normalized $T_{g(WLF)}$ value for hotpressed groups (150ºC and 200ºC) was due to the presence of many lower molecular weight and mobile polymer chains from lignin depolymerization. At lower pressing temperatures, amorphous polymers such as hemicelluloses decompose and lignin depolymerizes first. Competing reactions might take place at hotpressing higher than 200ºC, such as lignin depolymerization and lignin cross-linking, in addition to

cellulose realignment that is also taking place. The normalized $T_{g(WLF)}$ of lignin for hybrid poplar hotpressed at 250ºC was higher than for those hotpressed at lower temperatures, but similar to the control group. Higher normalized $T_{g(WLF)}$ was observed for hotpressing with 9% wood moisture content and this corresponded to a more complex lignin, possibly as a result of condensation and cross-linking during hotpressing at 250°C. This means moisture present during hotpressing at high temperature (250ºC) enhanced lignin cross-linking. In addition, thermal softening may also be affected by stiffening caused by an increase in the cellulose crystalline region, which reduced lignin flexibility to relax.

Another essential characteristic of viscoelastic polymers at the glass transition is relaxation activation energy. The relaxation activation energy of polymer chains at the lignin glass transition temperature $E_{a(WLF)}$ was calculated using Equation 4-12. For non-hotpressed hybrid poplar wood, $E_{a(WLF)}$ was around 281 ± 24 kJ/mol, which coincides with findings by Laborie, et al. (2004), who reported the $E_{a(WLF)}$ of EG plasticized yellow poplar to be approximately 274 ± 12 kJ/mol. Since $E_{a(WLF)}$ was implicitly dependent on the $T_{g(WLF)}$, it was speculated that this was also dependent on the solvent uptake. However, there was only a slight correlation between the $E_{a(WLF)}$ and solvent uptake (R^2=0.54) (Figure 4.14).

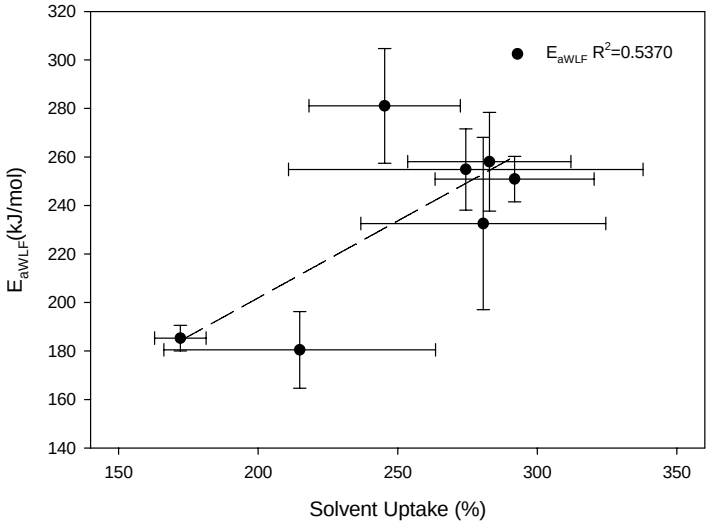

Figure 4.14 Relationship between solvent uptake and activation energy evaluated by WLF for control and hotpressed hybrid poplar wood (at least 3 replicates).

To further evaluate the impact of hotpressing, we performed an ANCOVA with solvent uptake as the covariate. Results showed that hotpressing did significantly affect the $E_{a(WLF)}$ (p value=0.008), but solvent uptake did not (p value=0.6339) (Table 4.5). After normalizing the $E_{a(WLF),}$ it was clearly seen from the ANOVA Tukey-Kramer grouping which indicated treatment did not affect the $nE_{a(WLF)}$ at an α level of 0.05 (p value=0.1197). Therefore, once the activation energy was normalized, it was not affected by hotpressing. The thermal requirement to initiate the segmental chain mobility at the lignin glass transition was not altered by hotpressing. This indicates that the T_g was not directly related to the activation energy; instead, other phenomena were taking place.

Table 4.5 Average value of lignin glass transition and relaxation activation energy evaluated by WLF equation. This includes the normalized value of solvent uptake for control and hotpressed hybrid poplar wood plasticized with EG and ANOVA Tukey-Kramer groupings letters.

Treatment	$T_{g(WLF)}$ (ºC)	Normalized $T_{g(WLF)}$ /Solvent $nT_{g(WLF)}$ (ºC)	C1	C2 (K)	$E_{a(WLF)}$ (kJ/mol)	Normalized $E_{a(WLF)}$ /Solvent $nE_{a(WLF)}$
Control	57 ± 6	0.24 ± 0.04 B,C	14 ± 1	107 ± 12	281 ± 24	1.16 ± 0.18
9%, 150ºC	45 ± 6	0.16 ± 0.02 C	7 ± 1	55 ± 4	251 ± 33	0.86 ± 0.05
9%, 200ºC	45 ± 3	0.16 ± 0.10 C	6 ± 1	49 ± 4	233 ± 39	0.83 ± 0.09
9%, 250ºC	65 ± 0	0.38 ± 0.13 A	5 ± 1	62 ± 9	185 ± 39	1.08 ± 0.15
0%, 150ºC	46 ± 6	0.17 ± 0.04 C	8 ± 5	63 ± 37	258 ± 20	0.92 ± 0.20
0%, 200ºC	46 ± 2	0.17 ± 0.05 C	14 ± 8	108 ± 42	255 ± 54	0.97 ± 0.31
0%, 250ºC	64 ± 2	0.31 ± 0.11 A,B	7 ± 3	77 ± 37	180 ± 0	0.88 ± 0.29
ANOVA p value	-	0.0001	-	-	-	0.1197
ANCOVA treatment p value	0.0011	-	-	-	0.0008	-
ANCOVA solvent uptake p	0.8180	-	-	-	0.6339	-

Although linear dependence on solvent uptake was observed for the storage and loss moduli, the drop in storage modulus, the lignin glass transition, and the flow activation energy, it was not observed for the fractional free volume (f_g) or the thermal expansion coefficient ($\Delta\alpha_f$) (Figure 4.15). Therefore, for properties that were not dependent on solvent uptake, ANOVA was performed to examine the significant effect of treatment on wood properties.

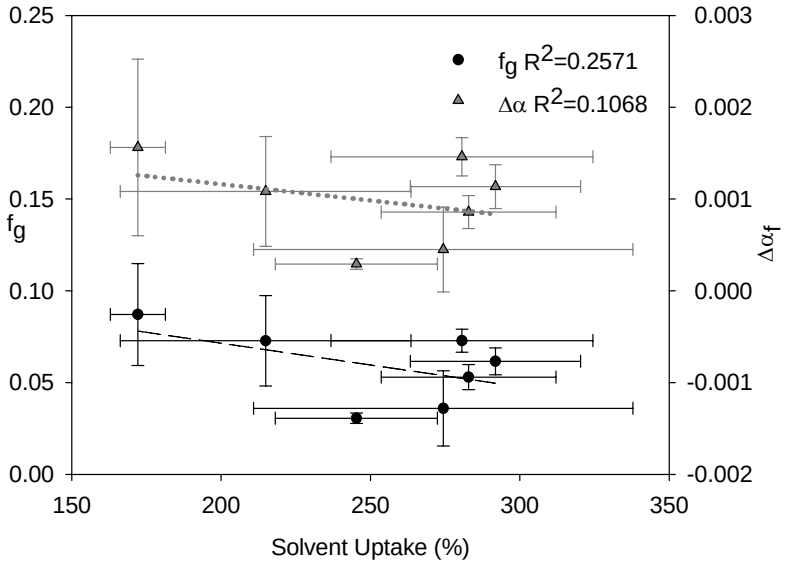

Figure 4.15 Relationship between solvent uptake and fractional free volume (circle) and between solvent uptake and thermal expansion coefficient (triangle).

Hotpressing at 250ºC at both dry and 9% wood moisture content resulted an increase in the fractional free volume compared to that of the control group (ANOVA p value=0.0009) (Table 4.6). This is also true for hybrid poplar hotpressed at 9%, 200°C. This corresponds to the increase of the thermal expansion coefficient of free volume at higher pressing temperatures, specifically for the 9% (ANOVA p value=0.006). The two-fold increase in free volume at the lignin glass transition for hotpressed samples regardless of moisture content suggests that free volume at T_g was more sensitive to pressing temperature than the wood moisture content.

Thermal expansion coefficient of free volume and fractional free volume exhibited direct dependence on pressing temperature observed for hotpressing at 9% wood moisture content. The trend between f_g and $\Delta\alpha_f$ is interestingly similar, in fact other researches had reported that both f_g and $\Delta\alpha_f$ were noted to decrease as thermal softening increases (Salmen & Olsson, 1992). Cross-linking of lignin was suspected to be the reason for the increase in thermal softening. In this study, the hotpressed group posed a higher f_g and $\Delta\alpha_f$ than the control group did, and the effect is

greater for samples hotpressed with 9% wood moisture content. Tukey-Kramer's grouping of free volume thermal expansion coefficient is shown in Figure 4.16.

Table 4.6 Average value of free volume and thermal expansion coefficient for free volume, evaluated with the WLF equation, including statistical significance and Tukey-Kramer grouping letters for control and hotpressed hybrid poplar wood plasticized with EG.

Treatment	f_g ($x10^2$)	$\Delta\alpha_f$ ($x10^{-4}deg^{-1}$)
Control	3.1 ± 0.3 C	2.9 ± 0.6 B
9%, 150ºC	6.2 ± 0.7 A,B,C	11.4 ± 2.4 A,B
9%, 200ºC	7.3 ± 0.6 A,B	14.6 ± 2.1 A
9%, 250ºC	8.7 ± 2.8 A	15.6 ± 9.6 A
0%, 150ºC	5.3 ± 0.7 A,B,C	8.6 ± 1.8 A,B
0%, 200ºC	3.6 ± 2.0 B,C	4.5 ± 4.6 A,B
0%, 250ºC	7.3 ± 2.5 A,B	10.8 ± 6.0 A,B
ANOVA p value	0.0009	0.0064

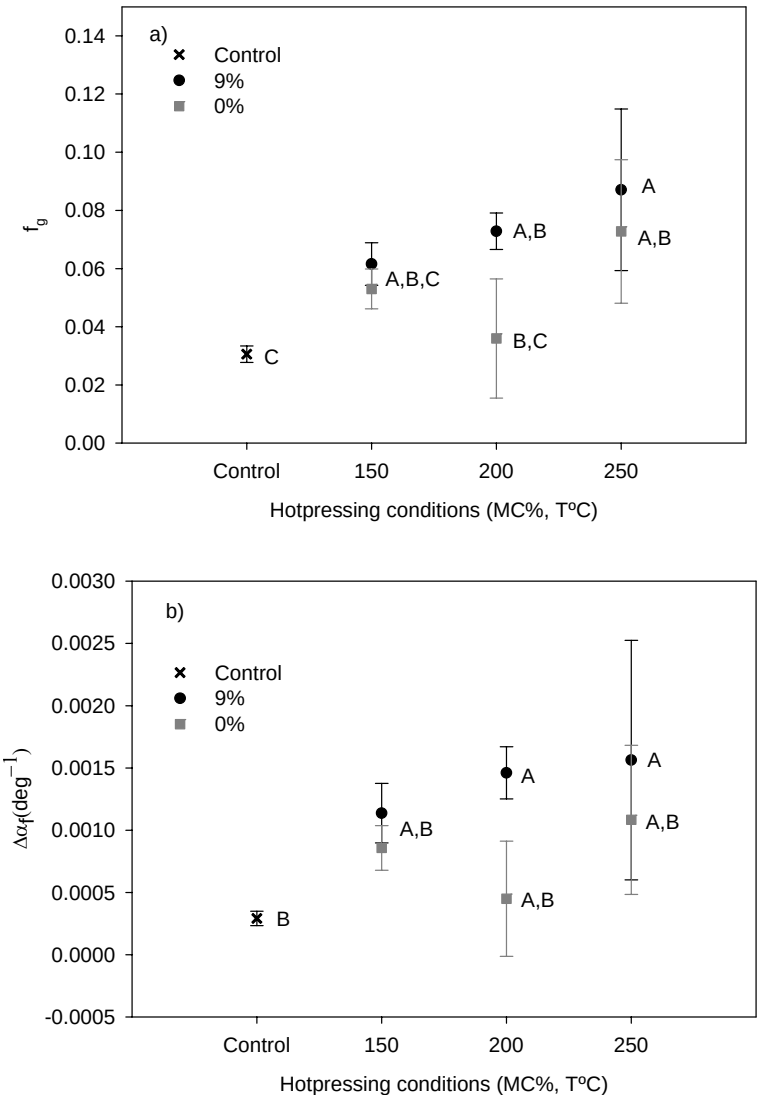

Figure 4.16 The Tukey-Kramer's grouping of a) fractional free volume and b) thermal expansion coefficient for control and hotpressed hybrid poplar wood (at least 3 replicates).

Lignin structure may be altered during hotpressing, which may cause an increase in free volume at T_g. Softwood has a higher thermal softening temperature than does hardwood (Olsson & Salmen, 1992; Hamdan, et al., 2000), and the main difference between the two types of wood is the composition of two different lignin forms: guaiacyl (G) and syringyl (S) (Sjostrom, 1983). Softwood is rich in guaiacyl, the less methoxilated phenolic structure, and therefore has more

reactive sites compared to hardwood, which contains a relatively similar amount of both G and S. As expected, hardwood lignin is bulkier, with fewer reactive sites; thus, it cross-links less upon polymerization compared with softwood (Olsson & Salmen, 1992). In hardwood, prolonged thermal treatment at 160 and 195ºC caused extensive breaking of β-O-4 bonds (Wikberg & Maunu, 2004). This suggested that hotpressing at 150 and 200ºC causes lignin depolymerization through aryl-ether linkages, and thus creates lignin of lower molecular weight and depresses the T_g. However, upon heating to extreme temperatures, lignin cross-linking occurs and creates a bulky lignin matrix compared to the lignin in the control wood. Essentially, the T_g is higher for samples pressed at 250ºC.

A full viscoelastic evaluation is shown by the shape and breadth of a master curve. The frequency window of the master curve provides some insight into the softening behavior for each hotpressed specimen. The breadth of the master curve was determined by subtracting the minimum from the maximum value of the logarithm of frequency, called the log frequency range (Figure 4.10). In general, this frequency window was extended from 3 decades of experimental frequency to 7-13 decades of master curve frequency resulting from TTS.

No relationship between log frequency range and solvent uptake was detected (R^2=0.18) (Figure 4.17 a). The breadth of master curve quantified by the range of log frequency range was affected significantly by hotpressing (ANOVA p value=0.0001) (Table 4.7). The Tukey-Kramer's grouping for log frequency is illustrated in Figure 4.7 b).

Table 4.7 lists the results for the log frequency range and coupling constant from the cooperativity analysis. Hotpressing induced different morphological features and different time dependencies, indicated by a shorter log frequency range compared to the control group Samples hotpressed at 9% wood moisture content consistently showed a shorter range of log frequency compared to the control group, and the shortest frequency range belonged to the samples pressed at the highest temperature (250°C). The shorter breadth of the master curves (Table 4.7) suggests that the distribution of relaxation behavior was narrow, and that the polymer chain exhibiting viscoelastic behavior was more uniform. This is exemplified by the fact that dominant wood polymers appeared to be mostly crystalline cellulose and some modified lignin, but no hemicelluloses at 250°C.

Laborie, et al. (2004) showed that the Ngai coupling model fits well with experimental data and describes the WLF equation for temperatures above T_g only. The coupling model proposed by Ngai is an empirical model developed for polymers to explain the glass transition phenomena from a kinetic point of view. In this study the master curve was reconstructed at the new equilibrium glass transition, called $T_{g(WLF),}$ where the temperature difference equals zero and the shift factor was plotted against the fractional deviation from the T_g $[(T-T_g)/ T_g]$. The dimensionless parameters of $(T-T_g)/T_g$ represent changes in rate as a function of available kinetic energy instead of free volume, as described by the WLF equation (Plazek & Ngai, 1991). From each master curve, the corresponding shift factor was then used to determine the applicability of the WLF equation on this wood (see the Data Analysis section). The validity of the WLF applicability for most polymers lies in the range of T_g + 100ºC (Ferry, 1980). However, in this study, the WLF equation fitted the experimental data only up to 100ºC, which was approximately T_g + 40ºC (Figure 4.11b). This is right in line with what other researchers have reported (Olsson

& Salmen, 1984; Laborie, et al., 2004). A shorter temperature range of WLF applicability might be due to polymers degradation at high temperature (corresponding to low frequency), interfering with the measurement.

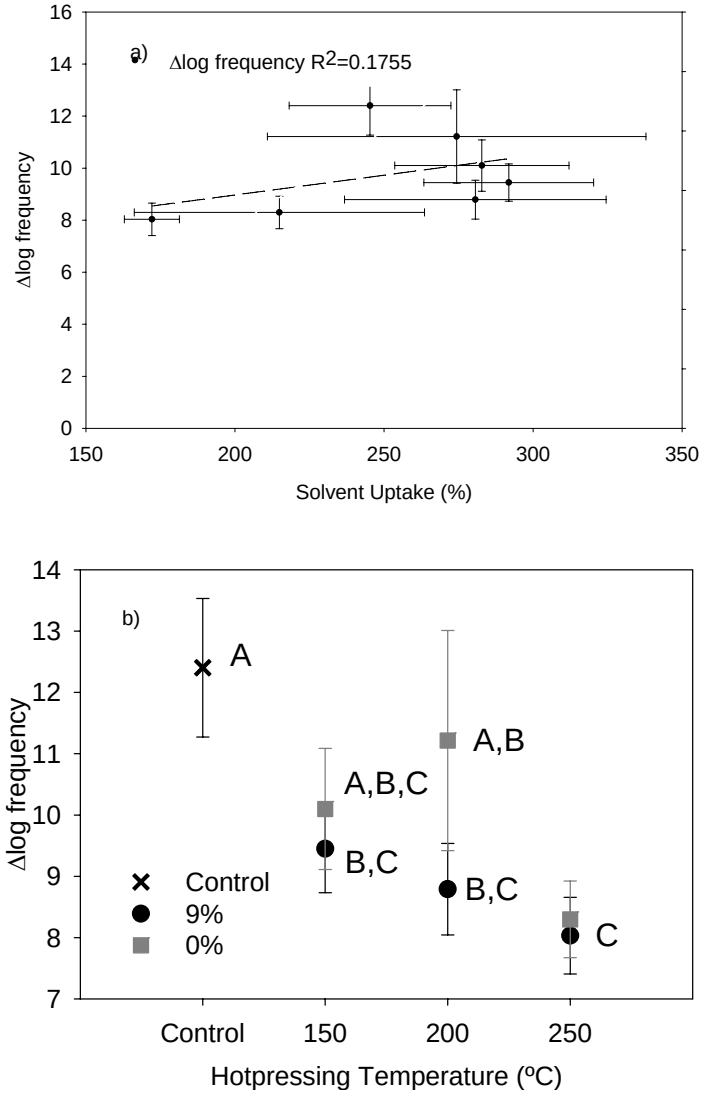

Figure 4.17 a) Relationship between solvent uptake and log frequency range and the b) Tukey-Kramer's grouping (at least 3 replicates).

Table 4.7 Results of cooperativity analysis

Treatment	$T_{g(WLF)}$ (ºC)	Coupling constant, n	n Nonlinear Regression (R^2)	Δlog frequency	Total Replicates
Control	65 ± 8	0.35 ± 0.04 A	0.98	12.4 ± 1.1 A	5
9%, 150ºC	50 ± 6	0.13 ± 0.06 B,C,D	1.00	9.4 ± 1.0 B,C	3
9%, 200ºC	47 ± 3	0.08 ± 0.06 D,C	1.00	8.8 ± 1.0 B,C	4
9%, 250ºC	67 ± 2	0 D	1.00	8.0 ± 0.9 C	3
0%, 150ºC	53 ± 10	0.21 ± 0.07 A,B,C	0.99	10.1 ± 1.4 A,B,C	3
0%, 200ºC	54 ± 2	0.30 ± 0.17 A,B	0.98	11.2 ± 2.4 A,B	4
0%, 250ºC	67 ± 2	0 D	0.99	8.4 ± 0.7 C	3
ANOVA p value		0.0001		0.0001	

Figure 4.18 shows the quality of the Ngai coupling model for the EG plasticized wood above the T_g of lignin. The fit was calculated using nonlinear regression with a weighted chi-square. In this study, the Ngai coupling constant (n) was found to be significantly affected by hotpressing (ANOVA p value = 0.0001) (Table 4.7). Hotpressing decreased the coupling constant, and in fact, the coupling constant for samples hotpressed at 250°C was zero, which essentially represents no cooperativity. Typical coupling constants for polymers lie in the range of 0.35–0.75 (Ngai &Roland, 1993). In this study, the coupling constants of native wood saturated in EG was found to be around 0.35 ± 0.04. This value was almost twice as high as that reported on yellow poplar under EG saturated conditions (Laborie, et al., 2004). This might be due to difference in species and structural arrangement.

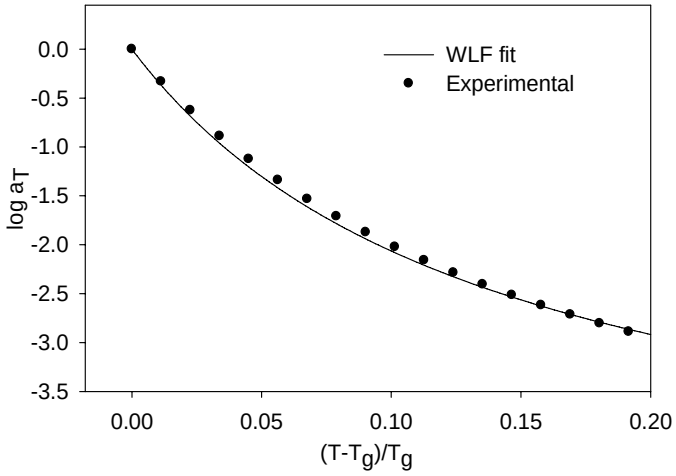

Figure 4.18 Evaluation of Ngai coupling model for EG plasticized wood above T_g of lignin.

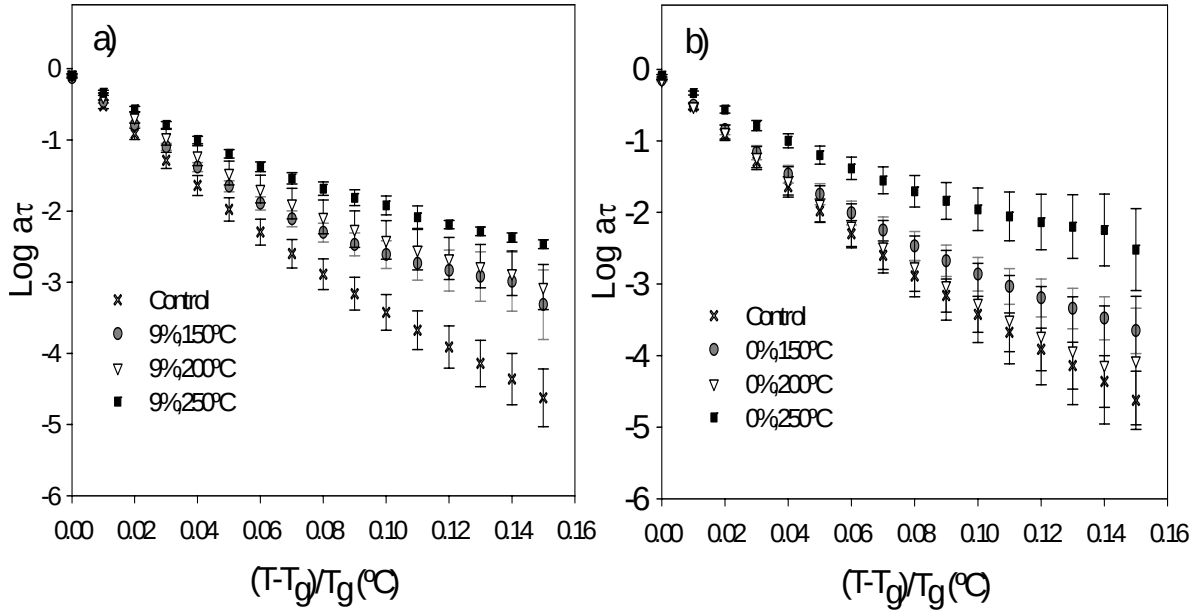

Figure 4.19 Average cooperativity plots for hybrid poplar wood hotpressed at a) 9% and b) 0% wood moisture content (with at least 3 replicates for each treatment group).

In addition, the coupling constants for hotpressed wood were much lower than for the control (observed from 0 to 0.19). Thus, hotpressing reduced the coupling constants, and this corresponded to a reduction in intermolecular cooperativity of a segmental chain with the

neighboring non-bonded segments. The cooperativity plots for control and hotpressed samples were constructed and shown in Figure 4.19. The coupling constant was observed to be not linearly dependent on solvent uptake either (R^2=0.25), as shown in Figure 4.20 a. The Tukey-Kramer's grouping for coupling constant is illustrated in Figure 4.20 b.

The lower the coupling constant, the more the segmental relaxation behavior follows that described by Arrhenius. The reduction of the coupling constant near in situ lignin T_g was postulated to be the consequence of the loss of non-bonded segments and a more uniform body of molecules surroundings the bulk lignin. In native wood, lignin covalently links with hemicelluloses, specifically with xylan (Salmen & Olsson, 1998). Thus, hemicellulose units may take part in the cooperativity of evaluated in situ lignin. In addition, hemicelluloses interact with cellulose through hydrogen bonding, which increases the complexity of interaction among wood polymers.

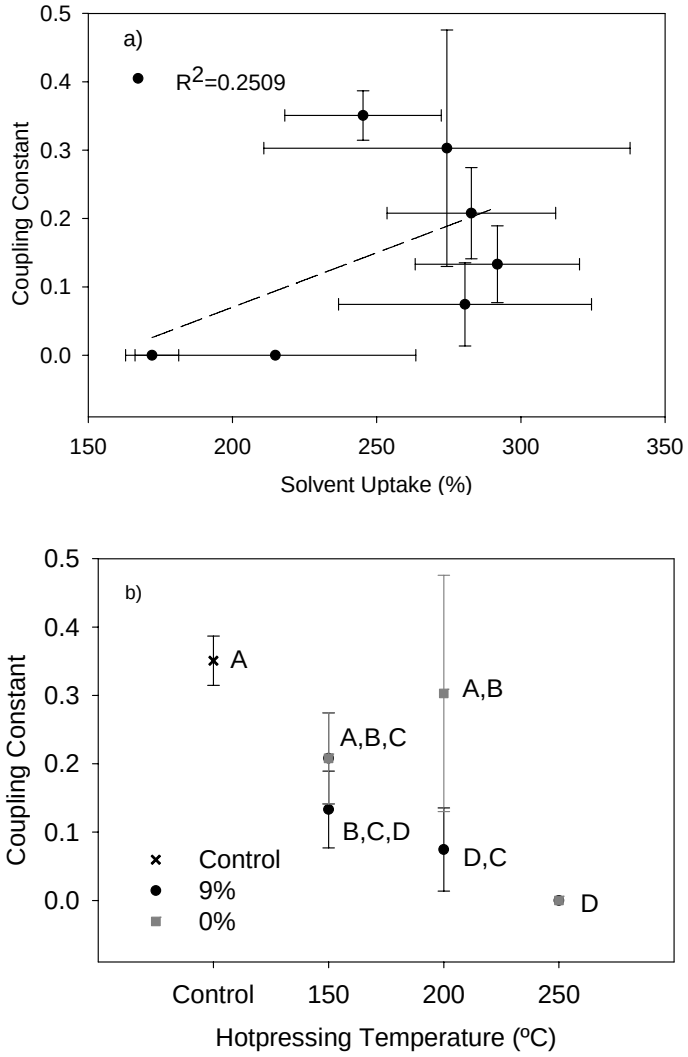

Figure 4.20 a) Relationship between solvent uptake and coupling constant and the b) Tukey-Kramer's grouping of coupling constant for hybrid poplar control and hotpressed wood (at least 3 replicates).

Hotpressing, in deed, reduced the intermolecular cooperativity of a segmental chain to the neighboring non-bonded segments and also affected the thermal softening of lignin. Further, the relationship between the coupling constant and glass transition temperature was investigated. For coupling constants greater than zero, the coupling constant was found to be linearly dependent

on normalized T_g as evaluated both with normalized $T_{g(App)}$ (R^2=0.78) shown in Figure 4.21 a and normalized $T_{g(WLF)}$ (R^2=0.61) shown in Figure 4.21 b.

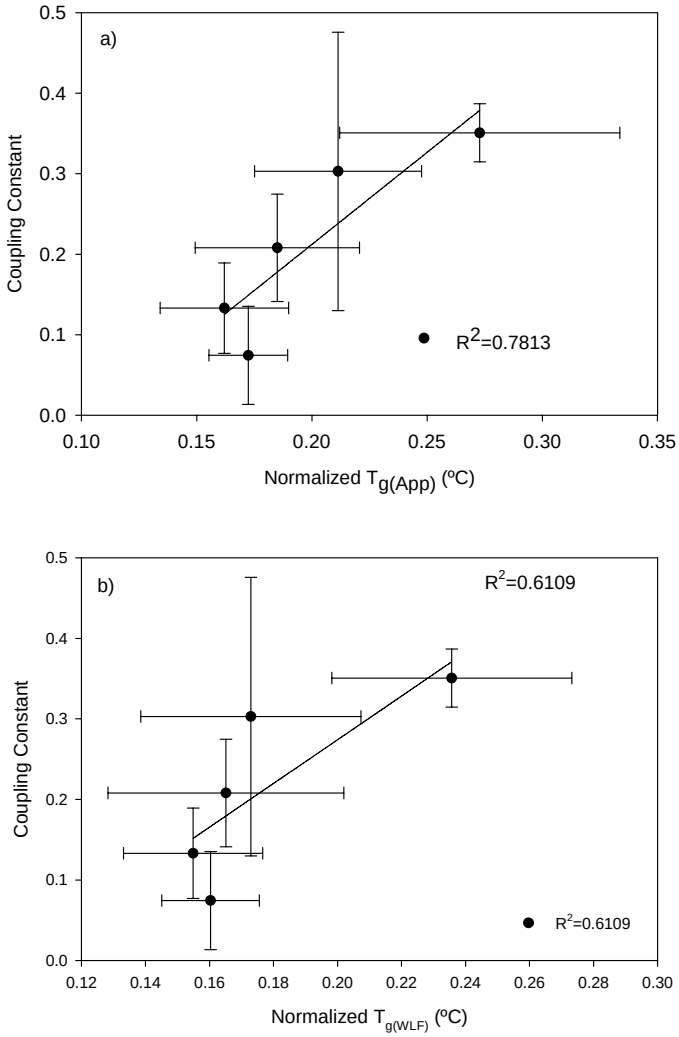

Figure 4.21 a) Relationship between coupling constant (n>0) and normalized $T_{g(App)}$ and b) the relationship between coupling constant (n>0) and normalized $T_{g(WLF)}$ and the for hybrid poplar control and hotpressed samples (at least 3 replicates).

This means that, as thermal softening increases, the coupling constant is expected to increase. Recall that the coupling constant bears information about polymers structure, stearic hindrance, and polarity. Thus, through the evaluation of lignin thermal softening, information about the interaction and chemical properties of polymers can be linked. This correlation is

useful for evaluation of viscoelastic properties and chemical properties. It was clearly observed that the in situ cooperativity of lignin was significantly altered by hotpressing conditions. At lower pressing temperatures, with the lower molecular weight of polymer chains from the partially degraded hemicelluloses and the depolymerization of lignin, intermolecular interaction was found to be greater than zero. Cooperativity analysis is useful for investigating the molecular features of in situ lignin relaxation (Laborie, et al., 2004). Our study showed that in situ cooperativity analysis could provide insight into the behavior of in situ lignin relaxation modified by hotpressing.

4.5 **Conclusions**

This study demonstrated that wood moisture content and high hotpressing temperature during hotpressing affected the thermal softening of lignin evaluated in situ and intermolecular cooperativity of hybrid poplar wood polymers. Characterization of in situ thermal softening behavior and cooperativity analysis related to the ascribed lignin segmental motion were successfully performed on the hotpressed wood. Correlation between properties evaluated and solvent uptake were examined to determine the intrinsic effect of hotpressing regardless solvent uptake condition. An increase in the normalized glass transition is observed as hotpressing temperatures increase and, in particular, displays a similar trend with increasing free volume and thermal expansion of free volume. While the relaxation activation energy was observed to not be affected by the hotpressing, the distribution of relaxation times for lignin was observed to be reduced significantly at higher pressing temperatures. Despite the complexity of wood, time-temperature superposition can be applied for both control wood samples and hotpressed wood samples. The quality of the master curve after shifting the storage modulus isotherm was

satisfactorily smooth and reproducible. A shorter relaxation time was observed for the hotpressed wood with 9% wood moisture content, indicating that a trace of water during hotpressing changed the wood morphology and its time dependence.

Hotpressing had a huge impact on molecular cooperativity at the thermal softening of lignin, as indicated by a reduction of the coupling constant and in fact, intermolecular interaction between segmental chains with non-bonded segments intermolecular coupling, was absent when hybrid poplar wood samples were pressed at 250ºC. It is speculated that at temperatures above 200ºC, two competing reactions affect the thermal softening of the lignin such as depolymerization of the lignin matrix and cross-linking of phenolic groups.

Knowledge gained from this research will help people in research in industry probe the impacts of hotpressing on molecular structure through the evaluation of lignin's in situ thermal softening behavior. A fundamental understanding of the combined effects of pressing temperature and wood moisture content is integral to enhancing the quality of forest products, such as oriented strand board. Further detailed chemical analysis is needed to better understand the thermal properties evaluated around the in situ thermal softening of lignin.

4.6 **References**

Angell, C.A. (1991). Thermodynamic aspects of the glass transition in liquids and plastic crystals. *Pure and Applied Chemistry, 63*(10), 1387–1392.

Back, E.L., & Salmen, N.L. (1982). Glass transitions of wood components hold implications for molding and pulping processes. *Tappi Journal, 65*(7), 107–110.

Bouchard, J., Lacelle, S., Chornet, E., Vidal, P.F., & Overend, R.P. (1993). Mechanism of depolymerization of cellulose by ethylene-glycol solvolysis. *Holzforschung, 47*(4), 291–296.

Doolittle, A.K. (1951). Newtonian flow. II. The dependence of the viscosity of liquids on free space. *Journal of Applied Physics, 22*, 1471–1475.

Dwianto, W., Morooka, T., Norimoto, M., & Kitajima, T. (1999). Stress relaxation of sugi (*Cryptomeria japonica* D.Don) wood in radial compression under high temperature steam. *Holzforschung, 53*(5), 541–546.

Ferry, J.D. (1980). Viscoelastic properties of polymers (2nd ed.). New York: John Wiley and Sons.

Gardner, D.J., Gunnells, D.W., Wolcott, M.P., & L. Amos (1993). Changes in wood polymers during the pressing of wood-composites. In J. F. Kennedy, G. O. Phillips & P. A. Williams (Eds.), *Cellulosics, Chemical, Biochemical and Material Aspects* (pp. 513–518). New York: Ellis Horwood.

Goring, D.A.I. (1963). Thermal softening of lignin, hemicellulose and cellulose. *Physical Chemistry Division, Pulp and Paper Research Institute of Canada, 64*(12), T517–T527.

Hall, C.K. (1982). Conformational state relaxation in polymers: Time-correlation functions. *Journal of Chemical Physics, 77*(6), 3275–3282.

Hsu, W.E., Schwald, W., Schwald, J., & Shields, J.A. (1988). Chemical and physical changes required for producing dimensionally stable wood-based composites. Part I: Steam pretreatment. *Wood Science and Technology, 22*, 281–289.

Irvine, G.M. (1984). The glass transition of lignin and hemicellulose and their measurement by differential thermal analysis. *Tappi Journal, 67*(5), 118.

Jensen, R.E., O'Brien, E., Wang, J., Bryant, J., Ward, T.C., James, L.T., & Lewis, D.A. (1998). Characterization of epoxy-surfactant interactions. *Journal of Polymer Science: Part B: Polymer Physics, 36*, 2781–2792.

Kelley, S.S., Rials, T.G., & Glasser, W.G. (1987). Relaxation behaviour of the amorphous components of wood. *Journal of Materials Science, 22*, 617–624.

Laborie, M.P. G., Salmen, L., & Frazier, C.E. (2004). Cooperativity analysis of the in situ lignin glass transition. *Holzforschung, 58,* 129–133.

Menard, K.P. (1999). Dynamic mechanical analysis: A practical introduction. Boca Raton, FL: CRC Press LLC.

Ngai, K.L. (1991). Test of expected correlation of polymer segmental chain dynamics with temperature-dependent time-scale shifts in concentrated solutions. *Macromolecules, 24*, 4865–4867.

Ngai, K.L., & Roland, C.M. (1993).Chemical structure and intermolecular cooperativity: Dielectric relaxation results. *Macromolecules, 26*, 2628–2830.

Olsson, A.M., & Salmen, L. (1992). Chapter 9: Viscoelasticity of in situ lignin as affected by structure. Softwood vs. hardwood. *Journal of the American Chemical Society (489)*, 133–143.

Osman, N., McDonald, A.G. & Laborie, M-P. (2009). Thermal Compression of Hybrid Poplar Wood: Vibrational spectroscopy analysis on the effects and behaviors of hot-pressed heat treatment (abstract). In: FPS 63rd International Convention, June 21-23; Boise, Idaho. Madion (WI): Forest Products Society.

Plazek, D.J., & Ngai, K.L. (1991). Correlation of polymer segmental chain dynamics with temperature-dependent time-scale shifts. *Macromolecules, 24*(5), 1222–1224.

Reinprecht, L., Kacik, F., & Solar, R. (1999). Relationship between the molecular structure and bending properties of the chemically and thermally degraded maplewood. *Cellulose Chemistry and Technology, 33*, 67–79.

Sadoh, T., & Ohgoshi, M. (1974). Viscoelastic properties of wood in solvent uptake systems. II. Viscoelastic properties of wood swollen with ethylene glycol and polyethylene glycols. *Mokuzai Gakkaishi, 20*(4), 177–181.

Sadoh, T. (1981). Viscoelastic properties of wood in solvent uptake systems. *Wood Science and Technology. 15*(1), 57–66.

Salmen, L. (1984). Viscoelastic properties of in situ lignin under water saturated conditions. *Journal of Material Science, 19*(9), 3090.

Salmen, L., & Olsson, A.M. (1998). Interaction between hemicelluloses, lignin and cellulose: structure–property relationships. *Journal of Pulp and Paper Science, 24*, 99–103.

Tjeerdsma, B.F., Boonstra, M., Pizzi, A., Tekely, P., & Militz, H. (1998). Characterization of thermally modified wood: Molecular reasons for wood performance improvement. *Holz als Roh- und Werkstoff, 56*, 149–153.

Verghese, K.N.E., Jensen, R.E., Lesko, J.J., & Ward, T.C. (2001). Effect of molecular relaxation behavior on sized carbon fiber-vinyl ester matrix composite properties. *Polymer, 42,* 1633–1645.

Wikberg, H., & Maunu, L. (2004). Characterization of thermally modified hard- and softwoods by ^{13}C CPMAS NMR. *Carbohydrate Polymers, 58,* 461–466.

Wolcott, M.P., Kamke, F.A., & Dillard, D.A. (1990). Fundamentals of flakeboard manufacture: Viscoelastic behavior of wood components. *Wood and Fiber Science, 22*(4), 345–361.

CHAPTER 5 CONCLUSIONS AND FUTURE WORK

5.1 Conclusions

Heat treatment has been utilized widely to improve wood properties, and its application combined with compression force is used in the manufacturing of oriented strand board. The expanding demand of wood products is not balanced with the resources available. Hybrid poplar is unique species of wood since the traits can be tailored for specific purposes. Utilizing genetic engineering avenues, its low density and fast growth characteristics make hybrid poplar an ideal candidate for alternative wood-based composites products. Despite this fact, hybrid poplar is not yet commonly used for structural materials and how its properties are impacted by processing is not completely known.

This study assessed the impact of hotpressing conditions (wood moisture content and pressing temperature) on the physical, chemical, and viscoelastic properties of hybrid poplar wood. Dynamic mechanical analysis was used to characterize viscoelastic behavior related to molecular motions because of its sensitivity to thermal softening of in situ lignin. Because this study evaluated the effects of hotpressing conditions commonly used in wood products manufacturing, results are useful for both research and industrial applications.

In Chapter 3, the investigation of hotpressing's effects on the physical and viscoelastic properties of dry wood samples was thoroughly presented. This study found that moisture content and pressing temperature together influenced the hygroscopic behavior, specific gravity, and bending dynamic mechanical properties of hybrid poplar wood. Samples exhibited less hygroscopicity when pressed at higher temperatures and moisture contents, indicated by a lower

EMC. Higher pressing temperatures resulted in higher stiffness and correlated to an increase in densification. Despite the dependence of stiffness on the specific gravity of wood, hotpressing increased the normalized storage modulus by 2 to 3 times compared to native wood. Project collaborators' results supported this finding, and they attributed an increase in stiffness to an increase in crystallinity. It is notable that specimens hotpressed at a 9% moisture content and 150ºC had the lowest peak height ratios and therefore low crystallinity, yet showed significantly more stiffness than other samples. This indicates a need for further research in the chemistry field to elucidate the interaction between wood moisture and pressing temperature. Despite the complexity of the dry wood structure, a satisfactory master curve for dry control specimens and hotpressed wood was constructed using additional vertical shifting on loss modulus isotherms. The viscous component was highly sensitive to fluctuations in density and moisture content during temperature testing, indicated by a visible loss modulus peak at 50ºC that was ascribed to the desorption of water molecules.

Chapter 4 explored the impact of hotpressing on in situ lignin thermal softening. The viscoelastic properties of wood under plasticized conditions are governed mainly by the time-temperature dependence behavior of lignin. This study showed that higher pressing temperatures cause less solvent uptake in hotpressed wood. Solvent uptake acts as a covariate for several properties evaluated in a plasticized system, and behaves in a similar manner to specific gravity in a dry wood system. This trend in T_g may be due to two competing reactions occurring in the temperature range of 200 to 250ºC, such as lignin depolymerization and cross-linking, which influenced the thermal softening of lignin. Lignin's segmental motion is also highly influenced by other wood constituents. The applicability of the WLF equation to the viscoelastic behavior of polymers at in situ lignin T_g in hotpressed wood suggests that a common phenomenon occurs

around the glass transition that is related to the viscoelastic properties of glass. Smooth master curves were constructed utilizing horizontal shifting, indicating that density variation was suppressed under plasticized conditions. One might hypothesize that the initial segmental motion of lignin is closely related to the energy barrier and free volume. However, this study showed that thermal softening alone cannot explain changes in relaxation activation energy and free volume. In addition, free volume was clearly proportional to the thermal expansion coefficient of free volume, as well as lignin thermal softening. This relationship became more pronounced in severe hotpressing conditions, such as those noted at 9% moisture content. Hotpressing at 0% MC and 200ºC showed a large deviation from the trend for free volume and thermal expansion coefficient of free volume, possibly related to the transition zone where the competing reactions occurred. The successfully constructed master curve showed significant reductions in range as pressing temperature increased. The distribution of temperature-dependent relaxation time is narrower for hotpressed wood, indicating a more uniform environment around the bulk lignin. The reduction of less ordered amorphous polymers such as hemicellulose and semicrystalline cellulose in wood may influence the manner in which lignin condenses.

This study has provided a better understanding of how moisture content and pressing temperature can impact the physical, chemical, and viscoelastic properties of hybrid poplar wood. Results can be used to forge new directions in the manufacture of oriented strand board. This exploration of softening behavior under plasticized conditions provides further insight into how hotpressing conditions alter the morphology of wood polymers and molecular motion.

5.2 **Future Work**

The scope of this study addressed only the initial step of investigation of using hybrid poplar as an alternative wood source for wood-based composites mainly for oriented strand board production. More research is needed to analyze the chemistry of hotpressed wood in order to link the physical and viscoelastic properties to the chemical modifications that occur during hotpressing. A basic understanding of the behavior of hybrid poplar during hotpressing needs to be investigated in order to enhance the understanding of wood/adhesive interphase systems, benefitting both the research and industrial fields.